Uniwersytet im. Adama Mickiewicza w Poznaniu

Wydział Chemii

Zastosowanie nanotechnologii w inżynierii tkanki chrzęstnej

Rozprawa doktorska

Tomasz Szymański

Poznań, 2024

Adam Mickiewicz University in Poznań

Faculty of Chemistry

Application of nanomaterials in cartilage tissue engineering

PhD dissertation

Tomasz Szymański

Poznań, 2024

Supervisor

prof. UAM dr hab. inż. Jakub D. Rybka

the Laboratory of Applied Biotechnology,

Center for Advanced Technology, Adam Mickiewicz University

Auxillary supervisor

dr Adam A. Mieloch

the Laboratory of Applied Biotechnology,

Center for Advanced Technology, Adam Mickiewicz University

PhD dissertation was performed at

the Laboratory of Applied Biotechnology

at Center for Advanced Technology,

Adam Mickiewicz University.

Acknowledgments

I'd like to express my gratitude to all of the people from the Laboratory of Advanced Biotechnology, where I work and where this dissertation was prepared:

To my supervisor Jakub, who is a great boss and manager, who can arrange almost impossible things, for his patience and support

To the rest of the team: Adam, Adam, Ania, Filip, Gosia, Julia, Monika, and Piotr for being great scientists and co-workers, but most importantly great people and friends

To prof. Michał Giersig, for his mentoring

&

For my fiancée Bogna, for daily support on good and bad days

Table of contents

List of scientific papers included in the scientific achievement

1. **<u>Szymański T</u>.,** Mieloch A.A., Richter M., Trzeciak T., Florek E., Rybka J.D., Giersig M Utilization of Carbon Nanotubes in Manufacturing of 3D Cartilage and Bone Scaffolds in orthopedics, *Materials* 2020, 13(18), 4039, https://doi.org/10.3390/ma13184039
IF: 3,4 (2022);
MNiSW: 140 (2024)
Citations: 29

2. **<u>Szymański T</u>.,** Kempa M., Giersig M., Rybka J.D Carbon Nanotubes Interference with Luminescence-Based Assays *Materials* 2020;13(19):4270*;*
https://doi.org/10.3390/ma13194270
IF: 3,4 (2022);
MNiSW: 140 (2024)
Citations: 7

3. **<u>Szymański T</u>**., Semba J.A**.,** Mieloch A.A., Cywoniuk P., Kempa M., and Rybka J.D. Hyaluronic acid and multiwalled carbon nanotubes as bioink additives for cartilage tissue engineering *Sci Rep* 13 (646); 2023, https://doi.org/10.1038/s41598-023-27901-z
IF: 4.6 (2022)
MNiSW: 140 (2024)
Citations: 4 (Google Scholar)

Scientific achievements

Education

2017-	**Adam Mickiewicz University in Poznań, Faculty of Chemistry** International PhD programme 'Cheminter'
2013-2015	**Adam Mickiewicz University in Poznań, Faculty of Chemistry** MSc in Biotechnology, programme taught in English, thesis title: 'In silico and experimental characterization of STAT3-SH2 inhibitors to block STAT1 activity in inflammation in atherosclerosis'
2009-2012	**Medical University in Poznań** Bachelor in Medical Biotechnology, thesis title: 'Suicide genes in cancer therapy'

Experience

2021-	**Adam Mickiewicz University in Poznań, Wielkopolska Centre of Advanced Technologies** Scientist in the NCBiR project TECHMATSTRATEG-III/0027/2019 (22 444 594 PLN) *'Development of bioinks for 3D bioprinting based on chemically modified porcines dECM, enriched with recombinant hybrid proteins, nanomaterials and synthetic polymers.'*
2021-2022	**Institute for Organic Synthesis and Photoreactivity, National Research Council of Italy, Bologna** Internship
2020-2021	**Adam Mickiewicz University in Poznań, Wielkopolska Centre of Advanced Technologies** Scientist in the NCBiR project SZPITALE-JEDNOIMIENNE/76/2020 (2 652 000 PLN): *'Development and verification of the effectiveness of the new COVID-19 immunodiagnostic tool'*

2018-2021	**Adam Mickiewicz University in Poznań, Wielkopolska Centre of Advanced Technologies**
	Scientist in the NCBiR project LIDER/34/0122/L-9/17/NCBR/2018 (1 199 906 PLN) '*MeniScaff 3D – bioprinted, carbon nanotube-enhanced scaffolds for stimulated chondrogenic differentiation of mesenchymal stem cells for meniscus implant*'
2017-2020	**Adam Mickiewicz University in Poznań, Faculty of Chemistry**
	Scientist in the OPUS project '*Synthesis, toxicological and functional studies on multi-walled carbon nanotubes as a scaffold for tissue engineering techniques in articular cartilage repair*'
2015-2018	**Polish Academy Of Sciences, Institute Of Human Genetics**
	Scientist in the NCBiR PBS project '*Molecular imaging (with the use of nanotechnology) to monitor implanted stem cells*'

Publications

1. Augustyniak A., **<u>Szymański T.</u>**, Porzucek F., Mieloch A.A, Semba J. A., Hubert K.A., Grajek D., Krela R., Rogalska Z., Zalc-Budziszewska E., Wysocki S., Sobczak K., Kuczyński L., Rybka J.D. A cohort study reveals different dynamics of SARS-CoV-2-specific antibody formation after Comirnaty and Vaxzevria vaccination, *Vaccine* 41 (34), 2023, 5037-5044 https://doi.org/10.1016/j.vaccine.2023.06.008
   IF: 7.7 (2022)
   MNiSW: 200 (2024)
   Citations: 1

2. **<u>Szymański T</u>**., Semba J.A., Mieloch A.A., Cywoniuk P., Kempa M., and Rybka J.D. Hyaluronic acid and multiwalled carbon nanotubes as bioink additives for cartilage tissue engineering *Scientific Reports* 13 (646); 2023, https://doi.org/10.1038/s41598-023-27901-z
   IF: 4.6 (2022)
   MNiSW: 140 (2024)
   Citations: 4

3. Sidorowicz A, **<u>Szymański T</u>**, Rybka JD. Photodegradation of Biohazardous Dye Brilliant Blue R Using Organometallic Silver Nanoparticles Synthesized through a Green Chemistry Method. *Biology* 2021 Aug 17;10(8):784. https://doi:10.3390/biology10080784
IF: 4.2 (2022)
MNiSW: 100 (2024)
Citations: 19

4. **<u>Szymański T.</u>**, Kempa M., Giersig M., Rybka J.D Carbon Nanotubes Interference with Luminescence-Based Assays *Materials* 2020;13(19):4270; https://doi.org/10.3390/ma13194270
IF: 3,4 (2022)
MNiSW: 140 (2024)
Citations: 7

5. **<u>Szymański T.</u>**, Mieloch A.A., Richter M., Trzeciak T., Florek E., Rybka J.D., Giersig M Utilization of Carbon Nanotubes in Manufacturing of 3D Cartilage and Bone Scaffolds *Materials* 2020, 13(18), 4039, https://doi.org/10.3390/ma13184039
IF: 3,4 (2022)
MNiSW: 140 (2024)
Citations: 29

6. Wierzbiński, K.R., **<u>Szymański, T</u>**., Rozwadowska, N. Rybka J.D., Zimna A., Zalewski T., Nowicka-Bauer K., Malcher A., Nowaczyk M., Krupiński M, Fiedorowicz M., Bogorodzki P., Grieb P., Giersig M., Kurpisz M.K. Potential use of superparamagnetic iron oxide nanoparticles for *in vitro* and *in vivo* bioimaging of human myoblasts. *Scientific Reports* 8, 3682 (2018) https://doi:10.1038/s41598-018-22018-0
IF: 4.6 (2022)
MNiSW: 140 (2024)
Citations: 85

Bibliometrics

Total citations: 145   h-index: 4 (Google Scholar)

Total citations: 119   h-index: 5 (Scopus)

Abstrakt

Uszkodzenia tkanki chrzęstnej są często występującymi schorzeniami, charakteryzującymi się słabą zdolnością do samodzielnej regeneracji. Dostępne metody leczenia zapewniają niedostateczną rekonwalescencję, poprzez częściową rekonstrukcję, złagodzenie dolegliwości lub interwencję operacyjną polegającą na wprowadzeniu endoprotezy. Jedną z najbardziej obiecujących metod inżynierii biomedycznej jest biodruk 3D, którego celem jest odtworzenie całej struktury narządu wraz z komórkami zapewniającymi prawidłowy metabolizm i funkcjonowanie takiego konstruktu. Głównym wyzwaniem tej technologii w zakresie tkanki chrzęstnej jest uzyskanie odpowiedniej wytrzymałości, która będzie w stanie wytrzymać siły działające w stawach. Nanorurki węglowe należą do nanomateriałów posiadających doskonałe właściwości mechaniczne i mogących służyć jako wzmocnienie struktury biodruku. W niniejszej rozprawie dokonano szerokiej analizy dotyczącej zastosowania w tym kontekście wielościennych nanorurek węglowych.

Badanie wpływu wielościennych nanorurek węglowych na żywotność komórek wykazało, że materiał ten interferuje z większością rutynowo stosowanych testów biologicznych opartych na absorbancji, fluorescencji i luminescencji, a stężenie 0,0625 mg/ml jest najwyższe, jakie można wiarygodnie zastosować w takich analizach. W dalszej części badań, do biodruku 3D rusztowań wykorzystano optymalną ilość nanorurek węglowych ustaloną w oparciu o żywotność, apoptozę i stres oksydacyjny. Analiza ekspresji genów markerów chondrogennych (*COL1A1, COL6A1, HIF1A, COMP, RUNX2 i POU5F1*) oraz testy mechaniczne wykazały stosowność zastosowania wielościennych nanorurek węglowych w takich konstruktach.

Abstract

Cartilage tissue injuries are prevalent disorders that are characterized by poor regeneration. The available treatment methods offer insufficient recovery by means of partial reconstruction, easing the pain or drastic intervention with prosthesis replacement that affects the patients' quality of life. One of the most promising methods in biomedical engineering is 3D bioprinting which aims at recreation of the whole structure of the organ along with the cells that provide proper metabolic function. The main struggle of this technique in the field of cartilage tissue is obtaining the proper robustness that could bear the forces in the joints. Carbon nanotubes are one of the nanomaterials which have excellent mechanical properties and can serve as a reinforcement of the bioprinted structure. In this dissertation, the broad analysis regarding the use of multi-walled carbon nanotubes in this context is presented.

The study of the impact of multi-walled carbon nanotubes on cell viability revealed that this material interferes with the majority of the routinely used biological assays. The concentration of 0,0625 mg/ml was determined as the highest that can be reliably used with the absorbance-, fluorescence-, and luminescence-based assays. Furthermore, the optimal amount of carbon nanotubes based on the *in vitro* viability, apoptosis, and oxidative stress was used in 3D bioprinting of scaffolds. Gene expression analysis of chondrogenic markers (*COL1A1*, *COL6A1*, *HIF1A*, *COMP*, *RUNX2*, and *POU5F1*) and mechanical testing showed the feasibility of multi-walled carbon nanotubes usage in such constructs.

Aim of the dissertation

The aim of the dissertation is to investigate the feasibility of multiwalled carbon nanotubes (MWCNTs) usage in the context of cartilage tissue engineering. MWCNTs are nanomaterials with exceptional mechanical properties. Therefore, using the broad experimental panel, the impact of MWCNTs on the cells in 2D culture, as well as on the cell condition and mechanical properties in 3D bioprinted constructs, was assessed.

Introduction

To gain an in-depth knowledge about the state-of-the-art in utilization of carbon nanotubes in tissue engineering a thorough literature research was conducted. The gathered knowledge was collected and published in a review article **'Utilization of Carbon Nanotubes in Manufacturing of 3D Cartilage and Bone Scaffolds**[1]**'**. I was responsible for the concept of the paper, literature collection, writing the original draft and preparation of figures. The article covers the topics of both cartilage and bone tissue, but since the dissertation is mainly focused on cartilage tissue, only this part is further highlighted. The article begins with a description of the complexity of cartilage tissue regarding its microarchitecture and cellular composition. In essence, it is a type of connective tissue, composed of the extracellular matrix (ECM), produced by the small number of residual cells. ECM is a mixture of structural proteins – mainly collagens, that give the tissue its tensile strength, and non-fibrous molecules such as hyaluronic acid and glycosaminoglycans (GAGs) responsible for the elasticity. Altogether, cartilage is often viewed as a relatively simple structure; however, within its small volume, it presents compartmentalization with distinct functionalities and cell types. Articular cartilage, which covers the surface of the bones is divided into 4 different zones (Fig.1). They differ in the amount and types of cells. Therefore, the ECM composition and collagen orientation vary
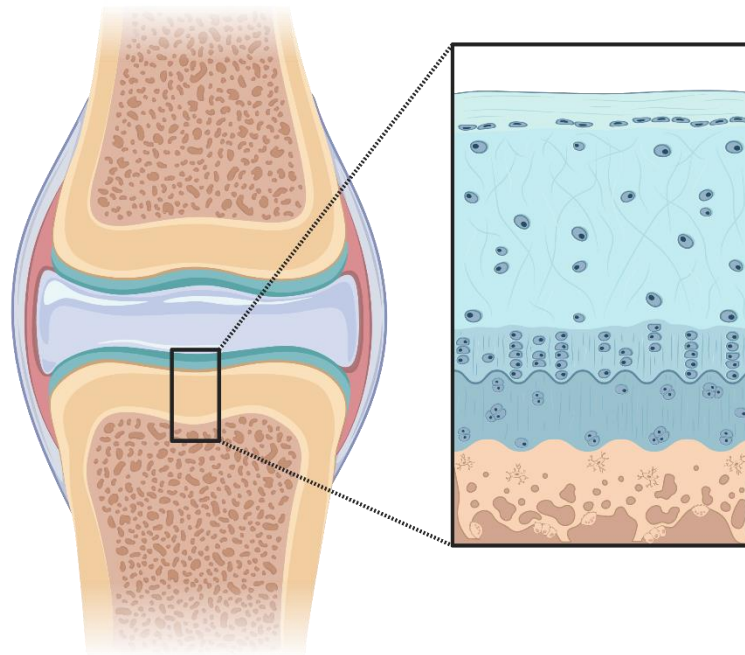

Fig. 1: Schematic cross-sectional representation of articular cartilage 4-layered structure. Figure created with Biorender.com

between them – this is the crucial aspect, responsible for the load-bearing capabilities of the whole structure[2]. Meniscus – a fibrocartilaginous structure in the knee, consists of 3 main zones – red-red, red-white, and white-white. The names come from the difference in vascularization – the red-red zone has relatively good blood flow, and the white-white zone is barely vascularized[3]. Given that the main function of cartilage tissue is to bear heavy loads during the movement, it is prone to injuries. Poor vascularization, which limits the cells, nutrients, and growth factors influx, is the main cause of poor recovery if damage occurs[4]. To date, there are no treatment methods, that provide a long-term, satisfactory recovery concerning the patient's quality of life[5,6]. To name a few, there are symptomatic treatments with the use of hyaluronic acid injections, experimental injections with platelet-rich plasma (PRP) or other growth factors, and stem cell combinations that aim at augmenting the self-regeneration, or radical interventions such as implants or endoprosthetic replacement[7]. One of the very promising technologies, that combines all of the abovementioned approaches is 3D bioprinting[8]. The technique is based on the precise extrusion of bioink, composed of structural components and live cells, that can be also stimulated with biological molecules such as growth factors. It gives a possibility to recreate the whole microenvironment of the native tissue, with the use of the patient's cells, and thus serve as a new organ for a direct replacement. One of the limitations that, to date, prevent the translation of 3D bioprinting to the clinic is the robustness of prepared constructs. The main challenge in the development of bioink for cartilage reconstruction is to provide sufficient mechanical properties while maintaining printability and cell survival. Since the hydrogel components, commonly used as a base for bioink are inherently brittle, there is a need for their physical reinforcement[9]. There are two main approaches, the addition of a robust ingredient such as fibers or plastics, or chemical modification, such as methacrylation[10,11].

Carbon nanotubes (CNTs) are the material, that possesses one of the best mechanical, both tensile and elastic, properties with values as high as 50 GPa and Young's modulus as high as 1 TPa, respectively. CNTs are graphene sheets rolled up in the form of cylinders. Based on the number of layers, we can distinguish two main types: single-walled carbon nanotubes (SWCNTs) or multi-walled carbon nanotubes (MWCNTs) SWCNTs have limited possible diameters of 0.5–2 nm, while MWCNTs may have diameters of 10–150 μm, depending on the number of concentric tubes forming the structure. Their length is mostly within the range of 0.5 to 30 μm, with a high aspect ratio, and a very wide range of possible dimensions, making them attractive for the fabrication of assembled nanoarchitectures [12,13]. Due to their sizes, as well as the graphene structure with inner cavities, they can adsorb or internalize many compounds, such

as metal ions, inorganic salts, and most importantly - in the context of biological application – organic molecules such proteins, nucleic acids, growth factors. It was also established that when in a proper arrangement, i.e. 'CNT forest' which is a tightly and perpendicularly grown layer of MWCNTs, they can promote cell adhesion and proliferation for such cells like chondrocytes[14]. One very important aspect, regarding the usage of MWCNTs in bioengineering is their toxicity. Scientific literature covered the topic, mostly with *in vitro*, and with few *in vivo* experiments, but with conflicting results and no scientific consensus. In the analysis of such studies, a few important aspects must be considered: (1) the dosages of CNTs used; often the amount of material per cell is much higher than what can be achieved in the environment, (2) CNT agglomeration, that has a vital influence on toxicity, (3) CNT sizes; usage of thin SWCNTs is often causing cell death because they can act as a 'needle' and break down the cell membrane, (4) whether the CNTs are constrained; it was shown that free-flowing CNTs could exhibit toxicity, whereas the same amount of CNTs embedded in 3D scaffolds can have the opposite effect.

Altogether, the abovementioned features indicate that MWCNTs resemble the native ECM in their role of mechanical support, adhesion, and biomolecule interactions, rendering them a great material for usage in 3D scaffolds. Hence, their impact on 3D bioprinted constructs was investigated in this dissertation.

The dissertation covers two main scientific achievements: 1) the evaluation of the assays used to determine the impact of multi-walled carbon nanotubes on cells; 2) the influence of multi-walled carbon nanotubes on cell metabolism and mechanical properties of 3D bioprinted scaffolds.

Research

Evaluation of the assays used to determine the impact of multi-walled carbon nanotubes on cells

The first experiments performed in the course of my dissertation were the preparation of biocompatible MWCNTs. After synthesis they are hydrophobic, hence there is a need to change their surface to render them water-soluble. For this purpose, an oxidation reaction in the mixture of concentrated sulfuric and nitric acid was carried out, which introduces carboxylic and carbonyl groups to the carbons of the graphene sheet. As prepared MWCNTs were then characterized using scanning electron microscopy (SEM) with energy-dispersive X-ray spectroscopy (EDS) and Fourier-transform infrared spectroscopy (FT-IR), to confirm their size,
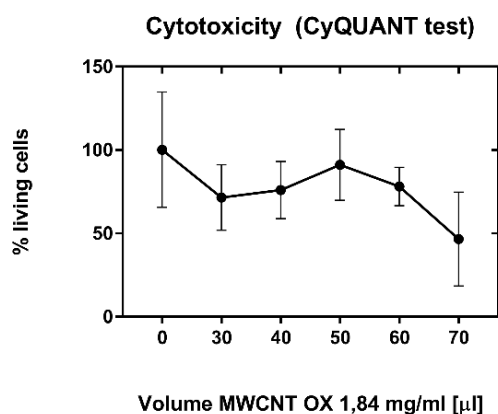
Cytotoxicity (CyQUANT test)

Fig. 2: Discrepancies in the replicates of absorbance-based tests. Data unpublished.

purity, and surface functionalization efficiency. Subsequently, the determination of the most optimal concentrations of MWCNTs in terms of cell viability or oxidative stress was performed on the NHAC-kn (Normal Human Articular Chondrocytes) cell line. There are many routinely used and well-established in the literature viability assays such as formazan crystal-based (MTT, MTS, XTT, WST-1), lactate dehydrogenase (LDH), Ki67, and BrdU measurements. They differ in the mechanism of how the signal is detected – it is usually absorbance (for the formazan crystal-based assays) or fluorescence. In the course of my research, I started to use MTT assay to determine the impact of oxidized, hydrophilic MWCNTs on the chondrocyte's viability. There were high discrepancies between various concentrations and technical replicates observed (Fig.2, data unpublished). During the literature research, I found out that there are reports of carbon nanotubes interfering with these assays. Wörle-Knirsch et al. observed a strong cytotoxic effect of SWCNTs in MTT assay on A549 cells[15]. It couldn't be confirmed by other assays—WST-1, LDH assay, mitochondrial membrane potential, and

Annexin V measured by flow cytometry. The false positive result was due to the physical absorption of insoluble formazan crystals at the surface of SWCNTs. Casey et al. has confirmed spectroscopically the SWCNTs' interference with a few routinely used viability assays based on absorption and fluorescence. (Fig. 3)[15,16,17]. Therefore, I decided to try luminescent-based assays in my work, as there were no reports in the literature on the possible interference.
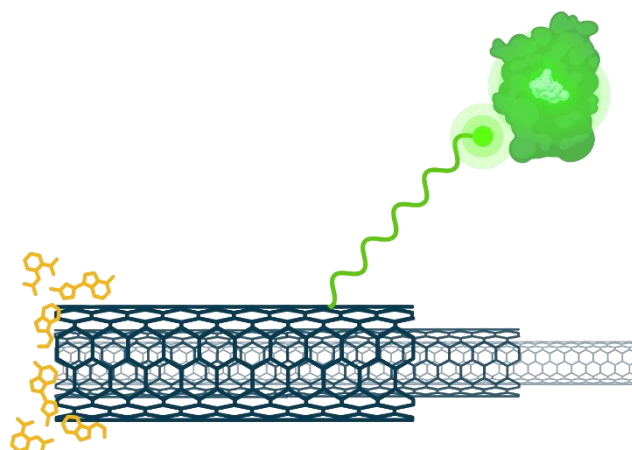

Fig. 3: Mechanisms of MWCNTs interference with biological assays. Yellow – precipitation and adsorption of molecules on the Surface of MWCNTs. Green – absorption of light emited (fluorescent and luminescent). Figure created with Biorender.com

The original research paper, **Carbon Nanotubes Interference with Luminescence-Based Assays**[18]**,** investigates the feasibility of luminescence-based assays in the presence of MWCNTs. First, two assays, measuring viability and reactive oxygen species generation, were performed on the NHAC-kn cell line with various concentrations of MWCNTs. Subsequently, to establish the reliability of the measurements, a similar experiment without cells, but with a known amount of substrate detected in the assay (adenosine triphosphate - ATP for the viability assay, and hydrogen peroxide – H_2O_2 for the ROS assay) was carried out. It was observed that with the increase of MWCNT concentration, the signal was diminished in the samples, where the same, known amount of substrate was tested. It is a direct indication, that concurs with the findings presented in the previous paragraph on the absorbance- and fluorescence-based assays, that MWCNTs interfere with the measurement. It was determined, that the highest concentration, not interfering with the measurement is 0.0625 mg/ml of MWCNTs. The findings were also confirmed with spectroscopic analysis. The absorbance spectrum overlaps partially with the luminescence spectra measured on the spectrofluorimeter. Based on this data, the almost linear trend of decreasing maximum luminescence intensities with increasing concentrations of MWCNTs was established.

Taking into account previously published discrepancies in absorbance and fluorescence-based assays [15,16], this research corroborates that many of the already published papers may contain false results. For example, Ursini et al. performed cytotoxicity analysis of oxidized MWCNTs with WST-1 assay on A549 and BEAS-2B cells[19]. The obtained results showed a similar pattern of a severe decrease in viability after incubation with increasing MWCNT-COOH. To evaluate the credibility of these results, a control with the known amount of hydrophilic formazan crystal formed in the WST-1 assay should be incubated with respective MWCNT-COOH concentrations. In my view, such controls should be included in all papers that use absorbance, fluorescence, or luminescence-based assays. Lack thereof should call into question the results. Such scrutiny, in the long term, may settle the field of carbon nanotubes toxicity, and lead to a more reliable consensus on this matter.

I was responsible for the design of the study, MWCNTs functionalization, handling of cell culture, cell viability measurements in 2D cultures, luminescence measurements of various MWCNTs solutions without cells, preparation of samples for SEM, FT-IR, absorbance measurements. Eventually, I curated the data, prepared figures for the respective analyses and wrote the original draft of the paper.

Influence of multi-walled carbon nanotubes on cell metabolism and mechanical properties of 3D-bioprinted scaffolds.

The original paper titled **Hyaluronic acid and multiwalled carbon nanotubes as bioink additives for cartilage tissue engineering**[20], presents a broad study of the influence of MWCNTs and hyaluronic acid on both 2D cell cultures and 3D bioprinted scaffolds. Firstly, the optimal concentrations of additives were determined in 2D cell cultures with two cell lines: Normal Articular Chondrocytes (NHAC-kn) and Adipose-Derived, Human Mesenchymal Stem Cells (hMSC-AT). The cell lines were chosen to compare the impact of MWCNTs on the native cells of the cartilage tissue (chondrocytes) to mesenchymal stem cells, that can differentiate into chondrocytes *in situ*. hMSC-AT are the main focus of my research since they are easily obtainable from the patient's fat tissue and can be further used to produce a personalized cartilage scaffold. This is possible due to the fact, that MSC cells have the potential to differentiate into a few types of cells, where chondrocytes, osteoblasts, and adipocytes are the most notable ones [21]. In fact, the ability to differentiate into these cell types is the crucial factor that defines the MSCs, along with the presence (CD73, CD90, CD105) and absence of particular surface markers (CD34, CD45)[22]. For the cells to be differentiated, a particular set of

conditions needs to be met. These always include stimulation with distinct compounds; for the chondrocytes, the essential ones are: dexamethasone, transforming growth factor-beta1 (TGF-beta1) and ascorbate, insulin, transferin, sodium pyruvate[23]. Such differentiation can be done in 2D cultures, with the use of commercially available media. However, for the proper stimulation and maintenance of cells phenotype, additional conditions are needed – in terms of chondrocytes, it is the spatial growth of cells. This can be achieved by culturing the cells in spheroids, in addition to embedding them in a 3D scaffold through bioprinting[24]. Bioprinting has also the advantage of applying pressure to the cells, a process called mechanotransduction, which is shown to activate various signaling pathways, such as TGF-beta1, that promote chondrogenic differentiation. It mimics the natural conditions, where cells present in cartilage are constantly subjected to pressure[25].
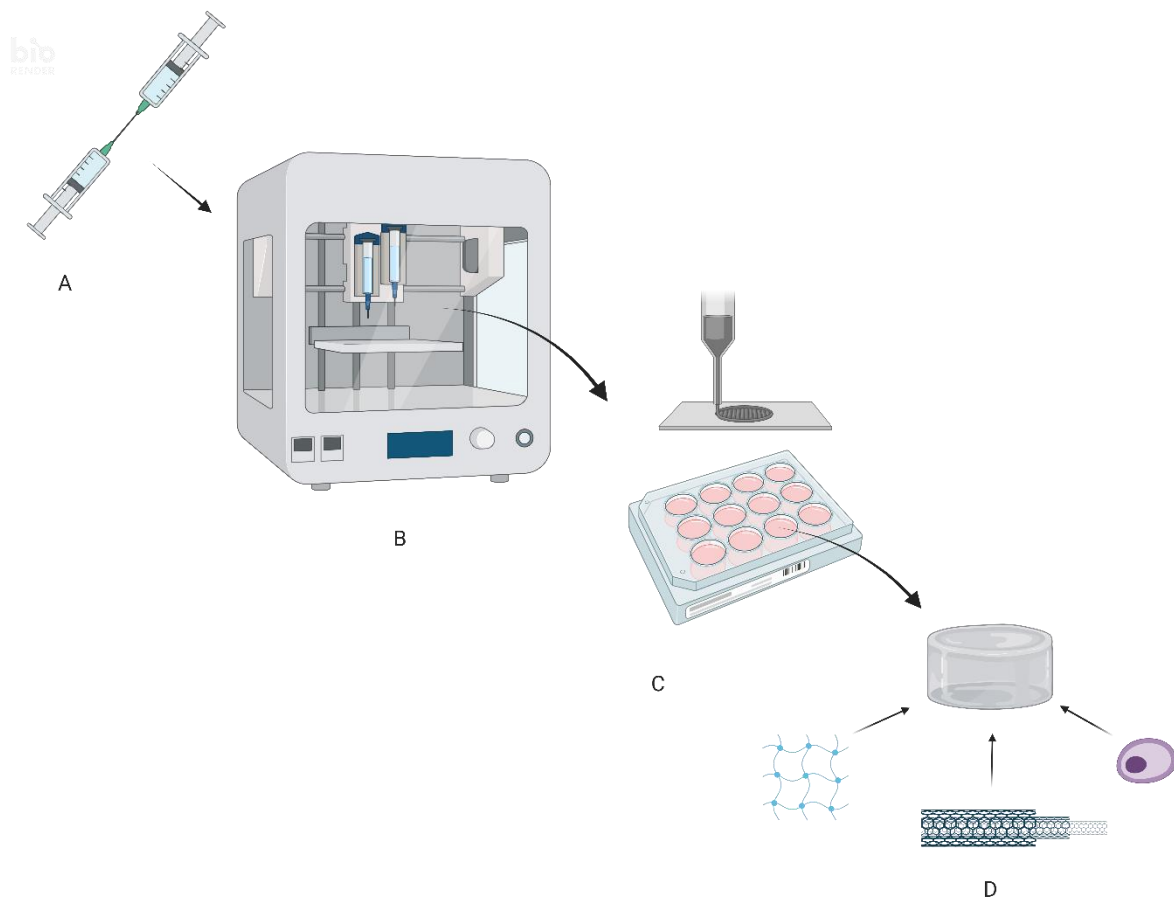

Fig 4: : Workflow of 3D-bioprinting. A – mixing of bioink ingredients with two syringes; B – syringe with mixed bioink is put into the bioprinter; C – extrusion bioprinting of scaffolds directly in the wells of a cell culture plate.; D – In each of the wells, there is a scaffold, composed of hydrogel base, MWCNTs, and cells. Figure created with Biorender.com

In my study, the influence of MWCNTs, the bioprinting process, and 3D growth in the scaffold was tested on the hMSC-AT cells. Firstly, the proper concentrations of MWCNTs,

which may have a positive impact on cell proliferation were determined in 2D cultures. In agreement with the previous study, the concentrations of MWCNTs above 0.0625 mg/ml resulted in measurement interference Therefore, it was decided to use the concentration of 0.0625 mg/ml for further studies, as the cells showed better viability compared to the lower concentrations. As a double check, measurement of caspases 3 and 7 was also performed, to compare whether the amount of dead cells is similar to the viability results. The base bioink was developed in our laboratory and is composed of 0.75% alginate, 4% gelatin, and 1.4% nanocrystalline cellulose fibers (CNCC), dissolved in 4.6% (w/v) d-mannitol, and additionally supplemented with MWCNTs[26]. To provide a good insight into the changes in cells over time, the bioprinted constructs were cultured for 28 days, and biological analyses were conducted at three time points (Fig. 4). Cells were cultured in a standard growth medium and the commercially available chondrogenic differentiation medium, for a reference to gene expression experiment. The viability was assessed with the LIVE/DEAD™ Viability/Cytotoxicity Kit. It is used to discriminate between live and dead cells by simultaneously staining them with green-fluorescent and red-fluorescent dye, respectively. The technique was chosen, because it allows for staining the cells in a 3D environment, and they can be observed with a confocal microscope. Most importantly, as it is a qualitative, not quantitative assay it is not prone to MWCNT interference with the fluorescent signal. It was determined that the addition of MWCNTs has a positive impact on cell viability over time, contrary to the scaffolds without MWCNTs, and to the behavior often reported in scientific literature. This may be attributed to the similarity to collagen fibers, which apart from having a structural role, also act as an embedding site for cells and have an impact on cellular signaling. In cartilage tissue, chondrocytes are attached to the ECM constituents (mainly fibronectin and collagens) through the integrin family of proteins. These proteins regulate cell proliferation, survival, differentiation, and matrix remodeling[27].

Additionally, a broad gene expression analysis was performed, with a panel of ECM and chondrogenic markers *COL1A1, COL6A1, COL10A1, HIF1A, COMP, RUNX2,* and *POU5F1*. It showed significant changes in gene expression with the overall loss of transcriptional activity, which indicates the embedded cells exhibit, at least partial, chondrogenic expression patterns. The most notable gene expression behavior, that is similar to the expression in cells cultured in a full differentiation medium is the high levels of *POU5F1, RUNX2,* and *COL6A1. POU5F1 (Oct-4)* is highly expressed in cells that undergo chondrogenic differentiation [28]. *RUNX2* is an essential transcription factor for chondrocyte maturation and

osteoblast differentiation and has been considered to be required for vascular invasion into the cartilage [29]. *COL6A1* expression is upregulated in the early events of chondrocyte differentiation[30], and it further stimulates chondrocyte proliferation [31]. This pattern shows that hMSCs may undergo differentiation in the chondrogenic lineage through the mechanotransduction exerted by the bioprinting process, the simple composition of the scaffold, and the spatial distribution of cells with the aid of MWCNTs. Higher expression of other tested genes such as *COL1A1* may indicate the influence of particular growth factors present in the full differentiation medium. Apart from biological analyses, the mechanical testing of 3D bioprinted scaffolds was performed by measuring the shear stress and viscosity. Despite the introduction of MWCNTs, the mechanical parameters did not increase substantially however, the bioink retained good printability as the shear stress and viscosity as a function of shear rate were not affected significantly.

I was responsible for the design of the study, and experiment supervision. I carried out the MWCNTs functionalization and determined the cell viability, reactive oxygen species, and apoptosis levels in 2D cell cultures stimulated with MWCNTs, 2-phospho-l-ascorbic acid, and hyaluronic acid. Eventually, I wrote the original draft and prepared Supplementary Fig. 1.

Additional research

During my PhD studies, I have also worked on other research concerning nanomaterials. In the work **Potential use of superparamagnetic iron oxide nanoparticles for *in vitro* and *in vivo* bioimaging of human myoblasts**[32] I was responsible for the synthesis, characterization, and testing of superparamagnetic iron oxide nanoparticles (SPIONs) that would be then used as an imaging agent to monitor the cells injected into the muscle. Iron oxide, as a bulk material possesses strong ferromagnetic properties, which means that it has significant magnetic permeability and coercivity and can retain its magnetization without the external magnetic field. However, when the material is sufficiently small, in the form of nanoparticles in the range of up to several dozen nanometers, it starts to exhibit superparamagnetic behavior and forms a ferrofluid. In ferrofluid, the SPIONs in the absence of an external magnetic field have an average magnetization of zero, but when the external magnetic field is applied, the nanoparticles become magnetized[33]. This behavior renders SPIONs usable in magnetic resonance imaging (MRI)[34]. In the work, I synthesized SPIONs with a very narrow size distribution (monodisperse) with an average diameter of 13 nm and subsequently functionalized them with *meso*-dimercaptosuccinic acid (DMSA), which rendered them hydrophilic and biocompatible. Modified nanoparticles were applied to the myoblast cells. They were internalized by the cells in high amounts, and a series of *in vitro* assays determined the optimal concentration of nanoparticles, not impacting the cell viability, oxidative stress, differentiation potential, angiogenesis ability, and iron metabolism. The cells labeled with SPIONs were then injected into the soleus muscle and left heart ventricle of mice, and could be detected by MRI after 5 and 12 days, with decreasing signal (Fig. 5) .
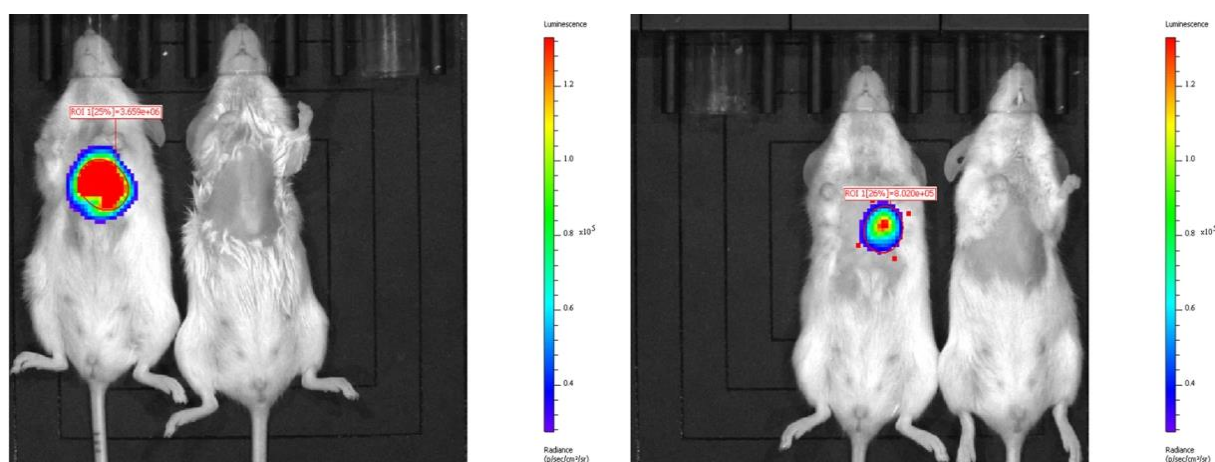

Fig. 5: Magnetic resonance imaging of cells labeled with modified SPIONs after 5 (left) and 12 (right) days.

This was caused mainly by the migration of implanted cells, and in partially by the efflux of SPIONs from the cells. The study showed that this is a feasible approach to monitor the implanted cells in muscle. Eventually, the implantation of various cells such as myoblasts and mesenchymal stem cells are to be used as a treatment of the post-infarcted heart.

In another original paper **Photodegradation of Biohazardous Dye Brilliant Blue R Using Organometallic Silver Nanoparticles Synthesized through a Green Chemistry Method**[35], I used silver nanoparticles as a catalyst for the degradation of an environmentally
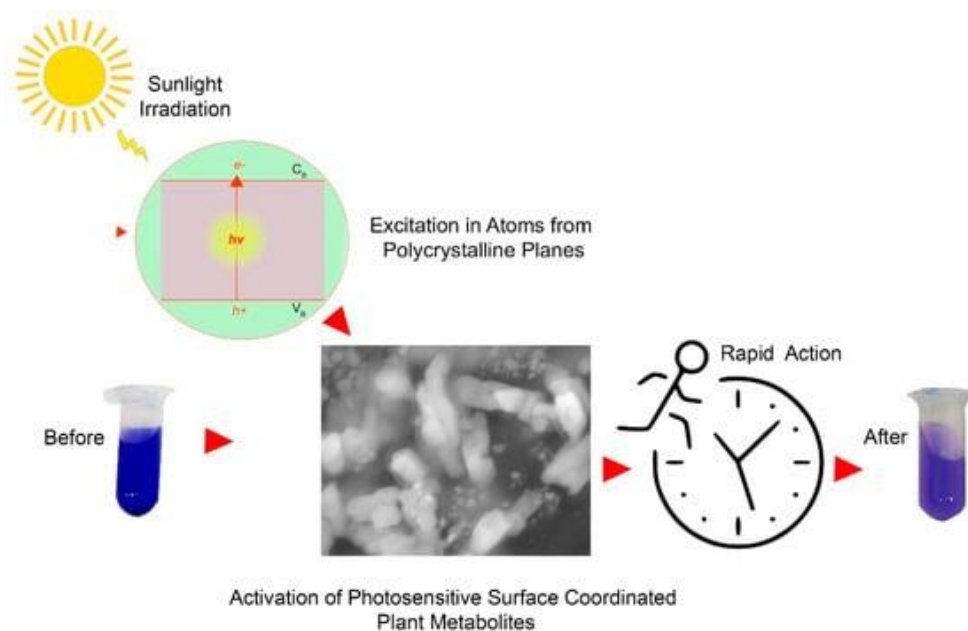

Fig. 6: A graphical summary of the green synthesis of silver nanoparticles and catalytic reduction of hazardous dye.

hazardous chemical. The work relies on the popular methods of green chemistry, which utilize as many natural and sustainable substrates as possible. The nanoparticles were synthesized from the simple silver salt by using only a plant extract from a commonly occurring herb *Cichorium intybus*. Another advantage of such extract is that it contains compounds that act both as a reducing agent for the silver salt and subsequently cap the surface of the particles, preventing aggregation. A few extracts were tested, but only one yielded monodisperse and stable nanoparticle suspension. These nanoparticles were then used to degrade the Brilliant Blue R dye, which is a problematic waste in many laboratories since it is difficult to eliminate from the wastewater. The solution of this chemical was subjected to catalytic degradation employing as-prepared silver nanoparticles and sunlight energy, and a degradation rate of above 50%, monitored by UV-Vis spectroscopy, was achieved within only 15 minutes. The work proved the feasibility of using green chemistry as a very cheap, sustainable method to neutralize hazardous substances in-house and in wastewater treatment facilities (Fig. 7).

My PhD studies were also affected by the SARS-CoV-2 pandemic period when my regular research had to be stalled. During this time, I was involved in a project where we produced SARS-CoV-2 antigens with molecular biology and genetic engineering techniques and used them for the development of serologic tests to detect the antibodies against SARS-CoV-2. It was used as a tool to monitor the serologic response after the vaccination. The work, **A cohort study reveals different dynamics of SARS-CoV-2-specific antibody formation after Comirnaty and Vaxzevria vaccination**[36], presents the results of this research. First, we used the expression plasmid pCAGGS with the coding sequence of the spike protein (S-protein) and its receptor binding domain (RBD) of the SARS-CoV-2 virus, to produce these proteins in an
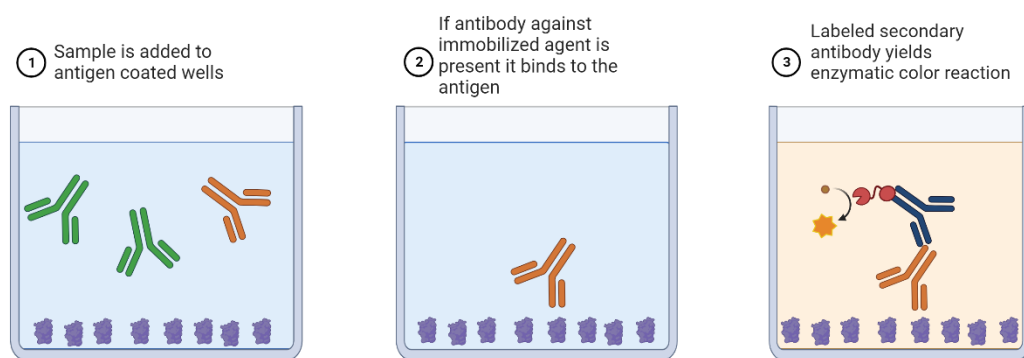

Fig. 7*: Workflow of ELISA reaction. 1 – the patient's serum is added to the antigen coated well; 2 – if in the serum there are antibodies specific to the antigen, it binds strongly to it. The rest of the unbound sample is washed away; 3 – secondary antibody labeled with enzyme is added, that is specific to the species and class of antibodies that we want to detect (in this case human). If there is primary antibody already present, it binds to it. The rest of the unbound antibody is washed away, and the substrate for the enzyme is added. It yields colourful signal, proportional to the bound antibodies. Created with Biorender.com

Expi293F® cell line (ThermoFisher Scientific). The coding sequences of the proteins were modified with the excretion peptide and His-Tag, which allows for the excretion of the proteins from cells to the medium and its purification with affinity chromatography using Ni-NTA resin, respectively. The purified antigens were then used for the enzyme-linked immunosorbent assay (ELISA) reaction, which detects quantitatively the amount of specific antibodies with very high sensitivity in the human serum (Fig. 7). The sera were obtained from the vaccinated patients, from the volunteers from Adam Mickiewicz University in Poznań, and the Provincial Specialist Hospital for Lung Diseases and Tuberculosis in Wolica, before and after the first and second vaccination. Eventually, a total of 1395 patients met the exclusion and inclusion criteria for the study and these samples were subjected to the ELISA testing and subsequent statistical analysis with the General Additive Model. With such a big cohort it was possible to generate a model of antibody production dynamics after each vaccination, with regard to the gender, age, time after vaccination, and type of vaccination (Comirnaty and Vaxzevria). Our model showed,

contradictory to many hypotheses, that there is no difference between the serological response between males and females. On the other hand, we revealed that the dynamics of antibody production are different in patients below 30, between 30 and 60, and above 60 years of age after the first dose, but do not differ after the booster dose. Additionally, the immune responses were different concerning the type of vaccination, however after 3 months after booster shot, it was not statistically different.

Summary and future perspective

Altogether, the dissertation presents an in-depth study of MWCNTs usage in tissue engineering. Starting from the 2D *in vitro* analyses, the finding that nanomaterials can interfere with many well-established techniques due to their inherent, distinct properties (such as π-π stacking, and strong optical absorption), is a reminder that data analysis should always be performed with critical assessment. The toxicity of nanomaterials in the context of medical use is the subject of ongoing scientific debate, often supported by conflicting data. This dichotomy may be attributed to the improper evaluation of already published work, that may show erroneous results, which was already discussed in detail in my work **Utilization of Carbon Nanotubes in Manufacturing of 3D Cartilage and Bone Scaffolds.** The methodology presented in the dissertation shows an interdisciplinary and broad range of techniques used in the evaluation of the influence of MWCNTs on cellular fate in 3D bioprinted scaffolds. The research fits very well with the concept of tissue engineering, which is broadly developed in today's science. Tissue engineering offers the possibility of creating personalized, biomimetic, cell-laden organs that may be an upgrade to the artificial implants, made from plastics or metallic materials, and serve as a direct replacement for the injured organ. The most promising technology to achieve it is 3D bioprinting. It offers layer-by-layer deposition of bioink, that may be organized similarly to the complex and non-homogenous architecture of the native organ. The main advantage is the usage of the patient's cells, vastly decreasing the risk of graft rejection and immune response. In terms of fibrocartilage engineering, which is the main topic of this dissertation, many approaches were applied to develop more robust scaffolds. Firstly, since the main structure of these tissues is the bearing of the heavy loads, various biomaterials were tested. There are various sacrificial materials, such as agarose, gelatin, and alginate. Their main advantages are biocompatibility, good printability, and they can be degraded over time, and replaced by the material excreted by the residual cells. The main drawback is, however, their brittleness. To overcome this issue, many reinforcing materials were tested: (1) thermoplastic polymers - polycaprolactone (PCL)[37] or poly(lactic acid) (PLA)[38]; (2) natural polymers – chitosan[39]; (3) nanofibers – nanocellulose[40], carbon nanotubes[41], (4) decellularized extracellular matrix from different species[42]. The latter one is also used in my further research, where the dECM is isolated from the porcine menisci using cryo-milling and supercritical CO_2 extraction. This is a very promising material since it's inherent similarity to the native human tissue. Another modification for the reinforcement of the scaffold is a chemical modification of

bioink components, to introduce crosslinking, e. g. methacrylation. This is also part of my research, where the abovementioned dECM is methacrylated, and thus can be crosslinked with the UV light (405 nm) after the bioprinting process, yielding stiffer material.

To fully understand the complexity of the tissue, powerful high throughput techniques such as RNA-seq and mass spectrometry, for the determination of the spatial tissue proteome and transcriptome distribution can be applied. By doing so, it is possible to determine the major biological components and cell lines within the subcompartments of the tissue, hence applying this knowledge to print the scaffolds with more precision, reflecting the natural ultrastructure.

In my additional research, broader application of nanotechnology was presented. Different types of nanoparticles were used as a green chemistry catalyst in organic reaction, and as a safe MRI contrast. Moreover, development of immunological test using molecular biology and genetic engineering techniques was shown, and its' subsequent usage in a large cohort study for the population analysis of immune response after vaccination against SARS-CoV-2 virus.

To conclude, the data presented in the dissertation shows that the addition of MWCNTs to 3D bioprinted scaffolds shows that they positively affects cellular proliferation and can stimulate the differentiation of mesenchymal stem cells to the chondrogenic lineage. The research is a solid base for further studies, that can elaborate on more advanced gene and protein expression analyses and a further modification of scaffolds with other additives (such as (dECM) that increase mechanical robustness, and biological molecules such as growth factors. Once sufficient parameters are achieved, such 3D-bioprinted constructs are to be evaluated *in vivo* in animal models to further prove their utility in the usage in tissue engineering as a replacement of damaged cartilage.

References

1. Szymański, T. *et al.* Utilization of carbon nanotubes in manufacturing of 3D cartilage and bone scaffolds. *Materials* vol. 13 1–25 (2020) doi:10.3390/ma13184039.

2. Gentili, C. & Cancedda, R. Cartilage and Bone Extracellular Matrix. *Curr. Pharm. Des.* **15**, 1334–1348 (2009) doi:10.2174/138161209787846739.

3. Bąkowski, P. *et al.* Meniscus repair via collagen matrix wrapping and bone marrow injection: clinical and biomolecular study. *Int. Orthop.* **47**, 2409–2417 (2023) doi:10.1007/s00264-023-05711-2.

4. Khan, I. M., Gilbert, S. J., Singhrao, S. K., Duance, V. C. & Archer, C. W. Cartilage integration: Evaluation of the reasons for failure of integration during cartilage repair. A review. *Eur. Cells Mater.* **16**, 26–39 (2008) doi:10.22203/eCM.v016a04.

5. Eyre, D. R., Weis, M. A. & Wu, J. J. Articular cartilage collagen: An irreplaceable framework? *European Cells and Materials* vol. 12 57–63 (2006) doi:10.22203/eCM.v012a07.

6. Mundi, R. *et al.* Cartilage Restoration of the Knee: A Systematic Review and Meta-analysis of Level 1 Studies. *Am. J. Sports Med.* **44**, 1888–1895 (2015) doi:10.1177/0363546515589167.

7. Medvedeva, E. V. *et al.* Repair of damaged articular cartilage: Current approaches and future directions. *Int. J. Mol. Sci.* **19**, (2018) doi:10.3390/ijms19082366.

8. Semba, J. A., Mieloch, A. A. & Rybka, J. D. Introduction to the state-of-the-art 3D bioprinting methods, design, and applications in orthopedics. *Bioprinting* **18**, (2020) doi:10.1016/j.bprint.2019.e00070.

9. Li, J., Chen, M., Fan, X. & Zhou, H. Recent advances in bioprinting techniques : approaches , applications and future prospects. *J. Transl. Med.* 1–15 (2016) doi:10.1186/s12967-016-1028-0.

10. Singh, D. *3D Bioprinting for Scaffold Fabrication. 3D Bioprinting for Reconstructive Surgery: Techniques and Applications* (Elsevier Ltd., 2018). doi:10.1016/B978-0-08-101103-4.00007-7.

11. Poldervaart, M. T. *et al.* 3D bioprinting of methacrylated hyaluronic acid (MeHA) hydrogel with intrinsic osteogenicity. *PLoS One* **12**, e0177628 (2017).

12. Nakanishi, W. *et al.* Bioactive nanocarbon assemblies: Nanoarchitectonics and applications. *Nano Today* **9**, 378–394 (2014) doi:10.1016/j.nantod.2014.05.002.

13. Tutak, W., Chhowalla, M. & Sesti, F. The chemical and physical characteristics of single-walled carbon nanotube film impact on osteoblastic cell response. *Nanotechnology* **21**, (2010) doi:10.1088/0957-4484/21/31/315102.

14. Pem, B. *et al.* Biocompatibility assessment of up-and down-converting nanoparticles: Implications of interferences with in vitro assays. *Methods Appl. Fluoresc.* **7**, (2019) doi:10.1088/2050-6120/aae9c8.

15. Wörle-Knirsch, J. M., Pulskamp, K. & Krug, H. F. Oops they did it again! Carbon nanotubes hoax scientists in viability assays. *Nano Lett.* **6**, 1261–1268 (2006) doi:10.1021/nl060177c.

16. Casey, A. *et al.* Spectroscopic analysis confirms the interactions between single walled carbon nanotubes and various dyes commonly used to assess cytotoxicity. *Carbon N. Y.* **45**, 1425–1432 (2007) doi:10.1016/J.CARBON.2007.03.033.

17. Scarcello, E., Lambremont, A., Vanbever, R., Jacques, P. J. & Lison, D. Mind your assays: Misleading cytotoxicity with the WST-1 assay in the presence of manganese. *PLoS One* **15**, 1–

14 (2020) doi:10.1371/journal.pone.0231634.

18. Szymański, T., Kempa, M., Giersig, M. & Rybka, J. D. Carbon nanotubes interference with luminescence-based assays. *Materials (Basel).* **13**, 1–14 (2020) doi:10.3390/MA13194270.

19. Ursini, C. L. *et al.* Differences in Cytotoxic, Genotoxic, and Inflammatory Response of Bronchial and Alveolar Human Lung Epithelial Cells to Pristine and COOH-Functionalized Multiwalled Carbon Nanotubes. *Biomed Res. Int.* **2014**, (2014) doi:10.1155/2014/359506.

20. Szymański, T. *et al.* Hyaluronic acid and multiwalled carbon nanotubes as bioink additives for cartilage tissue engineering. *Sci. Rep.* **13**, 1–10 (2023) doi:10.1038/s41598-023-27901-z.

21. Rastegar, F. *et al.* Mesenchymal stem cells: Molecular characteristics and clinical applications. *World J. Stem Cells* **2**, 67–80 (2010) doi:10.4252/wjsc.v2.i4.67.

22. Mushahary, D., Spittler, A., Kasper, C., Weber, V. & Charwat, V. Isolation, cultivation, and characterization of human mesenchymal stem cells. *Cytom. Part A J. Int. Soc. Anal. Cytol.* **93**, 19–31 (2018) doi:10.1002/cyto.a.23242.

23. Solchaga, L. A., Penick, K. J. & Welter, J. F. Chondrogenic Differentiation of Bone Marrow-Derived Mesenchymal Stem Cells: Tips and Tricks BT - Mesenchymal Stem Cell Assays and Applications. in (eds. Vemuri, M., Chase, L. G. & Rao, M. S.) 253–278 (Humana Press, Totowa, NJ, 2011).doi:10.1007/978-1-60761-999-4_20.

24. Yen, B. L. *et al.* Three-Dimensional Spheroid Culture of Human Mesenchymal Stem Cells: Offering Therapeutic Advantages and In Vitro Glimpses of the In Vivo State. *Stem Cells Transl. Med.* **12**, 235–244 (2023) doi:10.1093/stcltm/szad011.

25. Raman, N., Imran, S. A. M., Ahmad Amin Noordin, K. B., Zaman, W. S. W. K. & Nordin, F. Mechanotransduction in Mesenchymal Stem Cells (MSCs) Differentiation: A Review. *Int. J. Mol. Sci.* **23**, (2022) doi:10.3390/ijms23094580.

26. Semba, J. A., Mieloch, A. A., Tomaszewska, E., Cywoniuk, P. & Rybka, J. D. Formulation and evaluation of a bioink composed of alginate, gelatin, and nanocellulose for meniscal tissue engineering. *Int. J. Bioprinting* **9**, (2023) doi:10.18063/ijb.v9i1.621.

27. Loeser, R. F. Integrins and chondrocyte-matrix interactions in articular cartilage. *Matrix Biol.* **39**, 11–16 (2014) doi:10.1016/j.matbio.2014.08.007.

28. Li, L. *et al.* Oct4 facilitates chondrogenic differentiation of mesenchymal stem cells by mediating CIP2A expression. *Cell Tissue Res.* **389**, 11–21 (2022) doi:10.1007/s00441-022-03619-8.

29. Qin, X. *et al.* Runx2 is essential for the transdifferentiation of chondrocytes into osteoblasts. *PLOS Genet.* **16**, e1009169 (2020).

30. Quarto, R., Dozin, B., Bonaldo, P., Cancedda, R. & Colombatti, A. Type VI collagen expression is upregulated in the early events of chondrocyte differentiation. *Development* **117**, 245–251 (1993) doi:10.1242/dev.117.1.245.

31. Smeriglio, P. *et al.* Collagen VI enhances cartilage tissue generation by stimulating chondrocyte proliferation. *Tissue Eng. Part A* **21**, 840–849 (2015) doi:10.1089/ten.TEA.2014.0375.

32. Wierzbinski, K. R. *et al.* Potential use of superparamagnetic iron oxide nanoparticles for in vitro and in vivo bioimaging of human myoblasts. *Sci. Rep.* **8**, 1–17 (2018) doi:10.1038/s41598-018-22018-0.

33. Mahmoudi, M., Sant, S., Wang, B., Laurent, S. & Sen, T. Superparamagnetic iron oxide nanoparticles (SPIONs): Development , surface modi fi cation and applications in chemotherapy. *Adv. Drug Deliv. Rev.* **63**, 24–46 (2011) doi:10.1016/j.addr.2010.05.006.

34.   Mao, X., Xu, J. & Cui, H. Functional nanoparticles for magnetic resonance imaging. *Wiley Interdiscip. Rev. Nanomedicine Nanobiotechnology* (2016) doi:10.1002/wnan.1400 doi:10.1002/wnan.1400.

35.   Sidorowicz, A., Szymański, T. & Rybka, J. D. Photodegradation of biohazardous dye brilliant blue r using organometallic silver nanoparticles synthesized through a green chemistry method. *Biology (Basel).* **10**, (2021) doi:10.3390/biology10080784.

36.   Augustyniak, A. *et al.* A cohort study reveals different dynamics of SARS-CoV-2-specific antibody formation after Comirnaty and Vaxzevria vaccination. *Vaccine* **41**, 5037–5044 (2023) doi:10.1016/j.vaccine.2023.06.008.

37.   Mousavi Nejad, Z., Zamanian, A., Saeidifar, M., Vanaei, H. R. & Salar Amoli, M. 3D Bioprinting of Polycaprolactone-Based Scaffolds for Pulp-Dentin Regeneration: Investigation of Physicochemical and Biological Behavior. *Polymers (Basel).* **13**, (2021) doi:10.3390/polym13244442.

38.   Joseph, T. M. *et al.* 3D printing of polylactic acid: recent advances and opportunities. *Int. J. Adv. Manuf. Technol.* **125**, 1015–1035 (2023) doi:10.1007/s00170-022-10795-y.

39.   Agarwal, T. *et al.* Chitosan and its derivatives in 3D/4D (bio) printing for tissue engineering and drug delivery applications. *Int. J. Biol. Macromol.* **246**, 125669 (2023) doi:https://doi.org/10.1016/j.ijbiomac.2023.125669.

40.   Lin, L. *et al.* Application of 3D-bioprinted nanocellulose and cellulose derivative-based bio-inks in bone and cartilage tissue engineering. *Int. J. bioprinting* **9**, 637 (2023) doi:10.18063/ijb.v9i1.637.

41.   Moura, D., Pereira, R. F. & Gonçalves, I. C. Recent advances on bioprinting of hydrogels containing carbon materials. *Mater. Today Chem.* **23**, 100617 (2022) doi:https://doi.org/10.1016/j.mtchem.2021.100617.

42.   Liu, H. *et al.* Recent Advances in Decellularized Matrix-Derived Materials for Bioink and 3D Bioprinting. *Gels* vol. 9 at https://doi.org/10.3390/gels9030195 (2023) doi:10.3390/gels9030195.

Publications and author statements

Utilization of Carbon Nanotubes in Manufacturing of 3D Cartilage and Bone Scaffolds

Tomasz Szymański [1,2], Adam Aron Mieloch [1,2], Magdalena Richter [1,3], Tomasz Trzeciak [3], Ewa Florek [4], Jakub Dalibor Rybka [1,*] and Michael Giersig [1,5]

[1] Center for Advanced Technology, Adam Mickiewicz University in Poznań, Uniwersytetu Poznańskiego 10 Street, 61-614 Poznan, Poland; tszymanski@amu.edu.pl (T.S.); amieloch@amu.edu.pl (A.A.M.); mrichter@ump.edu.pl (M.R.); giersig@amu.edu.pl (M.G.)

[2] Faculty of Chemistry, Adam Mickiewicz University in Poznań, Uniwersytetu Poznańskiego 8 Street, 61-614 Poznan, Poland

[3] Department of Orthopedics and Traumatology, Poznan University of Medical Sciences, 28 czerwca 1956r. Street No. 135/147, 61-545 Poznan, Poland; tomasz.trzeciak@ump.edu.pl

[4] Laboratory of Environmental Research, Department of Toxicology, Poznan University of Medical Sciences, Dojazd 30, 60-631 Poznan, Poland; eflorek@ump.edu.pl

[5] Department of Physics, Institute of Experimental Physics, Freie Universität, Arnimallee 14, 14195 Berlin, Germany

*   Correspondence: jrybka@amu.edu.pl; Tel.: +48-61-829-1875

Abstract: Cartilage and bone injuries are prevalent ailments, affecting the quality of life of injured patients. Current methods of treatment are often imperfect and pose the risk of complications in the long term. Therefore, tissue engineering is a rapidly developing branch of science, which aims at discovering effective ways of replacing or repairing damaged tissues with the use of scaffolds. However, both cartilage and bone owe their exceptional mechanical properties to their complex ultrastructure, which is very difficult to reproduce artificially. To address this issue, nanotechnology was employed. One of the most promising nanomaterials in this respect is carbon nanotubes, due to their exceptional physico-chemical properties, which are similar to collagens—the main component of the extracellular matrix of these tissues. This review covers the important aspects of 3D scaffold development and sums up the existing research tackling the challenges of scaffold design. Moreover, carbon nanotubes-reinforced bone and cartilage scaffolds manufactured using the 3D bioprinting technique will be discussed as a novel tool that could facilitate the achievement of more biomimetic structures.

Keywords: tissue engineering; biomaterials; cartilage; bone; carbon nanotubes; scaffolds; bioprinting

1. Introduction

In recent years, due to a high incidence of cartilage and bone injuries and subsequent risk of complications in the future (e.g., osteoarthritis) [1–3], a significant extension of research regarding biocompatible scaffolds engineering and vast progress in biomaterials science, in general, has been observed. Through the combination of tissue engineering techniques and advancements in the synthesis of novel materials, the understanding of biomaterials has reached a new dimension. The robust development is especially seen in the field of motor organ repair concerning bone and cartilage tissue injuries in particular. Biomaterials are viewed as the next generation treatment for these conditions, resolving many of the inherent limitations of currently existing treatment procedures [4].

Articular cartilage (AC) covers the surface of the bone in diarthrodial (synovial) joints and provides a low-friction interface for a sliding motion and also propagates the applied forces to the subchondral

bone [5]. The most important drawback of an AC lesion is the fact that it does not heal spontaneously, mainly due to the small number of residual cells, limited vascular supply, and lymphatic drainage. Once injured, the lesion tends to progress and starts to deteriorate a patient's quality of life, being the 11th most frequent cause of disability globally [6–8].

Bones of the skeleton provide mechanical support for joints, tendons, and ligaments; they protect vital organs from damage and they have an important metabolic role as calcium and phosphate reservoirs. Unlike cartilage, bone tissue undergoes constant renewal, and in comparison to cartilage, when the bone tissue is injured, it possesses a better regeneration potential. However, many injuries such as severe fractures exceed the natural healing ability and require surgical intervention and the use of artificial bone fillers. The lack of or unsuitable interactions between materials and tissues remains a major concern, often resulting in the lack of implant integration and its failure. In terms of synthetic materials, the most prevalent problems are early failures due to interference in the healing process, caused by issues such as bleeding, infection, and the need for debridement and antibiotic treatment. In terms of porous scaffolds, often occurring problems are a lack of cell influx to the material, cell death, or the wrong nature of the created tissue due to improper microenvironment in the scaffold [9,10]. To improve the convalescence time and the quality of life, novel biomaterials are being developed [11,12].

An ideal scaffold must possess some essential characteristics to be able to mimic the natural tissue environment and therefore to serve its role in the regenerative process. It has to be made of biocompatible, bioresorbable, and biodegradable materials which can provide proper mechanical support necessary to resist mechanical stress applied to the cartilage and bone tissue. Moreover, the ultrastructure should be arranged to deliver porosity to assure interaction between the cells themselves and between the cells and the extracellular matrix (ECM). This, in turn, should promote an adequate reorganization of injured tissue by the residual cells, while the scaffolding is resorbed by the body [13,14].

Biomolecular recognition of scaffolds by cells is essential for proper cell metabolism. This recognition can be accomplished through the usage of proper materials or their modifications. One example of this approach is the use of bioactive molecules such as chains of native extracellular matrix proteins, carbon nanotubes (CNTs), or polymers, which can interact specifically with cellular receptors [15,16]. There are a plethora of other nanomaterials investigated for tissue engineering of bone or cartilage, e.g., nanofibrillated cellulose [17], electrospun nanofibers [18], mesoporous silica [19], nanohydroxyapatite [20], and bioactive glass-ceramic nanoparticles [21], which are beyond the scope of this review.

One of the most popular materials used in scaffolds for tissue engineering which was discovered in 1991 and which has revolutionized the research field is carbon nanotubes (CNTs). They are considered to be excellent reinforcements for bio-related applications due to their remarkable structural, mechanical, electrical, and thermal properties [22,23]. Their implantation in bone or cartilage may not only improve the mechanical properties of damaged bone tissue but can also stimulate bone regeneration, as nanofibers can mimic the extracellular matrix (ECM) and allow the differentiation of human mesenchymal stem cells (hMSCs) toward osteoblasts [24,25].

The limitation with most of the conventional scaffold fabrication techniques is that they do not allow the user to create precise pores, modify its distribution, or achieve high interconnectivity with detailed geometry. 3D bioprinting has been developed to overcome most of these limitations withholding the progress of tissue engineering. This technique allows the fabrication of versatile scaffolds with complex geometry that are capable of the homogenous distribution of cells and mimic the local extracellular matrix (ECM). Besides, cells can be directly blended with bioink and therefore reside in the scaffold without the need for infiltration. There are two main approaches regarding bioprinting:

(1) the biomimicry approach, where the prepared structure is aimed to be as close to the native one as possible;

(2)   the self-assembly approach, which attempts to replicate environmental and structural elements, which then promotes the assembly of a proper structure.

Therefore, bioprinting may be a revolutionary tool, able to produce complex, discrete, self-organizing units for tissue development.

This review will cover the intrinsic complexity of the native articular and bone tissue ultrastructure to depict the challenges in the bioengineering of biomimetic materials. Moreover, it will focus on structural and biological aspects of three-dimensional scaffolds reinforced with CNTs which are being researched as bone and articular cartilage replacements. Furthermore, the mechanisms by which CNTs enhance such structures will be outlined, as well as research utilizing 3D bioprinting as a useful tool to overcome the limitations of conventional scaffold fabrication techniques.

2. Articular Cartilage Structure and Function

Cartilage tissue is a specialized connective tissue consisting of a relatively small number of cells that are embedded in a well-organized, extracellular matrix (ECM) [26]. ECM is produced by the residual cells, the chondrocytes, and is composed of two main parts—fibrous, self-assembled elements; mainly collagens and elastin. The non-collagenous part is composed of glycoproteins and glycosamicoglycans (GAGs), such as hyaluronan and proteoglycans [27]. The dry mass is composed mainly (up to 60%) of collagens, whose unique structure defines the properties and function of the proteins themselves, as well as of the whole cartilage tissue.

Collagens are a family of fibrous proteins, whose basic structural unit consists of three polypeptide chains (α-chains), which can self-assemble to a closely intertwined, so-called superhelix. This twist is achieved because of the periodic occurrence of glycine, proline, and hydroxyproline amino acids which allow for tight adjacency and hydrogen bonding, respectively. These building blocks, called tropocollagens, are approximately 300 nm long, they are 1.5 nm in diameter, and they possess terminal amino acid chains. They are further arranged into long fibers, and they are stabilized due to their particular amino acid composition [28]. The fibrils' dimensions depend mainly on the type of collagen. In the articular cartilage, collagen type II is predominant, accounting for up to 90% of the total collagen content in an adult, and it forms fibrils with a diameter of up to 80 nm [29]. Type II fibers are enhanced by other collagen types (IX and XI) [30]. Collagen type IX is attached near the surface of the collagen type II fibrils in an antiparallel fashion. It has a distinct globular protein on one end, which serves a role in interactions between various other ECM molecules. On the other hand, collagen type XI crosslinks between collagen type II fibrils and enhances the integrity of the whole structure [30,31]. Together, due to the inherent complex structure, enforced with a plethora of bonds, this multi-collagen structure forms an intricate mesh responsible for the tensile strength of the whole tissue.

Other important molecules of the articular cartilage are proteoglycans, aggrecans in particular. They are located between the collagen fibrils and act as tissue organizers, regulating collagen fibrillogenesis, and interacting with growth factors and cytokines. They serve as a backbone for GAGs attachment, which is in part responsible for the proteoglycans' function. One of the most important GAGs is hyaluronic acid, which has exceptional water-attracting properties, forming a gel environment throughout the tissue. Hence, these non-collagenous molecules account for the elastic properties of the cartilage.

This complex, multimolecular network is further organized into four distinct subcompartments, as described originally by Bennighoff [32] and confirmed by Weiss et al. [33] (Figure 1). In the first, superficial zone, which is ~200 μm thick, the fibrils are thin (32 ± 5 nm) and tend to run primarily parallel to the plane of the articular surface. Moreover, they are much more closely packed, compared to deeper layers. A greater range of fibril diameters is seen in the transitional zone II (30–60 nm) and radial zone III (40–80 nm), which are 1.5–3.5 mm thick altogether. The organization in zone II appears more random. The cells present in this zone are bigger and they produce the essential ECM components to maintain the proper microenvironment of the whole tissue. However, they represent only up to 5% of the total cartilage volume. Nevertheless, they manage to serve their role in maintaining the

functionality of healthy tissue but struggle to repair it when more extensive damage occurs. In the radial zone of some joint regions, a preferred orientation of fibril bundles is vertical to the surface. The arcade-like micro-architecture of collagen responsible for this zonal appearance is anchored into the IV calcified zone.
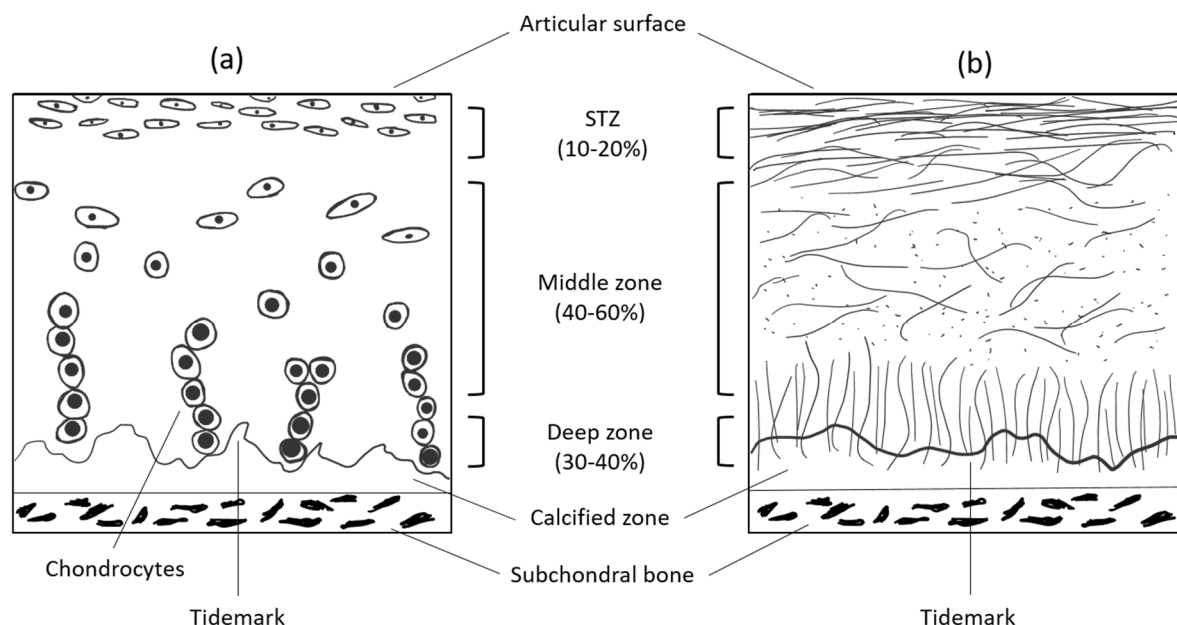

Figure 1. Schematic, cross-sectional diagram of healthy articular cartilage: (**a**) cellular organization in the zones of articular cartilage; (**b**) collagen fiber architecture.

Altogether, all of the components of articular cartilage create a very dynamic microenvironment of molecules secreted by the residual cells. This intricate ultrastructure of such a thin tissue yields exceptional tension resistance and elasticity at the same time. In general, the tensile modulus, hence the load the healthy cartilage tissue can bear, varies from 5 to 25 MPa, depending on the location, depth, and orientation within the joint surface. These well-known tensile properties demonstrate the inhomogeneous and anisotropic nature of articular cartilage [34].

3. Bone Structure and Function

Bone is a type of tissue with a similar composition to cartilage. Cartilage is a precursor of bone in most parts of the skeleton, gradually transforming into definitive bones during puberty and early adolescence by a process called endochondral ossification. Similar to its predecessor, the bone ECM is composed mainly of collagen fibrils; however, here type I prevails, comprising up to 90% of the organic part. This type of collagen fiber tends to have more covalent cross-linking sites than type II and therefore forms a more dense, less water-soluble, and rigid matrix, with a diameter of approximately 100 nm. This fibrous matrix is a site where the mineralization of bone occurs. Only a few types of inorganic crystals are deposited at the surface of and between fibrils, forming the basic building block of bone—mineralized collagen fibril. The vast majority of this inorganic matter consists of a plate or spindle-shaped crystals of hydroxyapatite $Ca_{10}(PO_4)_6(OH)_2$. They are very thin (2–7 nm), but polydisperse in length (15–200 nm) and width (10–80 nm). In total, they comprise about 60–70% of the bone's dry mass, the organic part making up the remainder [35]. The water content is also much lower, between 10–20% of the total mass. In conclusion, the mineralization of the ECM, the prevalence of collagen type I, and lower hydration enhance the bone's mechanical rigidity, which complements the tensile strength and elasticity provided by collagenous ECM.

The exceptional properties of bone tissue result from the intrinsic hierarchical structure in which its components are arranged (Figure 2). At the macroscopic level, two main anatomical types of bone tissue can be distinguished.

The first type is the dense cortical bone which forms the outer layers of bone and especially the shafts of the long bones. It is composed of osteons (Haversian systems), which are concentric lamellae of mineralized tissue and cells surrounding the central canal, where blood vessels are situated. These concentric fibrils are further organized into two distinct patterns: (a) dense, ordered, aligned, and parallel to the long axis of the bone, (b) disordered with randomly distributed fibers and visible porosity. These two patterns occur alternately, which yields a plywood-like structure with disordered material filling the spaces between aligned bundles of ordered fibrils [36–38].
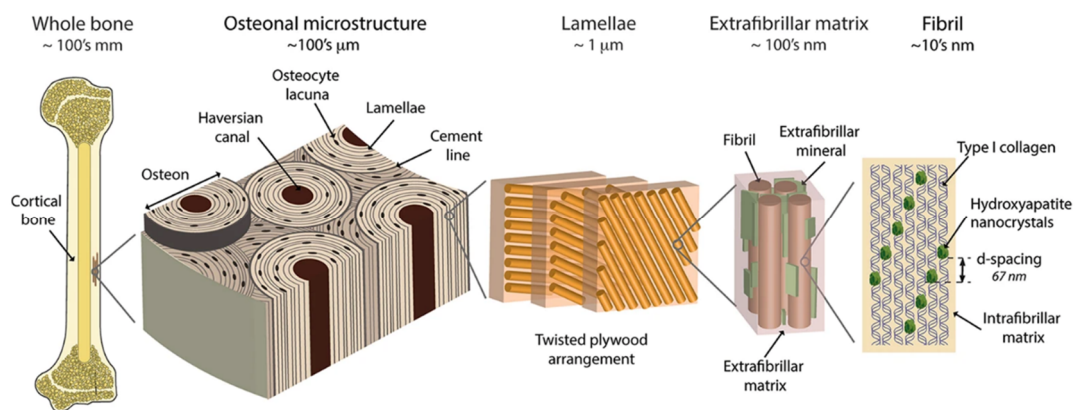

Figure 2. The hierarchical organization of cortical bone. On the first level, there are fibrils (~10 nm thick), composed of parallel aligned type I collagen strands, mineralized with evenly distributed hydroxyapatite crystals. Those fibrils are arranged in bundles, surrounded by extrafibrillar mineralized platelets. The bundles, arranged in the plywood-like structure form lamellae, where adjacent lamellae may have different orientation of bundles. The layers of concentrically aligned lamellae surrounding the Haversian canal forms a basic structural unit of bone—osteon (170–250 μm in diameter). Taken from [39].

The second anatomical type of human bone is called trabecular or cancellous bone (also known as spongy bone). It presents a lower density and a larger surface area than cortical bone. Trabecular bone fills the center of long bones, flat bones, and vertebrae, and consists of an interconnecting meshwork of bony trabeculae, separated by spaces filled with bone marrow [36].

The synthesis of all bone constituents, as well as maintenance of proper bone function, is carried out with residual cells of marrow origin, therefore cancellous bone has osteoinductive and osteogenic properties. Apart from the above-mentioned molecules, bone tissue is also made of non-fibrous proteins, which play an important role in many aspects of bone function and metabolism. The most notable of these proteins are osteopontin and osteocalcin, which act as a molecular Ca^{2+}-mediated adhesive at the interface between mineralized fibrils. They form a large mechanical network employing the so-called sacrificial bonds and hidden lengths, which dissipate energy during tensile stretching, greatly augmenting the tensile strength of the whole bone [40]. These unique arrangements and features give the trabecular bone Young's elastic modulus from 2 to 12 MPa and for the cortical bone as high as 12 to 18 GPa [41]. The latter is the major load-bearing part of the bone and therefore, in terms of successful bone-defect repair, the replacement material should have physical characteristics (e.g., Young's modulus) as similar as possible to the native bone.

4. Current Existing and Experimental Therapies for Articular Cartilage and Bone Injuries

Nowadays, there are no established procedures for the repair of damaged cartilage. Treatments of choice for articular cartilage lesions include those which temporarily alleviate symptoms—systemic drugs like corticosteroids and painkillers, as well as injections of hyaluronan into the joint, which acts

as a lubricant. Another procedure is a radical one called endoprosthesis replacement. There are three experimental approaches aiming at the permanent reconstruction of damaged tissue. The first one is an arthroscopic intervention combined with surgical access to the bone marrow, such as abrasion chondroplasty or micro fracturing, resulting in an influx of blood containing stem cells to the lumen of the joint, with the idea of the reconstruction of a new AC. The major limitation of this procedure is the complete removal of residual cartilage, even the healthy part, and subsequent immobilization of the joint for several weeks, with the recommendation of weight-bearing restriction, which affects the patient's quality of life. The result of the healing is fibrocartilaginous tissue, which has diminished resiliency, less stiffness, and poor wear characteristics, compared to the native hyaline cartilage, resulting in poor clinical outcomes [42,43]. The second one is the surgical transplantation of the osteochondral autograft from a different region of the body or an allograft of AC from a cadaver. The major concern in this technique is patient morbidity and the outcomes vary greatly depending on age (poor in patients > 40 years), sex, and size of the lesion [44]. The last approach is autologous chondrocyte implantation (ACI). The original two-step procedure involved cartilage harvesting from a non-weight bearing surface of the affected joint, followed by cell isolation, in vitro culture, and implantation of re-differentiated cells under the periosteal cover into the defect site (1st generation ACI). Since then, the procedure has evolved and collagen membranes instead of the periosteal flap were used (2nd generation ACI), later being used as a scaffold for cultured allografted chondrocytes or autologous mesenchymal stem cells (3rd generation ACI). However, these procedures are still in the experimental or clinical trials phase with mixed outcomes and they often involve long-lasting (weeks to months) recovery after surgery. [45,46]. Since long-term follow-up studies are not yet available, it is hard to draw any conclusions as to the future application of these techniques [47,48].

In terms of bone repair, the gold standard of treatment is autologous bone grafting, despite its inherent limited availability and patient morbidity, and metal alloys bone replacement, most often titanium alloys [49]. Titanium alloys are commonly used, because of their good biocompatibility, high strength, resistance to fatigue, and high ductility, which allows for cortical bone replacement. They are used as a replacement for jaw, heel, hip, cranial bones, and spinal fusion surgeries. However, they possess two major disadvantages. Firstly, there is evidence for the release of integrating metals into the surrounding microenvironment. Its biocompatibility is provided mainly by chemical inertness due to the nanometer-thin TiO_2 layer, which on the other hand is responsible for the lack of integration with the bone (osseointegration) often leading to implant failure. Secondly, much higher elastic modulus (120 GPa) can cause stress shielding and subsequent reduction in bone density due to the low load applied to the healthy part of the bone. One of the most successful approaches in reducing Young's modulus of titanium implants is by preparation of porous structures with the use of 3D printing. Such structures achieved elastic modulus values as low as 36 GPa. Porous architecture could also lead to better integration if the cells would be able to infiltrate the implant (osteoconductivity). However, it requires further modification of the inert surface. Several post-treatment techniques are employed to address this issue, such as plasma spraying, ion implementation, oxidation, and alkali-heat treatment. The titanium implants are good examples of scaffolding evolution, however, their inherent limitation is difficult post-processing, possible toxicity due to metal release, and that they are not resorbable [50–52]. Other experimental techniques employed are composites of natural bone components, e.g., hydroxyapatite (HA) and tricalcium phosphate (TCP) ceramics or cement, with polymers (e.g., collagens, poly-lactic acid, gelatin). There is also work on using growth factors to stimulate natural bone repair processes. These composite materials combine advantages of different materials (metallic, ceramic, and polymeric materials); they allow controlled degradation with better biocompatibility and physical characteristics than the polymers alone, however, they have not yet matched the bone tissue demands in vivo [53]. Nevertheless, these procedures have their downsides with the need for surgical intervention and subsequent stable hardware fixation often being the case, because of insufficient mechanical properties of the graft, or the need to hold the graft in place.

5. Carbon Nanotubes

Carbon nanotubes (CNTs) are single- or multi-layered graphene sheets rolled up in the form of cylinders. The former is known as single-walled carbon nanotubes (SWCNTs), and the latter are multi-walled carbon nanotubes (MWCNTs). SWCNTs may have limited possible diameters of 0.5–2 nm. On the other hand, MWCNTs consist of multiple sheets within a tube and may have diameters of 10–150 μm, depending on the number of concentric tubes forming the structure. Their length is mostly within the range from 0.5 to 30 μm. They have a high aspect ratio, with a very wide range of possible dimensions, making them attractive for the fabrication of assembled nanoarchitectures [54,55].

5.1. Synthesis of CNTs

The main methods of CNT synthesis are the arc discharge method, laser ablation method, and chemical vapor deposition (CVD). These methods use an electrical breakdown of gas (arc discharge) or thermal energy to recombine the carbon precursor into carbon nanotubes. Arc discharge was the first method of obtaining CNTs, described by Ijima [56]. The major disadvantage of this method is that they are another carbon product and the catalyst (often metal such as Fe, Ni, Co) is present as an impurity. The laser ablation technique offers a higher yield of CNTs and a lower amount of metallic impurities because they tend to evaporate after laser treatment. Moreover, the diameter of the CNTs can be better controlled. However, it is not an economically viable method, due to the high cost of equipment [57]. The most common synthesis method is chemical vapor deposition (CVD), due to its lower cost, lower temperature and pressure used, and the highest yield of CNTs, in comparison to other methods. These moderate parameters offer the best control over the dimension of produced CNTs, however, they possess a relatively high amount of defects in the structure [58]. For the biological application of CNTs, the most important factor in addition to dimensionality is purity. Therefore CNTs used in biological experiments are most often synthesized by the CVD method [22,59].

5.2. CNT Biomimics ECM Constituents

CNTs' intrinsic graphene structure possesses inner cavities where various compounds can be internalized and/or adsorbed, such as metal ions [60], inorganic salts [61], and organic molecules [62]. This is important in terms of the scaffolding's utility because CNTs can interact with biomolecules—nucleic acids, proteins, growth factors, collagens, adhesion molecules, and other ECM constituents. It was also found that the CNTs' surface promotes cell adhesion [63,64]. Due to their characteristic structure, CNTs can be grown perpendicular to the plane of the surface, yielding an arrangement which can be termed the "CNT forest", where CNTs are densely packed, parallel to each other. Various cells including Chinese hamster ovary cells (CHO) and human chondrocytes were cultured on such a surface (Figure 3) [65]. It was found that cells were aligned along with the MWCNT bundles. Reduced clustering of cells was observed, as well as a higher proliferation rate. Moreover, 16% of the cells had an aspect ratio of 3:1 or higher. This result indicates that CNTs favor cell adhesion and can act as a platform for cell growth. Additionally, ECM is a natural scaffold, providing mechanical support for the tissue. CNTs, with their exceptional physical properties with tensile strength as high as 50 GPa, and Young's modulus as high as 1 TPa, are a good candidate as a component of robust scaffolds.
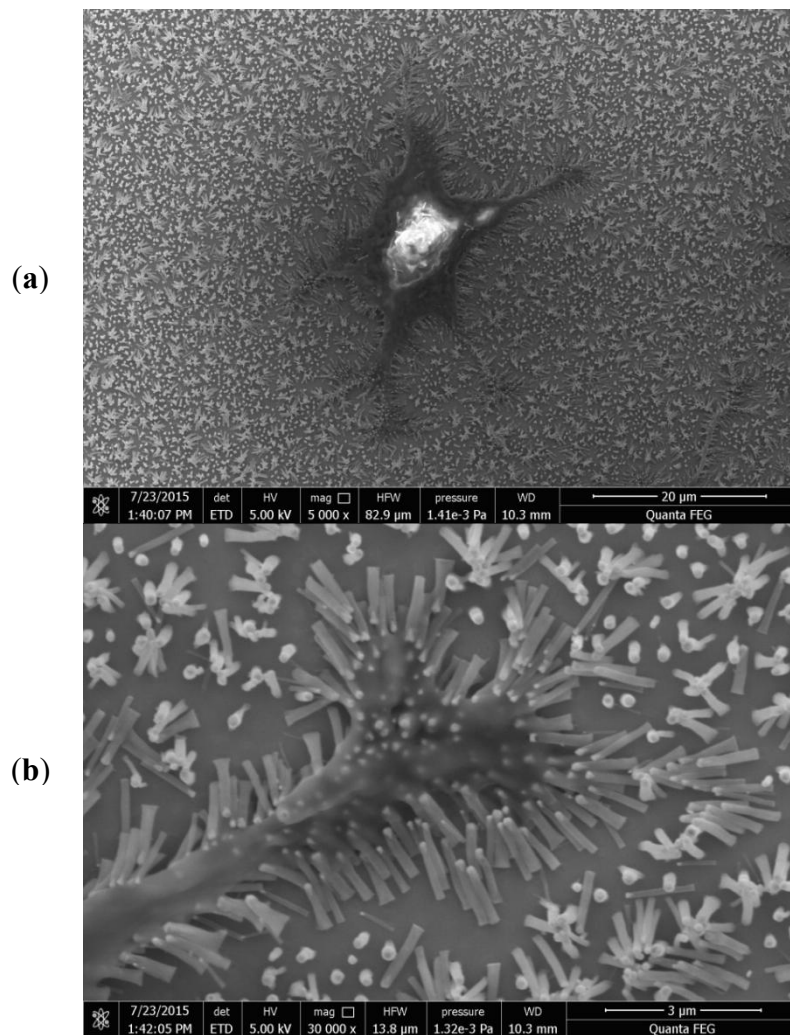
Figure 3. Chondrocyte was grown on perpendicularly aligned, chemical vapor deposition (CVD) synthesized multi-walled carbon nanotubes (MWCNTs), low magnification (**a**) and high magnification (**b**). Cytoplasmic extensions are visible. Note the cell adhesion to the scaffold. Phyllopodia bend the nanotubes to their purposes.

5.3. CNT Toxicity

One of the fundamental topics regarding the use of CNTs in bioengineering is their safety. The effects of CNTs on various cell types have been previously extensively reviewed [66–68]. They are mainly in vitro studies. On the other hand, in vivo animal studies have raised concerns, especially about pulmonary toxicity, due to their asbestos-like mechanism [69]. The summary of research regarding various features of CNTs, and its impact on toxicity is presented in Table 1. As it was noted by Castranova et al., it is important to take into consideration that many of these studies may be biased because of the following respective reasons: (1) the use of doses per cell that are much higher than those possible to achieve in the natural environment, (2) CNT agglomeration, and (3) adsorption of signals emitted by assay indicator dyes [70]. Therefore, care must be taken when analyzing in vitro results. Low doses of SWCNTs, which are more feasible to be achieved with daily exposure, such as 40 µg/mouse, aspirated by mice, exhibit low cytotoxicity. Conversely, a low dose of SWCNT exposure of lung fibroblasts increases the proliferation rate and collagen production [71]. Therefore, the rapid onset of an interstitial fibrotic response to pulmonary CNT exposure may be caused by direct interactions with CNTs (matrix effect), resulting in fibroblast activation [72]. Li et al. compared the effects of MWCNTs on lungs upon administration with intratracheal instillation and inhalation. They found an

inflammatory response and alveolar destruction after a single instillation of high dose MWCNTs and no inflammation with alveolar wall thickening after gradual inhalation of MWCNTs [73].

Consequently, many in vitro studies with CNTs have employed doses in the range of 10–100 µg/mL and have reported cytotoxicity. As it has been said, on a per-cell basis, such doses are orders of magnitude higher than those achieved in pulmonary exposure studies with rats or mice and may not be relevant to workplace exposure. National Institute of Occupational Safety and Health (NIOSH) researchers have determined the ratio between the CNT mass/surface area of cells, based on the lung's epithelial surface area in humans, rats, and mice. When such low doses are used in cellular experiments, the stimulation of lung fibroblast proliferation and collagen production rather than cytotoxicity was found, which mimics the fibrogenic effects of CNTs observed after pulmonary exposure. Such low doses also reveal CNT-induced cell transformation and aneuploidy instead of cell death [74].

Another crucial factor in CNTs' toxicity is their size. Equivocal results are published regarding toxicity and retention. For example, Takagi et al. reported the onset of mesothelioma after the intraperitoneal injection of long (28% >5 µm in length) MWCNTs [75], contrary to Muller et al., who reported no mesothelioma after the injection of 0.7 µm MWCNTs. Similarly, 81% of long MWCNTs (6 µm) were retained in the lungs after 60 days, in contrast to only 30% of short (0.7 µm) MWCNTs [76]. Similarly, Allegri et al. compared the influence of the MWCNTs' diameter and functionalization on macrophages' viability. With a diameter larger than 40 nm, no detrimental effects were observed, while mild cytotoxicity was found for diameters between 15 and 40 nm. However, when these MWCNTs were functionalized with either carboxyl or amine groups, the toxicity was mitigated. This phenomenon is attributed to the observed higher amount of serum proteins adsorbed on the surface of MWCNTs, which is called a protein corona. These proteins alter their surface chemistry, which eventually leads to the formation of larger aggregates, mitigating the biological effects on cells [77]. Sager et al. tested the influence of MWCNTs' carboxyl surface modification in C57BL/6 mice after lung instillation in comparison to unmodified MWCNTs. The results showed that functionalization significantly reduced inflammation and lung pathologies. Importantly, both MWCNT suspensions were prepared with surfactant (DPCC) and mouse albumin to promote dispersion, eliminating the possible aggregation factor. Thus, the surface modification, not dispersion status, was the primary driving force behind the differential activity of the MWCTs [78].

Mutlu et al. tested whether the aggregation of SWCNTs has an impact on toxicity. They instilled intratracheally, 40 mg of unpurified, aggregated, and highly dispersed SWCNTs in 1% Pluronic F 108NF to mice. The results showed that lung inflammation was induced by aggregated SWCNTs in phosphate buffer saline (PBS), while highly dispersed SWCNTs did not cause any inflammation or fibrosis [79].

Interestingly, increased reactive oxygen species (ROS) production by macrophages after exposure to CNTs was attributed to the CNTs' intracellular degradation. Elgrabli et al. reported two degradation mechanisms of MWCNTs with an outer diameter of 40–80 nm—a non-site specific thinning process of the walls and site-specific transversal drilling process on pre-existing defects of nanotubes. Both of these processes are mediated by the ROS produced by macrophages. Eventually, after 168 h of exposure, 51.1% of the MWCNTs' total surface was degraded [80].

Aldieri et al. examined the role of impurities left in CNTs which were used as catalysts in the process of synthesis. The tested MWCNTs were subjected to the additional step of purification to minimize iron remnants content. Only iron-rich MWCNTs exerted a cytotoxic effect, as well as oxidative stress on murine alveolar macrophages, which proves the detrimental role of such contaminants [81].

Tutak et al. compared osteoblast behavior on SWCNTs which were dissolved freely in the media to those which were firmly attached to the surface [82]. Interestingly, after 24 h free-flowing CNTs caused cell deaths; however, the resulting release of growth factors by dying cells stimulated the remaining ones to an enhanced secretion of ECM proteins. In contrast, neither cytotoxic effects nor enhanced ECM production was observed on the cells grown on the fixed SWCNTs. In another work, Tutak et al. compared the level of adhesion of MC3T3 cells on hydrophilic CNT films with different

surface roughness (60 and 100 nm) and determined that the 100 nm surface gives better adhesive properties [55].

Table 1. The table below summarizes the features of carbon nanotubes and their influence on cytotoxicity.

Aspect.	Condition	Result	116	Reference
Dose	40 μg of SWCNTs aspirated by mouse	Low toxicity	Dose probable to be encountered occupationally	[71]
Method of administration	Intratracheal instillation and inhalation	Alveolar destruction and inflammatory response upon instillation and no inflammatory cells and thickening of the alveolar wall upon inhalation	High doses of MWCNTs used	[73]
Length	5 um vs. 0.7 um MWCNTs injected peritoneally	Mesothelioma formation with long MWCNTs and no mesothelioma with short MWCNTs	-	[76]
Diameter	Macrophage viability upon exposure with <40 nm MWCNTs and 15–40 nm MWCNTs in diameter	No effects on viability with <40 nm MWCNTs and mild toxicity with 15-40 nm MWCNTs	-	[77]
Aggregation	Intratracheal instillation of aggregated and highly dispersed SWCNTs in 1% Pluronic F 108NF to mice	Lung inflammation was induced by aggregated SWCNTs in PBS, while highly dispersed SWCNTs do not cause any inflammation or fibrosis	Very high dose (40 mg) of SWCNTs was used	[79]
Purity	Cytotoxicity of MWCNTs with and without residual iron catalyst on murine alveolar macrophages	Toxic effects exerted only after treatment with unpurified MWCNTs	-	[81]
Surface functionalization	Unmodified and carboxyl modified MWCNTs instilled in C57BL/6 mouse lungs	Carboxyl functionalization reduces inflammation and lung pathologies	Dispersion status was not affecting the results, since both samples were well dispersed with surfactant	[78]
Method of detection	Toxicity of SWCNTs was tested on A549 cell line with Coomassie Blue, Alamar Blue[TM], Neutral Red, MTT and WST-1	Employment of different method yielded various results	-	[83]

The last essential aspect is the method used for cytotoxicity measurement. Casey et al. determined with the spectroscopic analysis that SWCNTs interact with various indicator dyes, such as Coomassie Blue, Alamar Blue[TM], Neutral Red, MTT, and WST-1. Consequently, the employment of different methods yielded various results [83]. Similarly, Wang et al. found discrepancies in the fluorescent LDH test, depending on the wavelength used for measurement, and proposed an algorithm for compensation to obtain more accurate results [84].

These findings lead to the conclusion that nanostructuring and carefully controlling the CNTs' sizes, doses, purity, and methods of administration are crucial in the determination of the CNTs' toxicity. It can be stated that CNTs, while embedded, do not inflict significant toxicity, and even if it can be observed, this may have a stimulating effect on cells and, eventually, have a positive impact on the tissue as a whole. Moreover, existing research demonstrates that cells can efficiently degrade residual CNTs within a range of sizes, which may diminish the concerns of the long-term toxicity caused by CNT retention in an organism. Finally, fixed CNTs have a positive effect on cell adhesion, proliferation, and cytoskeletal development, which presents CNTs as a possible enhancement in scaffold bioengineering.

6. Development of Bone and Cartilage Scaffolds

ECM plays an essential role in the tissue, as it provides an optimal environment for cell attachment, proliferation, and growth, as well as proper nutrients and cytokine flow. At the same time, it possesses sufficient mechanical strength to retain the shape and structure of the tissue and plays its role in the shock absorption properties. Both cartilage and bone tissue exhibit very complex and peculiar ultrastructure which is responsible for its function. So far, the biggest challenge and the Holy Grail in tissue engineering is to obtain such a structure, which is as close as possible to the natural one in terms of these attributes. Several aspects have to be addressed in fabricating such structures.

6.1. Biodegradability and Biocompatibility

The ideal material for a biomimetic scaffold has to be biocompatible, because it will house the cells and it will be implemented in the body, thus should not be toxic and elicit inflammatory responses. Secondly, the material has to be biodegradable (bioresorbable)—it should decompose over time, being exchanged by the tissue produced by the hosted cells. Therefore, synthetic and natural hydrogel-forming polymers turned out to be good candidates, because they possess all of those features [85]. PVA (polyvinyl alcohol) [86], PEG (polyethylene-glycol) [87], PLGA (polylactic-co-glycolic acid) [88], PLA (polylactic acid) [89], gelatin [90], alginate [91,92], collagen [93] and chitosan [94] have all been researched as a scaffold material for tissue engineering. These materials have the properties to support cell attachment and proliferation, especially osteocytes and chondrocytes [95]. They can be enhanced by supplementing the scaffold with particular proteins such as laminin to enhance adhesion [96]. Natural polymers such as collagen have the advantage that they can trigger specific cell signaling, such as to elicit osteogenesis [97]. They also can be degraded by the enzymes in our body, and the degradation rate can be modulated by either chemical modification, or altering the manufacturing process [98].

6.2. Mechanical Properties

As was described earlier, cartilage and bone serve a supportive function in the body, therefore scaffold replacing the tissue should have adequate mechanical properties such as Young's modulus. The hydrogels alone were too brittle to serve this function properly. To overcome this limitation, a lot of research has been conducted to incorporate reinforcing materials. One of the most researched reinforcing materials is PCL (poly-caprolactone). It is biocompatible, much tougher than the abovementioned polymers, and has a degradation time of two to three years. Therefore, PCL fibers are often used to prepare a composite material with hydrogel polymers. It is often electrospun or bioprinted in the form of a mesh, and eventually, the fibers are embedded in the polymer. Fibrous PCL can have an elastic modulus of 3.1 MPa, while a composite with various substances may augment its mechanical properties a few-fold [99]. Consequently, it enhances the mechanical properties of as-prepared composite materials, e.g., the composite of thick-fiber PCL (>88.5 μM), and GelMA had a stiffness of 16.1 MPa, which is similar to the native articular cartilage [100]. Another material used as a reinforcing material is cellulose nanofibers. They have a high surface area, broad chemical modification capacity, and similarity to collagen nanofibers. They have been used as a reinforcing material for alginate hydrogels for the cartilage scaffolds of human ear and sheep meniscus constructs [101]. Other research

was conducted presenting good biocompatibility, cell proliferation, and extracellular matrix formation, however, Young's modulus of as-prepared scaffolds are in the range of single to tens of kPa, which is not enough for articular cartilage and bone replacement [102,103]. CNTs, due to their mechanical and biological properties, are a perfect candidate to use as a reinforcing material, instead of plastic fibers like PCL and cellulose fibers [91,104,105].

6.3. Porosity

Another crucial aspect of a scaffold is the level of porosity and the size of the pores. This is important for the successful infiltration of cells, as well as diffusion of nutrients, gases, and metabolites into the deeper scaffold cavities. If they are too small, these processes are constrained. If too large, there is a limited surface area, which decreases the cell interactions and adhesion, both crucial phenomena for proper cellular function (Figure 4). On the other hand, if the material is too porous (>90%), it loses the mechanical sturdiness [13]. In terms of bone, it has been determined that the minimum pore size for bone growth is 75–100 μm with an optimal range of 100–135 μm [106]. However, it has also been reported that pores greater than 300 μm are essential for optimal vascularization [107]. Murphy and O'Brian experimented on collagen-glycosaminoglycan scaffolds with pore sizes of 96–151 μm and 85–325 μm. They found that within smaller pores, there was an initial rapid proliferation of cells; however, the process was quickly diminished. On the other hand, after a week, the cells within larger pores showed deeper penetration into the scaffold, combined with a higher number of cells overall. This was ascribed to the ease of the cellular expansion and better diffusion of nutrients [108].
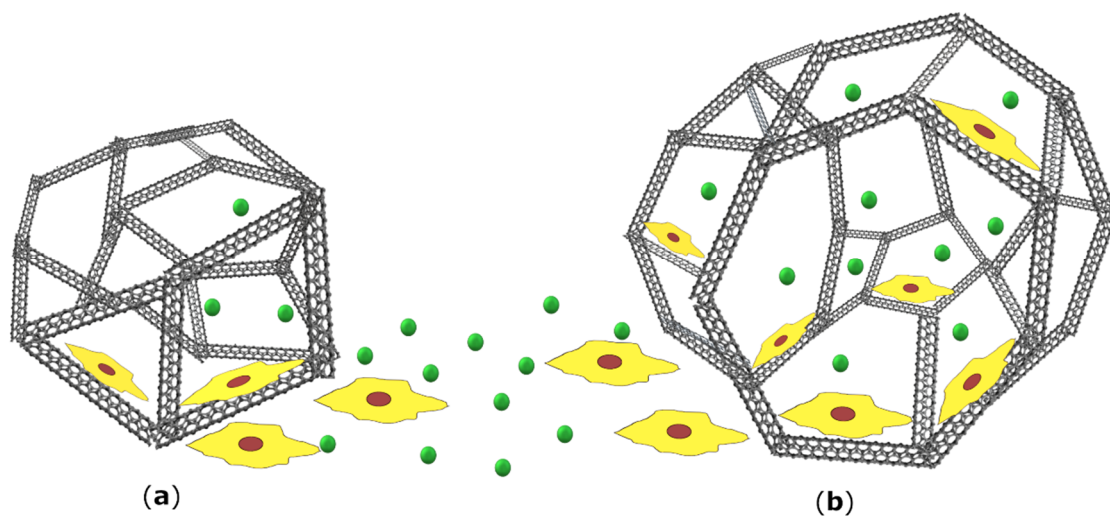

Figure 4. Porosity is a crucial factor in designing a scaffold. If pores are too small (**a**) there is a limited diffusion of nutrients and metabolites, as well as cell infiltration into deeper layers of the scaffold. However, such spatial constraint places cells near each other and therefore promotes proliferation, until the space becomes exhausted. On the other hand, if the pores are bigger (**b**) the flow of nutrients and cell penetration is much more efficient. Due to the low surface area, cell interactions and adhesion are exacerbated, which leads to slower cell proliferation. The figure is a schematic representation of a porous scaffold and it is not drawn to scale.

7. Advantages of CNTs' Usage in Scaffolds

Lalwani et al. presented a comprehensive cytocompatibility assessment of free-standing 3D constructs composed of CNTs, in comparison to the PLGA scaffold with similar porosity levels (80–90%) [109]. An average pore size, determined with the MicroCT technique, was 300–500 μm for PLGA and 100–400 μm for scaffolds prepared with MWCNTs and SWCNTs. Despite the difference in composition, the majority of tests carried out using MC3T3 cells (cytotoxicity, viability, proliferation, adhesion, infiltration) showed comparable results. Interestingly, the morphology of cells was different

among the scaffolds, with the elongated, spindle-like shape and more circular shape on MWCNT and SWCNT fabricated scaffolds, respectively. It was noted that this difference may be attributed to the difference in CNTs' dimensions. MWCNTs are thicker and longer compared to the used SWCNTs, which resulted in different surface roughness.

Joddar et al. developed an MWCNT-alginate composite by linking the alginate chains to –COOH-functionalized MWCNTs by Ca^{2+} ions. Unlike alginate alone and alginate with incorporated pristine MWCNTs, the prepared composite presented non-Newtonian pseudoplastic properties. It also presented a shear-thinning behavior characterized by decreasing viscosities with an increasing shear rate. The degradation time in the DMEM media of the scaffold was prolonged more than twofold. MWCNT addition to the amount of 1 mg/mL resulted in an increase in average pore size from $1.01 \pm 0.39\,\mu m$ to $1.98 \pm 1.08\,\mu m$ and, importantly, the pores were homogenously distributed and interconnected. This resulted in the clustering of HeLa cells in MWCNT-alginate scaffolds. This may be very promising for cartilage development since chondrocytes naturally grow in micromasses. It also resulted in a slight increase in the elastic modulus. All of these advantages are lost with increasing concentrations of MWCNTs. However, the authors declare that the level of MWCNT-alginate crosslinking is low and it can be increased by introducing more –COOH groups as well as increasing the Ca^{2+} ions' concentration. This would resemble natural complex ECM interconnections more closely, which should result in much better mechanical properties [91]. Similar findings were published by Lau et al., who analyzed various concentration levels of chitosan and CNTs to compare the porosity in three-dimensional chitosan–CNT scaffolds. The MWCNTs used in the experiment were of precisely defined dimensions of 20–30 nm outer diameter and 10–30 μm length. This size was selected due to the chitosan properties and mechanism of synthesis since such sized CNTs would not decrease the likelihood of entanglement and therefore the need for the use of a greater concentration of CNTs. Moreover, they were significantly larger than the average diameter of the chitosan pores. Such a scaffold was prepared with the TIPS method and exhibited 92–97% porosity, with pore sizes of 100–300 μm. Interestingly, the mechanical strength of the chitosan–CNT scaffold improved with the increasing concentration of CNT; however, beyond the optimum concentration of CNT, the scaffolds became more brittle and fragile.

Natural cartilage or bone tissue is composed of a plethora of interconnected molecules, and hence structures composed of diverse molecules were investigated. For example, chitosan–MWCNTs–HA nanocomposites prepared by Chen et al. demonstrated a sharp increase in the elastic modulus by 114% (from 509.9 to 1089.1 MPa) and compressive strength by 218% from 33.2 to 105.5 MPa, by increasing the MWCNT–chitosan weight ratios from 0% to 5%. Importantly, it did not affect cell viability. These values, though not as high as for the native bone, present that cooperation between different components may vastly increase the mechanical properties [104].

Kroustalli et al. showed that osteoblasts have increased adhesion properties, as well as proliferation and differentiation potential, on even pristine MWCNTs [110]. The MWCNTs with a mean diameter of 5–20 nm and >10 um were prepared as a thin film (243.4 ± 41.3 nm) of randomly oriented networks of aggregated CNTs. The MWCNTs accelerated human mesenchymal stem cell differentiation to a higher extent (three-and-a-half fold) than a plastic tissue culture, even in the absence of additional biochemical inducing agents, measured with alkaline phosphatase (ALP) activity. The pre-treatment with anti-integrin antibodies decreased the number of adherent cells and adhesion strength at 4–60%. In conclusion, even pristine MWCNTs can adsorb proteins and therefore allow osteoblasts to adhere via the integrin-mediated pattern.

Deligianni discussed the role of scaffold dimensions concerning cell shape and its impact on cell fate [111]. It has been concluded that the cell morphology correlates with the physiological behavior of the cells, especially that the cell growth is accelerated when cell adhesion is decreased. The study presented that on flat and polished surfaces, lower phyllopodia content was correlated with an increase in cell proliferation and a more elongated and spindle-like morphology. In contrast, on microrough surfaces, the cell bodies become more cuboidal and form polygonal shapes, with an accompanying lower proliferation rate. The clear correlation between cell shape and differentiation leads to the

assumption that changes in the assembly and disassembly of the actin cytoskeleton may be critical in supporting mesenchymal stem cell differentiation, especially into bone cell lineage. In conclusion, smaller MWCNTs of 30 nm in diameter promote adhesion, whereas larger (70 to 100 nm) MWCNTs elicit differentiation.

Chanine et al. cultured chondrocytes in composite mixtures of 2% agarose and two preparations of CNTs, carboxyl functionalized SWCNT–COOH, and covalent PEG-modified SWCNTs [112]. The SWCNT–COOH showed greater viability than a control scaffold, whereas the SWCNT–PEG scaffold showed inhibited proliferation. Interestingly, a higher concentration of SWCNT–PEG yielded much higher ECM production, despite the lowest cell viability. This is in concordance with the previously mentioned finding that the higher the adhesion level, the lower the proliferation rate, but the more active the metabolic state of the cell.

8. Methods of Scaffold Fabrication

There are several methods used for scaffold production. They are based on the formation of nanofibers from the biomaterial of choice with further attempts to organize them into desired spatial architecture. Current methods of scaffold fabrication are divided into conventional and rapid prototyping methods.

8.1. Conventional Techniques

Conventional techniques are defined as processes in which prepared scaffolds have continuous, uninterrupted pore structure, however, it lacks long-range channeling microarchitecture.

8.1.1. Electrospinning

One of the very first methods utilized is electrospinning. Electrostatic charge is applied to the polymer in liquid form, which is extruded through a small jet, resulting in the nanofibers which are deposited on the metallic collector [113]. Conventional electrospun fibers can be aligned randomly or in the vertically aligned fashion, creating a tightly packed, 2D mesh which is similar to native ECM of some tissues, e.g., skin [114]. However, as was noted before, the cartilage and bone are complex hierarchical structures. Therefore, it was attempted to create 3D structures with higher porosity to facilitate cell infiltration. One of the methods was to electrospun the fibers directly to the liquid collector instead of the flat one. It resulted in a more porous structure, however, with limited control over spatial arrangement [115]. There are several papers where CNTs are used in a composite material with PCL [116,117] and polyurethane [118,119].

8.1.2. Solvent Casting

This technique is based on the mixing of uniformly distributed salt particles in a particular solvent with a polymeric solution. After evaporation of the solvent, the matrix is submerged in water, leading to the dissolution of salt particles, leaving a porous scaffold.

8.1.3. Freeze-Drying

This process is also called lyophilization. Mao et al. developed a method to synthesize a collagen-based scaffold reinforced with SWCNTs using monodisperse ice crystals [120]. The ice particles, created by spraying the ultrapure water into liquid nitrogen, were sieved with 355 μm and 425 μm sieves at −15°C. They were mixed with a collagen solution and freeze-dried after another incubation step. Finally, the scaffold was immersed in a solution of collagen-coated SWCNTs. The process resulted in homogenous, interconnected pores with a narrow size distribution of 359 ± 53 μm in diameter. After two weeks, the number of cells and GAGs synthesis was significantly greater in the SWCNT-enforced scaffolds compared to the bare collagen.

8.1.4. Self-Assembly

Self-assembly is a process in which fibers arrange themselves spontaneously into fibers of the desired shape, due to intramolecular interactions. It is achieved by using particular functional motifs (e.g., amino acid sequences) [121], or chemical interactions in particular conditions (e.g., the polarity of solvent) [122]. Peptide self-assembled scaffolds have good biological activity, however, they are too brittle to carry the mechanical load as a scaffold.

8.1.5. Phase Separation

Phase separation is a technique that produces 3D nanofibrous structures with nanofibers of dimensions similar to collagen fibrils of ECM (50–500 μm). This technique employs two substances that are incompatible in a particular solvent, which results in the formation of a porous structure, followed by the replacement of the solvent. The fabrication process is convenient, however, it is restricted to certain specific polymer-solvent combinations and since they have high porosity the obtained scaffold is too brittle for cartilage and bone scaffolds. [123]. The modification of this method is a thermal-induced phase separation (TIPS), which utilizes temperature difference to separate the phases.

In general, scaffolds produced by conventional methods have poorly controlled pore sizes and spatial distribution. Thus, the cellular infiltration and diffusion of nutrients are limited [124].

8.2. Rapid Prototyping Technologies

Rapid prototyping technologies are bottom-up approaches, which are capable of producing specially designed forms and shapes with the use of computer-aided design (CAD).

8.2.1. 3D Bioprinting

3D bioprinting is a technique in which a biomaterial is precisely extruded in a layer-by-layer approach, thus giving much more control over the shape and microarchitecture of a printed scaffold. Therefore, it allows the creation of a construct that closely resembles native tissue. This is a crucial aspect, both in terms of mechanical support and for proper cellular function because, as was mentioned earlier, the local environment inside the tissue affects every aspect of cellular behavior such as metabolism, proliferation, and migration [125,126].

The biomaterial used in bioprinting is composed of a hydrogel matrix, in which living cells are uniformly suspended, and it is therefore called a bioink. An ideal bioink should have a few key features such as printability, shape stability, sufficient mechanical strength, biocompatibility, cytocompatibility, and degradability. Because it has to be bio- and cytocompatible, currently used bioinks are based mainly on natural polymers, such as alginate, agarose, gelatin, fibrin, chitosan, hyaluronate, and collagen; however, synthetic polymers, e.g., poloxamer (pluronic) or polyethylene glycol (PEG) are also exploited. Except for agarose and alginate, these materials have an inherent resemblance to the ECM. As relatively soft hydrogels, they have good printability parameters; however, they do not possess sufficient mechanical stability to resist the same continuously applied loads as a cartilage or bone replacement. Therefore, two approaches are utilized—crosslinking and augmentation with stiffer materials, generating a composite scaffold [127].

There are two types of crosslinking—physical and chemical. Physical crosslinking relies on ionic or hydrophobic interactions and hydrogen bonding. One of the most extensively used hydrogels, alginate, is physically crosslinked after printing by the addition of calcium salts (e.g., $CaCl_2$). Chemical crosslinking is based on the formation of covalent bonds, and therefore as-prepared scaffolds are mechanically stronger [128]. For this type of crosslinking, various chemical modifications of polymers are used, e.g., methacrylated or diacrylated moieties of PEG, cellulose, gelatin undergoes radical polymerization after UV light irradiation [129–131].

Composite scaffolds are made by the usage of rigid materials, in the form of an external mesh, or fibers and particles, along with the hydrogel formulation. An example of a widely used

synthetic material is polycaprolactone (PCL), due to its mechanical strength and biocompatibility. Daly et al. [132] printed a mesenchymal stem cell-laden scaffold on the pattern of vertebrae. In this study, alginate-based bioink, reinforced with PCL fibers, was utilized. This reinforcement led to a significant increase in the compressive modulus (3.867 ± 0.2187 vs. 1402 ± 157.8 kPa). This model was tested in vivo by subcutaneous implantation into mice. After 12 weeks, bioprinted vertebrae were extensively vascularized and mineralized; 24.6% ± 4.8% of the whole scaffold surface was bone tissue. Piard et al. co-printed osteon-like scaffolds with fibrin/gelatin bioink, along with a PCL supporting carrier scaffold. The application of the latter vastly increased the compressive modulus, which fell into the range of cortical bone [133]. On the other hand, Gao et al. printed a 3D scaffold made of poly(ethylene glycol)dimethacrylate (PEGDMA) in which nanoparticles of bioactive glass and hydroxyapatite were suspended [134]. The nanoparticles had a dual purpose—they reinforced the whole scaffold, increasing its compressive modulus, and hydroxyapatite was an osteogenic inducer to the mesenchymal stem cells present in the bioink.

8.2.2. Laser-assisted Bioprinting

Laser-assisted bioprinting (LAB) is a nozzle-free, non-contact technique, where the laser is pulsed on a three-layer material: laser-transparent layer, laser absorbing layer, and bioink. Energy from penetrating laser is absorbed and forms bubbles, which ejects the bioink from the laser surface onto the collector stage. Kerouredan et al. used this technique to print a pattern with labeled endothelial cells directly into the bone defect in mice, which was filled with a collagen matrix. The defined local cell density of endothelial cells allowed the generation of microvascular networks [135].

8.2.3. Fused Deposition Modeling

Fused deposition modeling (FDM) is a technique in which polymer filaments are inserted into a heated nozzle, melted and extruded.

8.2.4. Stereolithography and Digital Light Projection

Stereolithography (SLA) and digital light projection (DLP) are nozzle-free techniques that create objects through layer-by-layer photopolymerization.

Another promising direction in 3D bioprinting is the so-called 4D bioprinting, where the concept of time is added as a fourth dimension. This means that a 3D-bioprinted scaffold can change its characteristics, spontaneously, or under various stimuli, after the printing process [136]. The stimuli-responsive materials can "remember" their shapes due to their chemical composition. For instance, thermo-responsive materials can change their shape (e.g., polyurethane [137]), or achieve sol-gel transition below a particular temperature. Fabrication of such scaffolds has many potential advantages. Wu et al. prepared injectable chitosan/silk fibroin/bioactive glass nanoparticle hydrogel, which can be injected directly into the damaged bone. In body temperature it undergoes a gelling process, yielding porous filling. It was tested in rats, and after eight weeks it restored vascularized bone tissue and mineralized collagen deposits. No cells and growth factors were used, which suggests the infiltration of the scaffold by cells and its further replacement with native bone tissue [138].

There is a limited amount of research regarding CNT usage as a supplement in bioinks. One of the most interesting works was published by Goncalves et al. [105]. A three-phased HA–CNT–PCL composite was used to print a scaffold for bone cell growth. The CNT content was up to 10%, embedded in 50% PCL, HA being the remaining part. The addition of 2% CNT yielded the best mechanical and electrical properties, with a compressive strength of ~4 MPa, which is similar to that of a trabecular bone. On the other hand, the elastic moduli were measured 44 MPa for the 2% CNT supplement. Although 0.75% CNT yielded the highest Young's modulus (60 MPa), it was not conductive, which plays a role in regulating the physiological behavior of cells, e.g., the electrical stimulation of bone promotes osteogenesis [139], and therefore it is a desirable property for a bone

scaffold. The pore sizes could be adjusted from 450 to 700 μm. Moreover, the material elicited the adhesion and spreading of osteoblast-like cells.

Cui et al. used a tough polyion complex (PIC) mixed with MWCNTs for the extrusion-based printing of a scaffold for bone repair [140]. It was indicated that the addition of MWCNTs promoted the osteogenesis of embedded mesenchymal stem cells, resulting in a mineralized matrix formation and osteogenesis-related gene upregulation. Moreover, the scaffold had remarkable mechanical properties of the tensile strength (1.69 ± 0.11 MPa), Young's modulus (4.47 ± 0.5 MPa), and a compressive modulus (0.445 ± 0.029 MPa) and could be bent and fully recover its shape. It was used in an in vivo experiment, where it was implanted for osteogenic repair in a rat's cranial bone. It acted as a template for new bone tissue, which had ingrown in the pores of the scaffold. The promotion of new bone formation was significantly more effective with PIC/MWCNTs than PIC alone, which further indicates the MWCNTs' stimulatory effect.

Wang et al. [141] blended two different concentrations of MWCNTs (1% and 3 wt.%) with PCL and printed (with RegenHu Discovery bioprinter) 3D scaffold with a slice thickness of 220 μm, filament diameter of 330 μm, and pores of around 200 μm. The addition of MWCNTs slightly increased the compressive modulus, however, it vastly increased (more than two-and-a-half fold over two weeks) cell proliferation and exerted strong protein adhesion properties.

Huang et al. produced a 3D hierarchical scaffold by the screw-assisted extrusion 3D printing composed of a PCL/HA/MWCNTs composite. MWCNTs were highly aligned, surrounded by HA, which mimicked native bone structure. It was tested that MWCNTs promoted the early stage of osteogenesis differentiation of mesenchymal stem cells, while HA promoted the later stage of this process. The supplementation of PCL with MWCNTs and HA enhanced the compressive modulus from 55 to 85 MPa [142].

9. Discussion

Increasing demand for organs, limitations of currently existing treatment techniques, and shortage of suitable transplants have led to great advances in tissue engineering and regenerative medicine, specifically in the field of scaffold design. In terms of bone repair, two major techniques are used as a standard of treatment—autologous bone grafting and titanium implants. Both approaches suffer from patient morbidity; bone grafting is a technique with good outcomes, however, the amount of bone that can be grafted is limited [143]. Titanium implants, however, pose a risk of infection or rejection and may cause stress shielding which leads to embrittlement of the native bone [50]. In terms of articular cartilage repair, there is no effective gold standard method of treatment. Existing experimental methods rely on burdensome arthroscopic interventions combined with an influx of bone marrow, injections of stem cells, or grafting of different connective tissues. Those techniques are still in the experimental phases, with mixed outcomes and scarce long-term follow-up studies.

This led to the idea of external scaffolds, which may mimic the intrinsic complex ultrastructure of these tissues and serve as a direct replacement, which will be gradually replaced by the native tissue produced in situ by the residual cells. To achieve this, proper biocompatible materials should be developed with techniques to properly arrange the scaffold into a functional structure. Many hydrogel polymers have been tested, because of their biocompatibility and provision of aqueous environment needed to house the cells [81,92,144]. However, it was found that alone, they are too brittle to bear the load applied on either bone or cartilage. This led to the creation of composite materials where the hydrogel was reinforced with more robust molecules, such as PCL, native collagens or naturally occurring hydroxyapatite and tricalcium phosphate in terms of bone tissue. Such scaffolds were able to achieve physical characteristics comparable to the native tissues [104,145]. Due to the properties of CNTs, they were also tested for the scaffolds due to the following reasons: (1) their superior mechanical properties, with elastic moduli and tensile strength, far better than the other materials used [146]; (2) CNT size, shape, surface roughness, and surface area structurally mimics that of collagen fibers, providing a 3D network to support and guide cell proliferation, differentiation, and communication,

which is not the case for the polymeric fibers, such as PCL [91,140]; (3) CNTs' ability to interact with and adsorb extracellular proteins allows enhanced cell interaction and scaffold biocompatibility [110]; (4) CNTs offer increased cell support, which is important for angiogenesis and vascularization [147].

Nevertheless, the major problem at this stage of scaffold production is to properly arrange the fibers to, at least, obtain proper porosity, not to mention the hierarchical ultrastructure of the tissue, which is unattainable with the conventional techniques. Porosity should be high enough to provide the space for the cells and allow for the diffusion of metabolites, but the more porous the material is, the more brittle it becomes. Many conventional approaches were carried out to achieve this, e.g., using homogenous ice crystals as a mold for the polymers, which are later removed, leaving the monodisperse pores. However, the 3D bioprinting technique emerged, which is showing itself to be able to overcome the ultrastructural limitations with which scientists have been struggling to date [87]. Nowadays, 3D bioprinters offer a printing resolution of 5 μm (3DDiscovery™ Evolution, RegenHU) with several printheads and with few different printing techniques working in parallel, such as electrospinning. Nevertheless, to our knowledge, no produced scaffold exactly mimics the hierarchical ultrastructure of either bone or cartilage. The most important aspect of such scaffolds, besides the lack of toxicity, is to provide sufficient mechanical durability until the tissue regenerates. Therefore, if a scaffold possesses sufficient porosity to house the cells and sufficient mechanical properties, it seems that the fidelity in the ultrastructure of bone and cartilage can be omitted in the design of a scaffold. These ultrastructural features, such as distinct layers in cartilage (Figure 1), or a concentrated Haversian system in bone, are not necessarily required to be designed in the scaffold. Optimally, the scaffold would undergo biodegradation, at a rate similar to the ECM rebuilding, therefore these ultrastructural motifs could be remodeled by the residual cells. However, with the current state-of-the-art, it is possible to fabricate a CNT reinforced scaffold with mechanical properties similar to the native tissue, providing a microenvironment to house cells that is directly augmented by the incorporation of CNTs [140]. The scaffolds are shown to be effective in short-term in vivo studies in small animals. The current limitation in the field of 3D bioprinting is the lack of long-term research of produced scaffolds in vivo, especially in humans. Therefore, we do not have information on whether these scaffolds are sufficient to be translated to the market and used publicly. This is mostly attributed not to technical constraints because the bioprinting process itself is standardized and controlled by software, but to a high level of innovation and possible regulatory constraints preventing carrying out of such studies [147].

Conflicts of Interest: The authors declare no conflict of interest.

References

1. Muthuri, S.; McWilliams, D.F.; Doherty, M.; Zhang, W. History of knee injuries and knee osteoarthritis: A meta-analysis of observational studies. *Osteoarthr. Cartil.* **2011**, *19*, 1286–1293. [CrossRef] [PubMed]

2. Sasaki, E.; Ota, S.; Chiba, D.; Kimura, Y.; Sasaki, S.; Yamamoto, Y.; Tsuda, E.; Nakaji, S.; Ishibashi, Y. Early knee osteoarthritis prevalence is highest among middle-aged adult females with obesity based on new set of diagnostic criteria from a large sample cohort study in the Japanese general population. *Knee Surg. Sports Traumatol. Arthrosc.* **2019**, *28*, 984–994. [CrossRef] [PubMed]

3. Richter, M.; Trzeciak, T.; Rybka, J.D.; Suchorska, W.; Augustyniak, E.; Lach, M.; Kaczmarek, M.; Kaczmarczyk, J. Correlations between serum adipocytokine concentrations, disease stage, radiological status and total body fat content in the patients with primary knee osteoarthritis. *Int. Orthop.* **2016**, *41*, 983–989. [CrossRef] [PubMed]

4. Sefat, F.; Raja, T.I.; Zafar, M.S.; Khurshid, Z.; Najeeb, S.; Zohaib, S.; Ahmadi, E.D.; Rahmati, M.; Mozafari, M. Nanoengineered biomaterials for cartilage repair. In *Nanoengineered Biomaterials for Regenerative Medicine*; Elsevier BV: Amsterdam, The Netherlands, 2019; pp. 39–71.

5. Dewan, A.K.; Gibson, M.A.; Elisseeff, J.H.; Trice, M.E. Evolution of Autologous Chondrocyte Repair and Comparison to Other Cartilage Repair Techniques. *BioMed Res. Int.* **2014**, *2014*, 1–11. [CrossRef]

6. Wehling, P.; Evans, C.; Wehling, J.; Maixner, W. Effectiveness of intra-articular therapies in osteoarthritis: A literature review. *Ther. Adv. Musculoskelet. Dis.* **2017**, *9*, 183–196. [CrossRef]

7. Cross, M.J.; Smith, E.; Hoy, D.; Nolte, S.; Ackerman, I.N.; Fransen, M.; Bridgett, L.; Williams, S.; Guillemin, F.; Hill, C.L.; et al. The global burden of hip and knee osteoarthritis: Estimates from the Global Burden of Disease 2010 study. *Ann. Rheum. Dis.* **2014**, *73*, 1323–1330. [CrossRef]

8. Mieloch, A.A.; Richter, M.; Trzeciak, T.; Giersig, M.; Rybka, J.D. Osteoarthritis Severely Decreases the Elasticity and Hardness of Knee Joint Cartilage: A Nanoindentation Study. *J. Clin. Med.* **2019**, *8*, 1865. [CrossRef]

9. Khan, I.; Gilbert, S.; Singhrao, S.; Duance, V.; Archer, C. Evaluation of the reasons for failure of integration during cartilage repair. A review. *Eur. Cells Mater.* **2008**, *16*, 26–39. [CrossRef]

10. Talreja, P.S.; Gayathri, G.V.; Mehta, D.S. Treatment of an early failing implant by guided bone regeneration using resorbable collagen membrane and bioactive glass. *J. Indian Soc. Periodontol.* **2013**, *17*, 131–136. [CrossRef]

11. Przekora, A. Current Trends in Fabrication of Biomaterials for Bone and Cartilage Regeneration: Materials Modifications and Biophysical Stimulations. *Int. J. Mol. Sci.* **2019**, *20*, 435. [CrossRef]

12. Trzeciak, T.; Rybka, J.D.; Richter, M.; Kaczmarczyk, J.; Ramalingam, M.; Giersig, M. Cells and Nanomaterial-Based Tissue Engineering Techniques in the Treatment of Bone and Cartilage Injuries. *J. Nanosci. Nanotechnol.* **2016**, *16*, 8948–8952. [CrossRef]

13. Hollister, S. Porous scaffold design for tissue engineering. *Nat. Mater.* **2005**, *4*, 518–524. [CrossRef] [PubMed]

14. Sharma, B.; Elisseeff, J.H. Engineering structurally organized cartilage and bone tissues. *Ann. Biomed. Eng.* **2004**, *32*, 148–159. [CrossRef] [PubMed]

15. O'Brien, F.J. Biomaterials & scaffolds for tissue engineering. *Mater. Today* **2011**, *14*, 88–95. [CrossRef]

16. Marchesan, S.; Melchionna, M.; Prato, M. Carbon Nanostructures for Nanomedicine: Opportunities and Challenges. *Full- Nanotub. Carbon Nanostruct.* **2014**, *22*, 190–195. [CrossRef]

17. Hickey, R.J.; Pelling, A.E. Cellulose Biomaterials for Tissue Engineering. *Front. Bioeng. Biotechnol.* **2019**, *7*, 1–15. [CrossRef]

18. Chena, S.; Chenb, W.; Chenc, Y.; Mod, X.; Fana, C. Chondroitin Sulfate modified 3D Porous Electrospun Nanofiber Scaffolds Promote Cartilage Regeneration. *Mater. Sci. Eng. C* **2020**, *118*, 111312. [CrossRef]

19. Eivazzadeh-Keihan, R.; Chenab, K.K.; Taheri-Ledari, R.; Mosafer, J.; Hashemi, S.M.; Mokhtarzadeh, A.; Maleki, A.; Hamblin, M.R. Recent advances in the application of mesoporous silica-based nanomaterials for bone tissue engineering. *Mater. Sci. Eng. C* **2019**, *107*, 110267. [CrossRef]

20. Lowe, B.; Hardy, J.; Walsh, L.J. Optimizing Nanohydroxyapatite Nanocomposites for Bone Tissue Engineering. *ACS Omega* **2019**, *5*, 1–9. [CrossRef]

21. Oudadesse, H.; Najem, S.; Mosbahi, S.; Rocton, N.; Refifi, J.; El Feki, H.; Lefeuvre, B. Development of hybrid scaffold: Bioactive glass nanoparticles/chitosan for tissue engineering applications. *J. Biomed. Mater. Res. Part A* **2020**. [CrossRef]

22. Ibrahim, K.S. Carbon nanotubes-properties and applications: A review. *Carbon Lett.* **2013**, *14*, 131–144. [CrossRef]

23. Rahmati, M.; Mozafari, M. Biological Response to Carbon-Family Nanomaterials: Interactions at the Nano-Bio Interface. *Front. Bioeng. Biotechnol.* **2019**, *7*, 1–22. [CrossRef] [PubMed]

24. Edwards, S.L.; A Werkmeister, J.; Ramshaw, J.A. Carbon nanotubes in scaffolds for tissue engineering. *Expert Rev. Med Devices* **2009**, *6*, 499–505. [CrossRef] [PubMed]

25. Allaf, R.M.; Rivero, I.V.; Ivanov, I.N. Fabrication and Characterization of Multi-Walled Carbon Nanotube Loaded Interconnected Porous Nanocomposite Scaffolds. *Int. J. Polym. Mater.* **2016**, *66*, 183–192. [CrossRef]

26. Gentili, C.; Cancedda, R. Cartilage and Bone Extracellular Matrix. *Curr. Pharm. Des.* **2009**, *15*, 1334–1348. [CrossRef]

27. Fox, A.J.S.; Bedi, A.; Rodeo, S.A. The Basic Science of Articular Cartilage. *Sports Health A Multidiscip. Approach* **2009**, *1*, 461–468. [CrossRef]

28. Holmes, D.F.; Lu, Y.; Starborg, T.; Kadler, K.E. *Collagen Fibril Assembly and Function*; Elsevier BV: Amsterdam, The Netherlands, 2018.

29. Kolácná, L.; Bakesová, J.; Varga, F.; Kostáková, E.; Plánka, L.; Nečas, A.; Lukás, D.; Amler, E.; Pelouch, V. Biochemical and biophysical aspects of collagen nanostructure in the extracellular matrix. *Physiol. Res.* **2007**, *56*, 51–60.

30. Eyre, D.R. Articular cartilage and changes in Arthritis: Collagen of articular cartilage. *Arthritis Res.* **2001**, *4*, 30–35. [CrossRef]

31. Eyre, D.R.; Weis, M.A.; Wu, J.-J. Articular cartilage collagen: An irreplaceable framework? *Eur. Cells Mater.* **2006**, *12*, 57–63. [CrossRef]

32. Benninghoff, A. Form und Bau der Gelenkknorpel in ihren Beziehungen zur Funktion. *Cell Tissue Res.* **1925**, *2*, 783–862. [CrossRef]

33. Weiss, C.; Rosenberg, L.; Helfet, A.J. An Ultrastructural Study of Normal Young Adult Human Articular Cartilage. *J. Bone Jt. Surg. Am. Vol.* **1968**, *50*, 663–674. [CrossRef] [PubMed]

34. Mow, V.C.; Guo, X.E. Mechano-Electrochemical Properties Of Articular Cartilage: Their Inhomogeneities and Anisotropies. *Annu. Rev. Biomed. Eng.* **2002**, *4*, 175–209. [CrossRef] [PubMed]

35. Fratzl, P.; Gupta, H.S.; Paschalis, E.P.; Roschger, P. Structure and mechanical quality of the collagen–mineral nano-composite in bone. *J. Mater. Chem.* **2004**, *14*, 2115–2123. [CrossRef]

36. Ralston, S.H. Bone structure and metabolism. *Medicine* **2013**, *41*, 581–585. [CrossRef]

37. Reznikov, N.; Shahar, R.; Weiner, S. Three-dimensional structure of human lamellar bone: The presence of two different materials and new insights into the hierarchical organization. *Bone* **2014**, *59*, 93–104. [CrossRef]

38. Weiner, S.; Wagner, H.D. THE MATERIAL BONE: Structure-Mechanical Function Relations. *Annu. Rev. Mater. Res.* **1998**, *28*, 271–298. [CrossRef]

39. Zimmermann, E.A.; Schaible, E.; Gludovatz, B.; Schmidt, F.N.; Riedel, C.; Krause, M.; Vettorazzi, E.; Acevedo, C.; Hahn, M.; Püschel, K.; et al. Intrinsic mechanical behavior of femoral cortical bone in young, osteoporotic and bisphosphonate-treated individuals in low- and high energy fracture conditions. *Sci. Rep.* **2016**, *6*, 21072. [CrossRef]

40. Fantner, G.E.; Adams, J.; Turner, P.; Thurner, P.J.; Fisher, L.W.; Hansma, P.K. Nanoscale Ion Mediated Networks in Bone: Osteopontin Can Repeatedly Dissipate Large Amounts of Energy. *Nano Lett.* **2007**, *7*, 2491–2498. [CrossRef]

41. Qu, H.; Fu, H.; Han, Z.; Sun, Y. Biomaterials for bone tissue engineering scaffolds: A review. *RSC Adv.* **2019**, *9*, 26252–26262. [CrossRef]

42. Yang, D.S.; Lee, K.W.; Hwang, J.Y.; Kim, K.J.; Choy, W.S. Arthroscopic assessment of cartilage healing status after treatment of tibial plateau fracture. *Indian J. Orthop.* **2019**, *53*, 257. [CrossRef]

43. Richter, D.L.; Schenck, R.C.; Wascher, D.C.; Treme, G. Knee Articular Cartilage Repair and Restoration Techniques: A Review of the Literature. *Sports Health A Multidiscip. Approach* **2015**, *8*, 153–160. [CrossRef]

44. Solheim, E.; Hegna, J.; Øyen, J.; Harlem, T.; Strand, T. Results at 10 to 14 years after osteochondral autografting (mosaicplasty) in articular cartilage defects in the knee. *Knee* **2013**, *20*, 287–290. [CrossRef]

45. Mundi, R.; Chow, L.; Crouch, S.; Enselman, E.S.; Bedi, A.; Simunovic, N.; Ayeni, O.R. Cartilage Restoration of the Knee. *Am. J. Sports Med.* **2015**, *44*, 1888–1895. [CrossRef] [PubMed]

46. DiBartola, A.C.; Wright, B.M.; Magnussen, R.A.; Flanigan, D.C. Clinical Outcomes After Autologous Chondrocyte Implantation in Adolescents' Knees: A Systematic Review. *Arthrosc. J. Arthrosc. Relat. Surg.* **2016**, *32*, 1905–1916. [CrossRef] [PubMed]

47. Medvedeva, E.V.; Grebenik, E.A.; Gornostaeva, S.N.; Telpuhov, V.I.; Lychagin, A.; Timashev, P.; Chagin, A.S. Repair of Damaged Articular Cartilage: Current Approaches and Future Directions. *Int. J. Mol. Sci.* **2018**, *19*, 2366. [CrossRef] [PubMed]

48. Hunziker, E. Articular cartilage repair: Basic science and clinical progress. A review of the current status and prospects. *Osteoarthr. Cartil.* **2002**, *10*, 432–463. [CrossRef] [PubMed]

49. Campana, V.; Milano, G.; Pagano, E.; Barba, M.; Cicione, C.; Salonna, G.; Lattanzi, W.; Logroscino, G. Bone substitutes in orthopaedic surgery: From basic science to clinical practice. *J. Mater. Sci. Mater. Electron.* **2014**, *25*, 2445–2461. [CrossRef] [PubMed]

50. Song, P.; Hu, C.; Pei, X.; Sun, J.; Sun, H.; Wu, L.; Jiang, Q.; Fan, H.; Yang, B.; Zhou, C.; et al. Dual modulation of crystallinity and macro-/microstructures of 3D printed porous titanium implants to enhance stability and osseointegration. *J. Mater. Chem. B* **2019**, *7*, 2865–2877. [CrossRef]

51. Maksimkin, A.V.; Senatov, F.S.; Niaza, K.; Dayyoub, T.; Kaloshkin, S.D. Ultra-High Molecular Weight Polyethylene/Titanium-Hybrid Implant for Bone-Defect Replacement. *Materials* **2020**, *13*, 3010. [CrossRef]

52. Maggi, A.; Li, H.; Greer, J.R. Three-dimensional nano-architected scaffolds with tunable stiffness for efficient bone tissue growth. *Acta Biomater.* **2017**, *63*, 294–305. [CrossRef]

53. Ghassemi, T.; Shahroodi, A.; Ebrahimzadeh, M.H.; Mousavian, A.; Movaffagh, J.; Moradi, A. Current Concepts in Scaffolding for Bone Tissue Engineering. *Arch. bone Jt. Surg.* **2018**, *6*, 90–99. [PubMed]

54. Nakanishi, W.; Minami, K.; Shrestha, L.K.; Ji, Q.; Hill, J.P.; Ariga, K. Bioactive nanocarbon assemblies: Nanoarchitectonics and applications. *Nano Today* **2014**, *9*, 378–394. [CrossRef]

55. Tutak, W.; Chhowalla, M.; Sesti, F. The chemical and physical characteristics of single-walled carbon nanotube film impact on osteoblastic cell response. *Nanotechnology* **2010**, *21*, 315102. [CrossRef] [PubMed]

56. Iijima, S. Helical microtubules of graphitic carbon. *Nature* **1991**, *354*, 56–58. [CrossRef]

57. Prasek, J.; Drbohlavova, J.; Chomoucka, J.; Hubalek, J.; Jašek, O.; Adam, V.; Kizek, R. Methods for carbon nanotubes synthesis—Review. *J. Mater. Chem.* **2011**, *21*, 15872–15884. [CrossRef]

58. Gupta, N.; Gupta, S.M.; Sharma, S.K. Carbon nanotubes: Synthesis, properties and engineering applications. *Carbon Lett.* **2019**, *29*, 419–447. [CrossRef]

59. Nomanbhay, S.; Raziah, A.Z.; Junizah, A.R. Carbon Nanotubes: A Review on Structure and Their Interaction with Proteins. *J. Chem.* **2013**, *2013*, 1–18. [CrossRef]

60. Tofighy, M.A.; Mohammadi, T. Adsorption of divalent heavy metal ions from water using carbon nanotube sheets. *J. Hazard. Mater.* **2011**, *185*, 140–147. [CrossRef]

61. Yang, H.Y.; Han, Z.J.; Yu, S.F.; Pey, K.L.; Ostrikov, K.; Karnik, R. Carbon nanotube membranes with ultrahigh specific adsorption capacity for water desalination and purification. *Nat Commun.* **2013**, *4*, 2220. [CrossRef]

62. Resende, R.R.; Tonelli, F.M.P.; Santos, A.K.; Gomes, K.N.; Lorençon, E.; Ladeira, L.O.; Guatimosim, S. Carbon nanotube interaction with extracellular matrix proteins producing scaffolds for tissue engineering. *Int. J. Nanomed.* **2012**, *7*, 4511–4529. [CrossRef]

63. Imaninezhad, M.; Schober, J.; Griggs, D.; Ruminski, P.; Kuljanishvili, I.; Zustiak, S.P. Cell Attachment and Spreading on Carbon Nanotubes Is Facilitated by Integrin Binding. *Front. Bioeng. Biotechnol.* **2018**, *6*, 1–12. [CrossRef] [PubMed]

64. Trzeciak, T.; Rybka, J.D.; Akinoglu, E.M.; Richter, M.; Kaczmarczyk, J.; Giersig, M. In Vitro Evaluation of Carbon Nanotube-Based Scaffolds for Cartilage Tissue Engineering. *J. Nanosci. Nanotechnol.* **2016**, *16*, 9022–9025. [CrossRef]

65. Figarol, A.; Pourchez, J.; Boudard, D.; Forest, V.; Akono, C.; Tulliani, J.-M.; Lecompte, J.-P.; Cottier, M.; Bernache-Assollant, D.; Grosseau, P. In vitro toxicity of carbon nanotubes, nano-graphite and carbon black, similar impacts of acid functionalization. *Toxicol. Vitr.* **2015**, *30*, 476–485. [CrossRef] [PubMed]

66. Francis, A.P.; Thiyagarajan, D. Toxicity of carbon nanotubes: A review. *Toxicol. Ind. Health* **2018**, *34*, 200–210. [CrossRef] [PubMed]

67. Kobayashi, N.; Izumi, H.; Morimoto, Y. Review of toxicity studies of carbon nanotubes. *J. Occup. Health* **2017**, *59*, 394–407. [CrossRef]

68. Liu, Y.; Zhao, Y.; Sun, B.; Chen, C. Understanding the Toxicity of Carbon Nanotubes. *Acc. Chem. Res.* **2012**, *46*, 702–713. [CrossRef]

69. Castranova, V.; Schulte, P.A.; Zumwalde, R.D. Occupational Nanosafety Considerations for Carbon Nanotubes and Carbon Nanofibers. *Acc. Chem. Res.* **2012**, *46*, 642–649. [CrossRef]

70. Wang, L.; Mercer, R.R.; Rojanasakul, Y.; Qiu, A.; Lu, Y.; Scabilloni, J.F.; Wu, N.; Castranova, V. Direct Fibrogenic Effects of Dispersed Single-Walled Carbon Nanotubes on Human Lung Fibroblasts. *J. Toxicol. Environ. Health Part A* **2010**, *73*, 410–422. [CrossRef]

71. Johnston, H.J.; Hutchison, G.R.; Christensen, F.M.; Peters, S.; Hankin, S.; Aschberger, K.; Stone, V. A critical review of the biological mechanisms underlying thein vivoandin vitrotoxicity of carbon nanotubes: The contribution of physico-chemical characteristics. *Nanotoxicology* **2010**, *4*, 207–246. [CrossRef]

72. Li, J.-G.; Li, W.-X.; Xu, J.-Y.; Cai, X.-Q.; Liu, R.-L.; Li, Y.; Zhao, Q.-F.; Li, Q. Comparative study of pathological lesions induced by multiwalled carbon nanotubes in lungs of mice by intratracheal instillation and inhalation. *Environ. Toxicol.* **2007**, *22*, 415–421. [CrossRef]

73. Sargent, L.M.; Reynolds, S.H.; Castranova, V. Potential pulmonary effects of engineered carbon nanotubes:in vitrogenotoxic effects. *Nanotoxicology* **2010**, *4*, 396–408. [CrossRef]

74.   Takagi, A.; Hirose, A.; Nishimura, T.; Fukumori, N.; Ogata, A.; Ohashi, N.; Kitajima, S.; Kanno, J. Induction of mesothelioma in p53+/- mouse by intraperitoneal application of multi-wall carbon nanotube. *J. Toxicol. Sci.* **2008**, *33*, 105–116. [CrossRef]

75.   Muller, J.; Huaux, F.; Moreau, N.; Misson, P.; Heilier, J.-F.; Delos, M.; Arras, M.; Fonseca, A.; Nagy, J.B.; Lison, D. Respiratory toxicity of multi-wall carbon nanotubes. *Toxicol. Appl. Pharmacol.* **2005**, *207*, 221–231. [CrossRef]

76.   Allegri, M.; Perivoliotis, D.K.; Bianchi, M.G.; Chiu, M.; Pagliaro, A.; Koklioti, M.A.; Trompeta, A.-F.; Bergamaschi, E.; Bussolati, O.; Charitidis, C. Toxicity determinants of multi-walled carbon nanotubes: The relationship between functionalization and agglomeration. *Toxicol. Rep.* **2016**, *3*, 230–243. [CrossRef]

77.   Sager, T.M.; Wolfarth, M.W.; Andrew, M.; Hubbs, A.; Friend, S.; Chen, T.-H.; Porter, D.W.; Wu, N.; Yang, F.; Hamilton, R.F.; et al. Effect of multi-walled carbon nanotube surface modification on bioactivity in the C57BL/6 mouse model. *Nanotoxicology* **2013**, *8*, 317–327. [CrossRef]

78.   Mutlu, G.M.; Budinger, G.R.S.; Green, A.A.; Urich, D.; Soberanes, S.; Chiarella, S.E.; Alheid, G.F.; McCrimmon, D.R.; Szleifer, I.; Hersam, M.C. Biocompatible Nanoscale Dispersion of Single-Walled Carbon Nanotubes Minimizes in vivo Pulmonary Toxicity. *Nano Lett.* **2010**, *10*, 1664–1670. [CrossRef]

79.   Elgrabli, D.; Dachraoui, W.; Ménard-Moyon, C.; Liu, X.J.; Bégin, D.; Bégin-Colin, S.; Bianco, A.; Gazeau, F.; Alloyeau, D. Carbon Nanotube Degradation in Macrophages: Live Nanoscale Monitoring and Understanding of Biological Pathway. *ACS Nano* **2015**, *9*, 10113–10124. [CrossRef]

80.   Aldieri, E.; Fenoglio, I.; Cesano, F.; Gazzano, E.; Gulino, G.; Scarano, D.; Attanasio, A.; Mazzucco, G.; Ghigo, D.; Fubini, B. The Role of Iron Impurities in the Toxic Effects Exerted by Short Multiwalled Carbon Nanotubes (MWCNT) in Murine Alveolar Macrophages. *J. Toxicol. Environ. Health Part A* **2013**, *76*, 1056–1071. [CrossRef]

81.   Tutak, W.; Park, K.H.; Vasilov, A.; Starovoytov, V.; Fanchini, G.; Cai, S.-Q.; Partridge, N.C.; Sesti, F.; Chhowalla, M. Toxicity induced enhanced extracellular matrix production in osteoblastic cells cultured on single-walled carbon nanotube networks. *Nanotechnol.* **2009**, *20*, 255101. [CrossRef]

82.   Casey, A.; Herzog, E.; Davoren, M.; Lyng, F.M.; Byrne, H.J.; Chambers, G. Spectroscopic analysis confirms the interactions between single walled carbon nanotubes and various dyes commonly used to assess cytotoxicity. *Carbon* **2007**, *45*, 1425–1432. [CrossRef]

83.   Wang, G.; Zhang, J.; Dewilde, A.H.; Pal, A.K.; Bello, D.; Therrien, J.M.; Braunhut, S.; Marx, K.A. Understanding and correcting for carbon nanotube interferences with a commercial LDH cytotoxicity assay. *Toxicology* **2012**, *299*, 99–111. [CrossRef] [PubMed]

84.   Jeznach, O.; Kołbuk, D.; Sajkiewicz, P.; Sajkiewicz, P. Injectable hydrogels and nanocomposite hydrogels for cartilage regeneration. *J. Biomed. Mater. Res. Part A* **2018**, *106*, 2762–2776. [CrossRef] [PubMed]

85.   Dattola, E.; Parrotta, E.I.; Scalise, S.; Perozziello, G.; Limongi, T.; Candeloro, P.; Coluccio, M.L.; Maletta, C.; Bruno, L.; De Angelis, M.T.; et al. Development of 3D PVA scaffolds for cardiac tissue engineering and cell screening applications. *RSC Adv.* **2019**, *9*, 4246–4257. [CrossRef]

86.   Raic, A.; Rödling, L.; Kalbacher, H.; Lee-Thedieck, C. Biomimetic macroporous PEG hydrogels as 3D scaffolds for the multiplication of human hematopoietic stem and progenitor cells. *Biomaterials* **2014**, *35*, 929–940. [CrossRef] [PubMed]

87.   Ahmad, H.; Arya, A.; Agrawal, S.; Dwivedi, A.K. PLGA scaffolds: Building blocks for new age therapeutics. *Mater. Biomed. Eng.* **2019**, 155–201. [CrossRef]

88.   Singh, D.; Babbar, A.; Jain, V.; Gupta, D.; Saxena, S.; Dwibedi, V. Synthesis, characterization, and bioactivity investigation of biomimetic biodegradable PLA scaffold fabricated by fused filament fabrication process. *J. Braz. Soc. Mech. Sci. Eng.* **2019**, *41*, 121. [CrossRef]

89.   Afewerki, S.; Sheikhi, A.; Kannan, S.; Ahadian, S.; Khademhosseini, A. Gelatin-polysaccharide composite scaffolds for 3D cell culture and tissue engineering: Towards natural therapeutics. *Bioeng. Transl. Med.* **2018**, *4*, 96–115. [CrossRef]

90.   Joddar, B.; Garcia, E.; Casas, A.; Stewart, C.M. Development of functionalized multi-walled carbon-nanotube-based alginate hydrogels for enabling biomimetic technologies. *Sci. Rep.* **2016**, *6*, 32456. [CrossRef]

91.   Farokhi, M.; Shariatzadeh, F.J.; Solouk, A.; Mirzadeh, H. Alginate Based Scaffolds for Cartilage Tissue Engineering: A Review. *Int. J. Polym. Mater.* **2019**, *69*, 230–247. [CrossRef]

92. Irawan, V.; Sung, T.-C.; Higuchi, A.; Ikoma, T. Collagen Scaffolds in Cartilage Tissue Engineering and Relevant Approaches for Future Development. *Tissue Eng. Regen. Med.* **2018**, *15*, 673–697. [CrossRef]

93. Aguilar, A.; Zein, N.; Harmouch, E.; Hafdi, B.; Bornert, F.; Offner, D.; Clauss, F.; Fioretti, F.; Huck, O.; Benkirane-Jessel, N.; et al. Application of Chitosan in Bone and Dental Engineering. *Molecules* **2019**, *24*, 3009. [CrossRef] [PubMed]

94. Parisi, L.; Toffoli, A.; Ghiacci, G.; Macaluso, G.M. Tailoring the Interface of Biomaterials to Design Effective Scaffolds. *J. Funct. Biomater.* **2018**, *9*, 50. [CrossRef] [PubMed]

95. Garg, K.; Talovic, M.M.M.; Ziemkiewicz, K.G.N. Laminin Enriched Scaffolds for Tissue Engineering Applications. *Adv. Tissue Eng. Regen. Med. Open Access* **2017**, *2*, 1–8. [CrossRef]

96. Duan, W.; Haque, M.; Kearney, M.T.; Lopez, M.J. Collagen and Hydroxyapatite Scaffolds Activate Distinct Osteogenesis Signaling Pathways in Adult Adipose-Derived Multipotent Stromal Cells. *Tissue Eng. Part C Methods* **2017**, *23*, 592–603. [CrossRef] [PubMed]

97. Tian, H.; Tang, Z.; Zhuang, X.; Chen, X.; Jing, X. Biodegradable synthetic polymers: Preparation, functionalization and biomedical application. *Prog. Polym. Sci.* **2012**, *37*, 237–280. [CrossRef]

98. Dwivedi, R.; Kumar, S.; Pandey, R.; Mahajan, A.; Nandana, D.; Katti, D.S.; Mehrotra, D. Polycaprolactone as biomaterial for bone scaffolds: Review of literature. *J. Oral Boil. Craniofacial Res.* **2020**, *10*, 381–388. [CrossRef]

99. Visser, J.; Melchels, F.P.; Jeon, J.E.; Van Bussel, E.M.; Kimpton, L.S.; Byrne, H.M.; Dhert, W.J.A.; Dalton, P.D.; Hutmacher, D.W.; Malda, J. Reinforcement of hydrogels using three-dimensionally printed microfibres. *Nat. Commun.* **2015**, *6*, 6933. [CrossRef]

100. Ávila, H.M.; Schwarz, S.; Feldmann, E.-M.; Mantas, A.; Von Bomhard, A.; Gatenholm, P.; Rotter, N. Biocompatibility evaluation of densified bacterial nanocellulose hydrogel as an implant material for auricular cartilage regeneration. *Appl. Microbiol. Biotechnol.* **2014**, *98*, 7423–7435. [CrossRef]

101. Markstedt, K.; Mantas, A.; Tournier, I.; Ávila, H.M.; Hägg, D.; Gatenholm, P. 3D Bioprinting Human Chondrocytes with Nanocellulose–Alginate Bioink for Cartilage Tissue Engineering Applications. *Biomacromolecules* **2015**, *16*, 1489–1496. [CrossRef]

102. Athukoralalage, S.S.; Balu, R.; Dutta, N.K.; Choudhury, N.R. 3D Bioprinted Nanocellulose-Based Hydrogels for Tissue Engineering Applications: A Brief Review. *Polymers* **2019**, *11*, 898. [CrossRef]

103. Chen, L.; Hu, J.; Shen, X.; Tong, H. Synthesis and characterization of chitosan–multiwalled carbon nanotubes/hydroxyapatite nanocomposites for bone tissue engineering. *J. Mater. Sci. Mater. Electron.* **2013**, *24*, 1843–1851. [CrossRef] [PubMed]

104. Gonçalves, E.M.; Oliveira, F.; Silva, R.M.F.; Neto, M.A.; Fernandes, M.H.; Amaral, M.; Vallet-Regí, M.; Vila, M. Three-dimensional printed PCL-hydroxyapatite scaffolds filled with CNTs for bone cell growth stimulation. *J. Biomed. Mater. Res. Part B Appl. Biomater.* **2015**, *104*, 1210–1219. [CrossRef] [PubMed]

105. Klawitter, J.J.; Bagwell, J.G.; Weinstein, A.M.; Sauer, B.W.; Pruitt, J.R. An evaluation of bone growth into porous high density polyethylene. *J. Biomed. Mater. Res.* **1976**, *10*, 311–323. [CrossRef] [PubMed]

106. Tsuruga, E.; Takita, H.; Itoh, H.; Wakisaka, Y.; Kuboki, Y. Pore Size of Porous Hydroxyapatite as the Cell-Substratum Controls BMP-Induced Osteogenesis. *J. Biochem.* **1997**, *121*, 317–324. [CrossRef] [PubMed]

107. Murphy, C.M.; O'Brien, F.J. Understanding the effect of mean pore size on cell activity in collagen-glycosaminoglycan scaffolds. *Cell Adhes. Migr.* **2010**, *4*, 377–381. [CrossRef]

108. Lalwani, G.; Gopalan, A.; D'Agati, M.; Sankaran, J.S.; Judex, S.; Qin, Y.-X.; Sitharaman, B. Porous three-dimensional carbon nanotube scaffolds for tissue engineering. *J. Biomed. Mater. Res. Part A* **2015**, *103*, 3212–3225. [CrossRef]

109. Kroustalli, A.; Kotsikoris, V.; Karamitri, A.; Topouzis, S.; Deligianni, D. Mechanoresponses of human primary osteoblasts grown on carbon nanotubes. *J. Biomed. Mater. Res. Part A* **2014**, *103*, 1038–1044. [CrossRef]

110. Deligianni, D.D. Multiwalled carbon nanotubes enhance human bone marrow mesenchymal stem cells' spreading but delay their proliferation in the direction of differentiation acceleration. *Cell Adhes. Migr.* **2014**, *8*, 558–562. [CrossRef]

111. Chahine, N.O.; Collette, N.M.; Thomas, C.B.; Genetos, D.C.; Loots, G.G. Nanocomposite Scaffold for Chondrocyte Growth and Cartilage Tissue Engineering: Effects of Carbon Nanotube Surface Functionalization. *Tissue Eng. Part A* **2014**, *20*, 2305–2315. [CrossRef]

112. Jun, I.; Han, H.-S.; Edwards, J.R.; Jeon, H. Electrospun Fibrous Scaffolds for Tissue Engineering: Viewpoints on Architecture and Fabrication. *Int. J. Mol. Sci.* **2018**, *19*, 745. [CrossRef]

113. Keirouz, A.; Chung, M.; Kwon, J.; Fortunato, G.; Radacsi, N. 2D and 3D electrospinning technologies for the fabrication of nanofibrous scaffolds for skin tissue engineering: A review. *Wiley Interdiscip. Rev. Nanomed. Nanobiotechnol.* **2020**, *12*, e01626. [CrossRef] [PubMed]

114. Li, S.; Lee, B.-K. Electrospinning of circumferentially aligned polymer nanofibers floating on rotating water collector. *J. Appl. Polym. Sci.* **2019**, *137*, 48759. [CrossRef]

115. Tohidlou, H.; Shafiei, S.; Abbasi, S.; Asadi-Eydivand, M.; Fathi-Roudsari, M. Amine-functionalized Single-walled Carbon Nanotube/Polycaprolactone Electrospun Scaffold for Bone Tissue Engineering: In vitro Study. *Fibers Polym.* **2019**, *20*, 1869–1882. [CrossRef]

116. Zadehnajar, P.; Akbari, B.; Karbasi, S.; Mirmusavi, M.H. Preparation and characterization of poly ε-caprolactone-gelatin/multi-walled carbon nanotubes electrospun scaffolds for cartilage tissue engineering applications. *Int. J. Polym. Mater.* **2019**, *69*, 326–337. [CrossRef]

117. Tondnevis, F.; Keshvari, H.; Mohandesi, J.A. Fabrication, characterization, and in vitro evaluation of electrospun polyurethane-gelatin-carbon nanotube scaffolds for cardiovascular tissue engineering applications. *J. Biomed. Mater. Res. Part B Appl. Biomater.* **2020**, *108*, 2276–2293. [CrossRef]

118. Stocco, T.D.; Antonioli, E.; Romagnolli, M.L.; Sousa, G.F.; Ferretti, M.; Lobo, A.O. Aligned biomimetic scaffolds based on carbon nanotubes-reinforced polymeric nanofibers for knee meniscus tissue engineering. *Mater. Lett.* **2020**, *264*, 127351. [CrossRef]

119. Mao, H.; Kawazoe, N.; Chen, G. Cell response to single-walled carbon nanotubes in hybrid porous collagen sponges. *Colloids Surfaces B Biointerfaces* **2015**, *126*, 63–69. [CrossRef]

120. Chen, J.; Zou, X.-N. Self-assemble peptide biomaterials and their biomedical applications. *Bioact. Mater.* **2019**, *4*, 120–131. [CrossRef]

121. Zhang, S.; Xing, M.; Li, B. Biomimetic Layer-by-Layer Self-Assembly of Nanofilms, Nanocoatings, and 3D Scaffolds for Tissue Engineering. *Int. J. Mol. Sci.* **2018**, *19*, 1641. [CrossRef]

122. Zhang, T.; Zhang, H.; Zhang, L.; Shuaijun, J.; Liu, J.; Xiong, Z.; Sun, W. Biomimetic design and fabrication of multilayered osteochondral scaffolds by low-temperature deposition manufacturing and thermal-induced phase-separation techniques. *Biofabrication* **2017**, *9*, 025021. [CrossRef]

123. Kundu, J.; Pati, F.; Shim, J.-H.; Cho, D.-W. *Rapid Prototyping Technology for Bone Regeneration*; Elsevier BV: Amsterdam, The Netherlands, 2014; pp. 254–284.

124. Noh, I. *Biomimetic Medical Materials: From Nanotechnology to 3D Bioprinting*; Springer: Singapore, 2018.

125. Moniruzzaman, M.; O'Neal, C.; Bhuiyan, A.; Egan, P.F. Design and Mechanical Testing of 3D Printed Hierarchical Lattices Using Biocompatible Stereolithography. *Designs* **2020**, *4*, 22. [CrossRef]

126. Gungor-Ozkerim, P.S.; Inci, I.; Zhang, Y.S.; Khademhosseini, A.; Dokmeci, M.R. Bioinks for 3D bioprinting: An overview. *Biomater. Sci.* **2018**, *6*, 915–946. [CrossRef]

127. Axpe, E.; Oyen, M.L. Applications of Alginate-Based Bioinks in 3D Bioprinting. *Int. J. Mol. Sci.* **2016**, *17*, 1976. [CrossRef] [PubMed]

128. Klotz, B.J.; Gawlitta, D.; Rosenberg, A.J.; Malda, J.; Melchels, F.P. Gelatin-Methacryloyl Hydrogels: Towards Biofabrication-Based Tissue Repair. *Trends Biotechnol.* **2016**, *34*, 394–407. [CrossRef]

129. Poldervaart, M.T.; Goversen, B.; De Ruijter, M.; Abbadessa, A.; Melchels, F.P.W.; Oner, F.C.; Dhert, W.J.A.; Vermonden, T.; Alblas, J. 3D bioprinting of methacrylated hyaluronic acid (MeHA) hydrogel with intrinsic osteogenicity. *PLoS ONE* **2017**, *12*, e0177628. [CrossRef] [PubMed]

130. Wu, D.; Yu, Y.; Tan, J.; Huang, L.; Luo, B.; Lu, L.; Zhou, C. 3D bioprinting of gellan gum and poly (ethylene glycol) diacrylate based hydrogels to produce human-scale constructs with high-fidelity. *Mater. Des.* **2018**, *160*, 486–495. [CrossRef]

131. Li, J.; Chen, M.; Fan, X.-Q.; Zhou, H. Recent advances in bioprinting techniques: Approaches, applications and future prospects. *J. Transl. Med.* **2016**, *14*, 271. [CrossRef] [PubMed]

132. Piard, C.; Baker, H.; Kamalitdinov, T.; Fisher, J.P. Bioprinted osteon-like scaffolds enhance in vivo neovascularization. *Biofabrication* **2019**, *11*, 025013. [CrossRef]

133. Gao, G.; Schilling, A.F.; Yonezawa, T.; Wang, J.; Dai, G.; Cui, X. Bioactive nanoparticles stimulate bone tissue formation in bioprinted three-dimensional scaffold and human mesenchymal stem cells. *Biotechnol. J.* **2014**, *9*, 1304–1311. [CrossRef]

134. Kérourédan, O.; Hakobyan, D.; Rémy, M.; Ziane, S.; Dusserre, N.; Fricain, J.-C.; Delmond, S.; Thébaud, N.B.; Devillard, R. In situ prevascularization designed by laser-assisted bioprinting: Effect on bone regeneration. *Biofabrication* **2019**, *11*, 045002. [CrossRef]

135. Wan, Z.; Zhang, P.; Liu, Y.; Lv, L.; Zhou, Y. Four-dimensional bioprinting: Current developments and applications in bone tissue engineering. *Acta Biomater.* **2019**, *101*, 26–42. [CrossRef]

136. Hendrikson, W.J.; Rouwkema, J.; Clementi, F.; Van Blitterswijk, C.A.; Fare', S.; Moroni, L. Towards 4D printed scaffolds for tissue engineering: Exploiting 3D shape memory polymers to deliver time-controlled stimulus on cultured cells. *Biofabrication* **2017**, *9*, 031001. [CrossRef] [PubMed]

137. Wu, J.; Zheng, K.; Huang, X.; Liu, J.; Liu, H.; Boccaccini, A.R.; Wan, Y.; Guo, X.; Shao, Z. Thermally triggered injectable chitosan/silk fibroin/bioactive glass nanoparticle hydrogels for in-situ bone formation in rat calvarial bone defects. *Acta Biomater.* **2019**, *91*, 60–71. [CrossRef] [PubMed]

138. Balmer, T.W.; Vesztergom, S.; Broekmann, P.; Stahel, A.; Büchler, P. Characterization of the electrical conductivity of bone and its correlation to osseous structure. *Sci. Rep.* **2018**, *8*, 8601. [CrossRef]

139. Cui, H.; Yu, Y.; Li, X.; Sun, Z.; Ruan, J.; Wu, Z.L.; Qian, J.; Yin, J. Direct 3D printing of a tough hydrogel incorporated with carbon nanotubes for bone regeneration. *J. Mater. Chem. B* **2019**, *7*, 7207–7217. [CrossRef]

140. Wang, W.; Huang, B.; Byun, J.J.; Bartolo, P. Assessment of PCL/carbon material scaffolds for bone regeneration. *J. Mech. Behav. Biomed. Mater.* **2019**, *93*, 52–60. [CrossRef]

141. Huang, B.; Vyas, C.; Byun, J.J.; El-Newehy, M.; Huang, Z.; Bartolo, P. Aligned multi-walled carbon nanotubes with nanohydroxyapatite in a 3D printed polycaprolactone scaffold stimulates osteogenic differentiation. *Mater. Sci. Eng. C* **2020**, *108*, 110374. [CrossRef]

142. Beheshtizadeh, N.; Lotfibakhshaiesh, N.; Pazhouhnia, Z.; Hoseinpour, M.; Nafari, M. A review of 3D bio-printing for bone and skin tissue engineering: A commercial approach. *J. Mater. Sci.* **2019**, *55*, 3729–3749. [CrossRef]

143. Saravanan, S.; Leena, R.; Selvamurugan, N. Chitosan based biocomposite scaffolds for bone tissue engineering. *Int. J. Boil. Macromol.* **2016**, *93*, 1354–1365. [CrossRef]

144. Bruyas, A.; Lou, F.; Stahl, A.M.; Gardner, M.J.; Maloney, W.J.; Goodman, S.; Yang, Y.P. Systematic characterization of 3D-printed PCL/β-TCP scaffolds for biomedical devices and bone tissue engineering: Influence of composition and porosity. *J. Mater. Res.* **2018**, *33*, 1948–1959. [CrossRef]

145. Gorain, B.; Choudhury, H.; Pandey, M.; Kesharwani, P.; Abeer, M.M.; Tekade, R.K.; Hussain, Z. Carbon nanotube scaffolds as emerging nanoplatform for myocardial tissue regeneration: A review of recent developments and therapeutic implications. *Biomed. Pharmacother.* **2018**, *104*, 496–508. [CrossRef] [PubMed]

146. Cui, L.; Liang, J.; Liu, M.H.; Zhang, K.; Li, J. Nanomaterials for Angiogenesis in Skin Tissue Engineering. *Tissue Eng. Part B Rev.* **2020**, *26*, 203–216. [CrossRef] [PubMed]

147. Costa, P. Translating Biofabrication to the Market. *Trends Biotechnol.* **2019**, *37*, 1032–1036. [CrossRef] [PubMed]

Tomasz Szymański
Faculty of Chemistry;
Laboratory of Applied Biotechnology
Center for Advanced Technology
Adam Mickiewicz University in Poznań
e-mail: tomszy1@amu.edu.pl

Author contribution statement

I declare that I am the co-author of the article "**Utilization of Carbon Nanotubes in Manufacturing of 3D Cartilage and Bone Scaffolds**" by Tomasz Szymański, Adam Aron Mieloch, Magdalena Richter, Tomasz Trzeciak, Ewa Florek, Jakub Dalibor Rybka and Michael Giersig published in *Materials* in 2020. The author's contribution is as follows:

Tomasz Szymański was responsible for the idea on the paper, literature collection, writing the original draft and preparation of figures.

Adam Aron Mieloch was responsible for the revision of the original draft.

Magdalena Richter was a critical reviewer of the part concerning cartilage and bone tissue anatomy, as well as methods of treatment.

Tomasz Trzeciak was a critical reviewer of the part concerning cartilage and bone tissue anatomy, as well as methods of treatment.

Ewa Florek was a critical reviewer of the part concerning MWCNTs toxicity in *in vitro* and *in vivo* experiments.

Jakub Dalibor Rybka was responsible for conceptualization, revised the original draft and was a critical reviewer of the part regarding MWCNTs and tissue engineering. He was also responsible for the correspondence with journals and reviewers.

Michael Giersig revised the original draft.

Date: 8.12.2023

Signature: _Szymański_

prof. UAM dr hab. inż. Jakub D. Rybka

Dr Adam Mieloch
Laboratory of Applied Biotechnology
Center for Advanced Technology
Adam Mickiewicz University in Poznań
e-mail: amieloch@amu.edu.pl

Author contribution statement

I declare that I am the co-author of the article "**Utilization of Carbon Nanotubes in Manufacturing of 3D Cartilage and Bone Scaffolds**" by Tomasz Szymański, Adam Aron Mieloch, Magdalena Richter, Tomasz Trzeciak, Ewa Florek, Jakub Dalibor Rybka and Michael Giersig published in *Materials* in 2020. The author's contribution is as follows:

Tomasz Szymański was responsible for the idea on the paper, literature collection, writing the original draft and preparation of figures.

Adam Aron Mieloch was responsible for the revision of the original draft.

Magdalena Richter was a critical reviewer of the part concerning cartilage and bone tissue anatomy, as well as methods of treatment.

Tomasz Trzeciak was a critical reviewer of the part concerning cartilage and bone tissue anatomy, as well as methods of treatment.
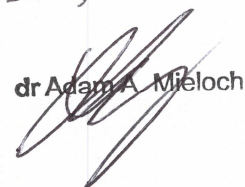
Ewa Florek was a critical reviewer of the part concerning MWCNTs toxicity in *in vitro* and *in vivo* experiments.

Jakub Dalibor Rybka was responsible for conceptualization, revised the original draft and was a critical reviewer of the part regarding MWCNTs and tissue engineering. He was also responsible for the correspondence with journals and reviewers.

Michael Giersig revised the original draft.

Date: 04.12.2023

Signature: dr Adam A. Mieloch

Dr hab. inż. Jakub Rybka, prof. UAM
Laboratory of Applied Biotechnology
Center for Advanced Technology
Adam Mickiewicz University in Poznań
e-mail: jrybka@amu.edu.pl

Author contribution statement

I declare that I am the co-author of the article "**Utilization of Carbon Nanotubes in Manufacturing of 3D Cartilage and Bone Scaffolds**" by Tomasz Szymański, Adam Aron Mieloch, Magdalena Richter, Tomasz Trzeciak, Ewa Florek, Jakub Dalibor Rybka and Michael Giersig published in *Materials* in 2020. The author's contribution is as follows:

Tomasz Szymański was responsible for the idea on the paper, literature collection, writing the original draft and preparation of figures.

Adam Aron Mieloch was responsible for the revision of the original draft.

Magdalena Richter was a critical reviewer of the part concerning cartilage and bone tissue anatomy, as well as methods of treatment.

Tomasz Trzeciak was a critical reviewer of the part concerning cartilage and bone tissue anatomy, as well as methods of treatment.

Ewa Florek was a critical reviewer of the part concerning MWCNTs toxicity in *in vitro* and *in vivo* experiments.

Jakub Dalibor Rybka was responsible for conceptualization, revised the original draft and was a critical reviewer of the part regarding MWCNTs and tissue engineering. He was also responsible for the correspondence with journals and reviewers.

Michael Giersig revised the original draft.

Date: 08. 01. 2024

Signature: prof. UAM dr hab. inż. Jakub D. Rybka

Michael Giersig

Department of Theory of Continuous Media and Nanostructures),
Institute of Fundamental Technological Research
Polish Academy of Sciences
Ul. Pawińskiego 5B; 02-106 Warsaw, Poland;
e-mail: mgiersig@ippt.pan.pl

Author contribution statement

I declare that I am the co-author of the article "**Utilization of Carbon Nanotubes in Manufacturing of 3D Cartilage and Bone Scaffolds**" by Tomasz Szymański, Adam Aron Mieloch, Magdalena Richter, Tomasz Trzeciak, Ewa Florek, Jakub Dalibor Rybka and Michael Giersig published in *Materials* in 2020. The author's contribution is as follows:

Tomasz Szymański was responsible for the idea on the paper, literature collection, writing the original draft and preparation of figures.

Adam Aron Mieloch was responsible for the revision of the original draft.

Magdalena Richter was a critical reviewer of the part concerning cartilage and bone tissue anatomy, as well as methods of treatment.

Tomasz Trzeciak was a critical reviewer of the part concerning cartilage and bone tissue anatomy, as well as methods of treatment.

Ewa Florek was a critical reviewer of the part concerning MWCNTs toxicity in *in vitro* and *in vivo* experiments.

Jakub Dalibor Rybka was responsible for conceptualization, revised the original draft and was a critical reviewer of the part regarding MWCNTs and tissue engineering. He was also responsible for the correspondence with journals and reviewers.

Michael Giersig revised the original draft.

Date: 2 2. 01. 2024

Signature: *prof. dr hab. Michał Giersig*

Magdalena Richter

Department of Orthopedics and Traumatology,
Poznań University of Medical Sciences,
28 czerwca 1956r. Street No. 135/147,
61-545 Poznan, Poland;
e-mail: mrichter@ump.edu.pl

Author contribution statement

I declare that I am the co-author of the article "**Utilization of Carbon Nanotubes in Manufacturing of 3D Cartilage and Bone Scaffolds**" by Tomasz Szymański, Adam Aron Mieloch, Magdalena Richter, Tomasz Trzeciak, Ewa Florek, Jakub Dalibor Rybka and Michael Giersig published in *Materials* in 2020. The author's contribution is as follows:

Tomasz Szymański was responsible for the idea on the paper, literature collection, writing the original draft and preparation of figures.

Adam Aron Mieloch was responsible for the revision of the original draft.

Magdalena Richter was a critical reviewer of the part concerning cartilage and bone tissue anatomy, as well as methods of treatment.

Tomasz Trzeciak was a critical reviewer of the part concerning cartilage and bone tissue anatomy, as well as methods of treatment.

Ewa Florek was a critical reviewer of the part concerning MWCNTs toxicity in *in vitro* and *in vivo* experiments.

Jakub Dalibor Rybka was responsible for conceptualization, revised the original draft and was a critical reviewer of the part regarding MWCNTs and tissue engineering. He was also responsible for the correspondence with journals and reviewers.

Michael Giersig revised the original draft.

Date: 08.01.2024

Signature: Richter

MDPI

Article

Carbon Nanotubes Interference with Luminescence-Based Assays

Tomasz Szymański [1,2], **Marcelina Kempa** [1,3], **Michael Giersig** [1,4] **and Jakub Dalibor Rybka** [1,*]

[1] Center for Advanced Technology, Adam Mickiewicz University, Uniwersytetu Poznańskiego 10 Street, 61-614 Poznan, Poland; tszymanski@amu.edu.pl (T.S.); marcelina.kempa@op.pl (M.K.); giersig@amu.edu.pl (M.G.)

[2] Faculty of Chemistry, Adam Mickiewicz University, Uniwersytetu Poznańskiego 8 Street, 61-614 Poznan, Poland

[3] Faculty of Biology, Adam Mickiewicz University, Uniwersytetu Poznańskiego 6, 61-614 Poznań, Poland

[4] Department of Physics, Institute of Experimental Physics, Freie Universität, Arnimallee 14, 14195 Berlin, Germany

[*] Correspondence: jrybka@amu.edu.pl; Tel.: +48-61-829-1875

check for updates

Abstract: Carbon nanotubes (CNTs) are one of the most promising nanomaterials synthesized to date. Thanks to their unique mechanical, electronic, and optical properties, they have found a wide application in electronics in the production of biosensors and nanocomposites. The functionalization of multiwalled carbon nanotubes (MWCNTs) is aimed at making them biocompatible by adding hydrophilic groups on their surface, increasing their solubility and thus rendering them applicable in the regenerative medicine. So far, there is conflicting information about carbon nanotubes in biological systems. This paper investigates the effect of functionalized, oxidized, multiwalled carbon nanotubes (MWCNT-Ox) on the cytotoxicity of normal human articular chondrocytes (NHAC-kn cell line). Since absorbance-based and fluorescence-based assays were shown to interfere with carbon nanotubes, luminescence-based tests were carried out, as they work on a different method of detection and provide advantages over the mentioned ones. Cell viability and reactive oxygen species (ROS) tests were carried out. The cell viability assay showed that with the increasing MWCNTs concentration, the number of viable chondrocytes was significantly decreasing. Exposure to MWCNT-Ox indicated oxidative stress in the lowest investigated concentration with a decreased amount of ROS with higher concentrations. However, control experiments with adenosine triphosphate (ATP) and H_2O_2—molecules that are detected by the assays—showed that carbon nanotubes interfere directly with measurement, thus rendering the results unreliable. To understand the exact interference mechanisms, further studies must be taken. In conclusion, this study shows that luminescence-based tests yield erroneous results, confirming that in vitro experiments in the literature concerning carbon nanotubes should be analyzed with caution.

Keywords: tissue engineering; biomaterials; carbon nanotubes; scaffolds; cytotoxicity; chondrocytes

1. Introduction

1.1. Carbon Nanotubes (CNTs)

Carbon nanotubes (CNTs) are allotropic forms of carbon, made of cylindrical folded graphene layers discovered by Sumio Iijima in 1991 [1]. They constitute a diverse group of nanomaterials in terms of structure, size, shape, and properties. The carbon nanotube has a honeycomb-shaped hexagonal graphene network that periodically repeats in space, which gives CNTs impressive mechanical,

physico-chemical, and optical properties. The diameter of nanotubes is expressed in nanometers, while the length of nanotubes can be up to several millimeters. The ratio of their length to the diameter is in the range of 10:3 to 10:5 [2–4]. There are two types of carbon nanotubes: single-walled carbon nanotubes (SWCNTs) and multiwalled carbon nanotubes (MWCNTs). SWCNTs are made of a single, cylindrical rolled graphene layer. The diameter of most single-walled carbon nanotubes reaches 1 nm. MWCNTs are made of many concentrically rolled individual graphene layers forming a cylindrical structure [5].

Due to the unique properties, nanotubes have enormous application potential and are the subject of research for scientists around the world. The mechanical properties of CNTs result from the combination of rigidity, strength, and flexibility; they also possess exceptional conductive and thermal properties [5,6]. Therefore, they are applied in many fields, such as materials science [7], medicine [8–11] electronics [12], and energy storage [13].

1.2. CNTs Toxicity

Since nanotechnology is one of the dynamically developing fields, and its products can be widely used in medicine, the food industry, and electronics, it is necessary to know exactly the nature and impact of CNTs on the health and functioning of the body. This is especially important for the biomedical use of carbon nanotubes. In recent years, researchers' interest in the use of scaffolds from CNTs for the production of implants has grown, among others, for the treatment of cartilage injuries [14–18]. Carbon nanotubes are attractive for this type of application due to their very high mechanical strength, excellent flexibility, and size, similar to extracellular matrix (ECM) molecules [19]. There is a number of studies that show the positive impact of CNTs on cells, stimulating their proliferation and proper metabolism [20–23]. However, it was noticed that 3D cultured chondrocytes showed higher tolerance to increasing concentration of carbon nanotubes, compared to 2D culture in which viability decreased with increasing amounts of CNTs. Differences in cell survival in 2D cultures may be caused by carbon nanotubes diffusion into the medium, which facilitates cellular uptake by endocytosis. In 3D culture, carbon nanotubes are embedded in a hydrogel matrix, which limits their ability to be absorbed by the cells [24]. On the other hand, there is much research, carried out either in vitro or in vivo showing that carbon nanotubes are toxic to cells in many aspects [25–27].

It was shown that size [28], level of aggregation [29], dose [30], surface modification [31], and purity [32] all have an impact on toxicity. It was also shown that CNTs may cause reactive oxygen species (ROS) production [33]. Carbon nanotubes are characterized by a highly hydrophobic character and very poor solubility in polar and non-polar solvents. Additionally, after synthesis, carbon nanotubes are contaminated with large amounts of amorphous carbon and catalyst particles, e.g., iron, nickel [34].

The initial methods of purification and functionalization of nanotubes are designed to introduce changes in their structure and increase solubility, e.g., in aqueous solutions, which makes it possible to use CNTs in biological systems [19].

1.3. CNTs Interactions with Biological Assays

When determining the influence of CNTs on a cell in vitro, the well-established assays are often performed, such as MTT, MTS, WST-1, and LDH measurement. As was described, CNTs interact with a plethora of molecules. The nature of these interactions has been researched and is attributed mainly to van der Waals forces and π–π stacking [35]. Some studies that show interference with widely used molecular assays based on absorbance and fluorescence. Wörle-Knirsch et al. performed MTT assay on A549 cells with various doses of SWCNTs and a strong cytotoxic effect was observed of almost 60% [36]. However, different tests—WST-1, LDH assay, mitochondrial membrane potential, and Annexin V measured by flow cytometry—have not confirmed these results and showed that SWCNTs have a negligible effect on cellular function. Interestingly, MTT and WST-1 tests are based on the same principle—they measure the absorption of the formazan crystals formed by the reduction of

tetrazolium substrate by living cells. The only difference between these two tests is that in MTT assay, the end product is water-insoluble, contrary to the WST-1 test, where formed crystals are hydrophilic. Researchers found in TEM images precipitates attached to the SWCNTs that were treated with the MTT test, and no such precipitates on SWCNTs from the WST-1 test. They attribute it to the strong adsorption of insoluble crystals to the surface of carbon nanotubes, yielding false-positive results, since adsorbed crystals are not detected during measurement. Casey et al. assessed the interaction of SWCNTs with a broad panel of indicator dyes that are used routinely for the cellular viability measurement—Comassie Blue, Alamar Blue[TM] (AB), Neutral Red (NR), MTT, and WST-1—on the same A549 cell line [37]. He determined by spectroscopic measurements that SWCNTs interact with varying degrees with each of those tests, even WST-1 assay, resulting potentially in false-positive outcomes. Such results cast doubt on the validity of such experiments carried out in other research.

The investigated tests are based either on absorbance or fluorescence measurement. These are well-established, relatively cheap, widely used assays that are suitable for use in multiwell-plate formats and high-throughput screening. Since carbon nanotubes are heavily researched in the biomedical and bioengineering field and consensus about their toxicity is not yet reached, there is a need to have such a tool that could be applied for carbon nanotubes experiments and would not interfere with the tested compound. In terms of existing technologies, there is one more, which to our knowledge was not tested with carbon nanotubes: luminescence-based assays. Here, the luminescent signal is generated upon the interaction of recombinant luciferase with the measured substance. There are a few advantages of this technology compared to absorbance and fluorescence-based assays: (1) luminescence is a continuous light source, which is produced 'in situ', without the need for an external light source, (2) the signal generated by existing recombinant luciferases are stable for hours, (3) very high sensitivity, because the emitted light is broad across many wavelengths (with a peak emission wavelength $\lambda = 565$ nm), and since eukaryotic cells do not intrinsically produce light, sample background is very low [38].

Taking into account these features, such assays seems promising to use with carbon nanotubes.

The purpose of this work is to measure the impact of functionalized, multiwalled carbon nanotubes (MWCNT-Ox) on the viability and reactive oxygen species using luminescent-based tests and determine whether MWCNTs interact with the luminescent signal generated in the assays.

2. Materials and Methods

2.1. MWCNTs

MWCNTs with a diameter of 15–30 nm, length of 15–20 μm, and purity of up to 95% produced by chemical vapor deposition (CVD) were supplied by Nanolab Inc., Boston, MA, USA

2.2. MWCNTs Functionalization

MWCNTs were functionalized to oxidize their surface according to the following method. First, 30 mg of MWCNTs were sonicated at 70 °C in a mixture of concentrated sulfur VI (H_2SO_4) and nitric V (HNO_3) acids in a 3:1 ratio. Then, the mixture was neutralized with 300 mL of 3M sodium hydroxide (NaOH). The purification of oxidized carbon nanotubes was carried out through a centrifugation cycle at the speed 9000× *g*, 20 °C for (a) 15 min, (b) 30 min, and (c) 40 min, with subsequent centrifugation at 12,000× *g*, 4 °C for 40 min. The resulting carbon nanotubes solution was dried using a vacuum evaporator. MWCNTs were suspended in phosphate buffer (PBS). The thermogravimetric method determined the mass of nanotubes in a given volume of solution, and on this basis, the MWCNT-Ox concentration was determined.

2.3. MWCNTs Characterization

MWCNTs were characterized using scanning electron microscopy (SEM) to confirm their size and subsequent energy-dispersive X-ray spectroscopy (EDS) analysis to check their purity before and after functionalization. The experiments were carried out on high-resolution Quanta 250 FEG,

FEI, microscope. Diameters of MWCNTs were measured with ImageJ software. Fourier-transform infrared spectroscopy (FTIR,) was performed to check the level of functionalization. Briefly, 2 mg of dried MWCNTs and functionalized, oxidized, multiwalled carbon nanotubes (MWCNTs-Ox) were mixed with 250 mg of KBr. The mixture was pressed to form a pellet and was degassed under vacuum. The pellet was analyzed on a Jasco 4700A spectrometer (Jasco Corporation, Tokio, Japan), and the IR spectra were obtained within the range of 4000–400 cm^{-1} with the resolution of 1 cm^{-1}.

2.4. Cell Culture

The studies were carried out on the established NHAC-kn normal human articular cartilage cell line (Lonza Group, Basel, Switzerland). Cells were cultured in full culture medium composed of DMEM (Corning Inc., Corning, NY, USA) supplemented with 10% fetal bovine serum (FBS) (Corning), 1% penicillin/streptomycin (Corning), and 50 μg/mL 2-phospho-L-ascorbic acid trisodium salt (Sigma Aldrich), at 37 °C and 5% CO$_2$. Cells were grown on 75 cm^2 flasks, and when confluence reached ≈80%, cells were detached with TrypLE™ Express Enzyme (Thermo Fisher Scientific, Waltham, MA, USA. For experiments, cells were plated at the density of 1×10^4 cells/well in opaque, white 96-well plates with the clear bottom in a volume of full culture medium specified in the manufacturers' protocol. Cells were allowed to attach and grow for 24 h. After this time, growth medium was discarded and replaced with fresh medium or solutions of appropriate concentrations (0.0625 mg/mL, 0.25 mg/mL, 0.5 mg/mL, 1 mg/mL), diluted in full fresh medium.

2.5. Viability Test

The test used in the experiment was CellTiter-Glo$^{®}$ Luminescent Cell Viability Assay (Promega, Madison, WI, USA). It determines the number of viable, metabolically active cells based on the quantitative ATP assay. As a result of cell lysis, ATP is released and a luminescent signal is generated, which is proportional to the number of live cells.

The experiment was carried out according to the manufacturer protocol. NHAC-kn cells were plated on an opaque, white 96-well plate with clear bottom (1×10^4 cells/well) with MWCNTs-Ox concentrations: 0.0625 mg/mL, 0.25 mg/mL, 0.5 mg/mL, and 1 mg/mL in a volume of 100 μL/well and incubated for 48 h at 37 °C and 5% CO$_2$. Doxorubicin at a concentration of 350 μg/mL was used as a positive control [39]. After 48 h incubation, the assay was performed. The luminescent signal was read (from the top) using a microplate reader (Infinite$^{®}$ 200 PRO, TECAN, Männedorf, Switzerland).

2.6. ROS Assay

To determine the reactive oxygen species production, ROS-Glo™ H$_2$O$_2$ Assay (Promega, Madison, WI, USA) was used. The test is based on a substrate that reacts directly with hydrogen peroxide to form the luciferin precursor. The addition of recombinant luciferase and D-cysteine leads to the conversion of the luciferin precursor into luciferin, which then reacts with the enzyme to generate a luminescent signal. The luminescence signal is proportional to the amount of H$_2$O$_2$. The experiment was carried out according to the manufacturer's protocol. NHAC-kn cells were plated on an opaque, white 96-well plate with a clear bottom (1×10^4 cells/well) with MWCNTs-Ox concentrations of 0.0625, 0.25, 0.5, and 1 mg/mL in a volume of 80 μL/well and incubated 24 h at 37 °C and 5% CO$_2$. Menadione at a concentration of 100 μM was used as a positive control and added 8 h before measurement. After 48 h, the level of ROS was measured, using a microplate reader (Infinite$^{®}$ 200 PRO, TECAN, Männedorf, Switzerland).

2.7. Measurement of MWCNTs Absorption and Luminescence Spectra

To determine the absorption spectra of MWCNT-Ox, 100 μL of 0.0625, 0.25, 0.5, and 1 mg/mL MWCNT-Ox solutions diluted in growth medium were put into a 96-well plate, and the absorbance was measured within the range of 260 to 1000 nm, with 2 nm intervals. As a reference, PBS and growth medium in the same amount as in the sample were used. The measured optical densities (ODs) were

subtracted from the MWCNT-Ox ODs. Measurements were performed on an Infinite® 200 PRO, TECAN (Männedorf, Switzerland) microplate reader.

Luminescence spectra were obtained on a Cary Eclipse Spectrofluorimeter (Agilent, Santa Clara, CA, USA) for the same concentrations of MWCNTs-Ox, diluted in PBS. First, 30 μL of 1 μM ATP solution and 100 μL of CellTiter-Glo® reagent was added to MWCNTs solutions. After 10 min, 100 μL of the prepared solutions were added to a quartz cuvette, and the measurement of emitted light was performed, with the emission range from 400 to 700 nm, 1 nm interval. Intensities of light were expressed in arbitrary units (A.U.).

2.8. MWCNTs Interference with Luminescence

For CellTiter-Glo® Luminescent Cell Viability Assay, 100 μL of MWCNTs-Ox in concentrations of 0.0625, 0.25, 0.5, and 1 mg/mL was incubated with 1 μM ATP solution for 24 h at 37 °C and 5% CO_2. The ATP concentration was taken from the manufacturers' protocol, as it is suggested to be used for a standard curve preparation. Accordingly, for the interference with ROS-Glo ™ H_2O_2 Assay, 10 μM of H_2O_2 was added to the MWCNTs solutions. The test was performed immediately after the addition of H_2O_2 due to its chemical instability. The luminescent signal was read using the Infinite® 200 PRO, TECAN microplate reader.

3. Results

3.1. MWCNTs Characterization

SEM of both MWCNTs (Figure 1A,B) and functionalized MWCNT-Ox (Figure 1C,D), confirmed the diameters of the CNTs provided by the manufacturer—they are between 15–30 nm, as measured with the ImageJ software (Figure 1B).
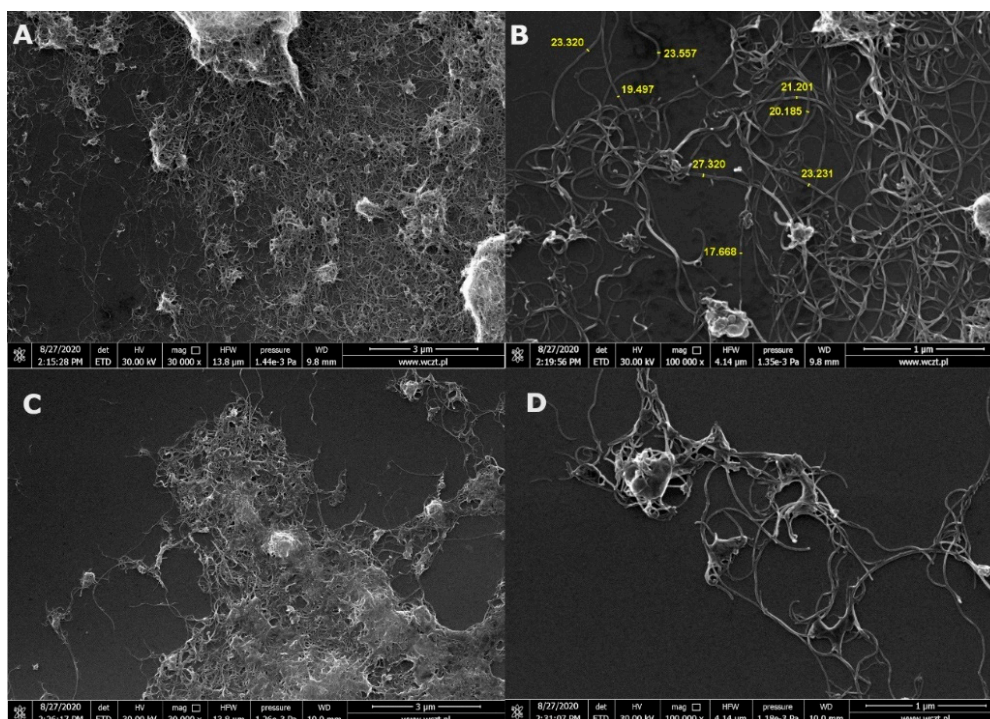

Figure 1. Scanning electron microscopy (SEM) images of both multiwalled carbon nanotubes (MWCNTs) (**A**,**B**) and functionalized oxidized, multiwalled carbon nanotubes (MWCNT-Ox) (**C**,**D**).

Visible aggregates were formed for the MWCNT sample because MWCNT powder was dissolved in ethanol in order to apply them on the silica grid. MWCNT-Ox was already dissolved in PBS.

EDS analysis for MWCNTs (Figure 2A) showed aluminum impurities, which is the leftover after synthesis (most probably, an aluminum-based material was used as a support in CVD synthesis).
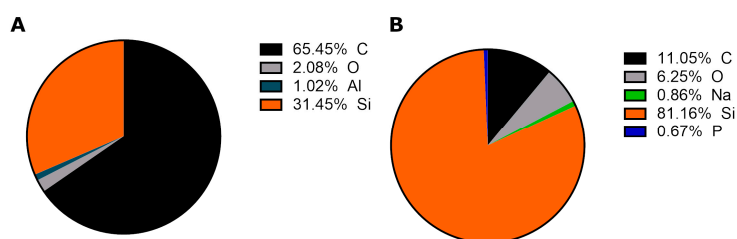

Figure 2. EDS analysis of MWCNTs (**A**) and functionalized MWCNT-Ox (**B**).

However, aluminum is not visible after functionalization (Figure 2B). The reaction reagents are concentrated strong acids—sulfuric and nitric, which dissolve the residual metal, and it is subsequently removed with the series of washes. The sodium and phosphorus come from the PBS—a buffer, in which the sample was dissolved. The signal from silicon is derived from the silicon mount used in SEM, and oxygen in the MWCNTs sample may derive from the ethanol used for solubilization of the MWCNTs in powder form to apply them on the mount.

FTIR spectra were obtained to compare surface groups on MWCNTs before and after functionalization (Figure 3).
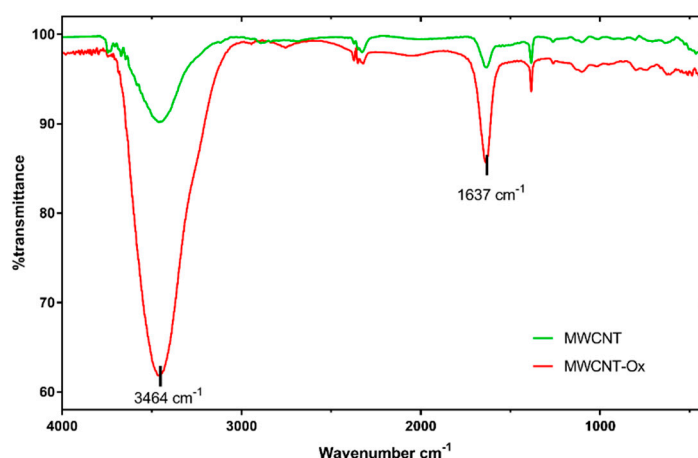
Figure 3. Fourier-transform infrared spectroscopy (FTIR) spectra of pristine MWCNTs and MWCNT-Ox.

There is a vast decrease in transmittance in two peaks in the MWCNT-Ox spectrum compared to pristine MWCNT. The first peak at 3464 cm^{-1} is a characteristic of the O-H stretch of a hydroxyl group, which can be ascribed to the oscillation of carboxyl groups. The peak at 1637 cm^{-1} corresponds to carbonyl groups, which were formed in the place of new defects and further oxidation during the functionalization reaction. They may also be a part of the carboxyl group. In conclusion, the FTIR spectra show that MWCNTs were oxidized.

3.2. Chondrocyte Viability

After 48 h of incubation with MWCNT-Ox solutions, chondrocytes exhibited a significant decrease in the luminescent signal. At the lowest concentration, i.e., 0.0625 mg/mL, the measured signal shows that the viability of chondrocytes decreased by half compared to control, and it is decreasing with each subsequent concentration, suggesting the deaths of most of the cells (Figure 4).
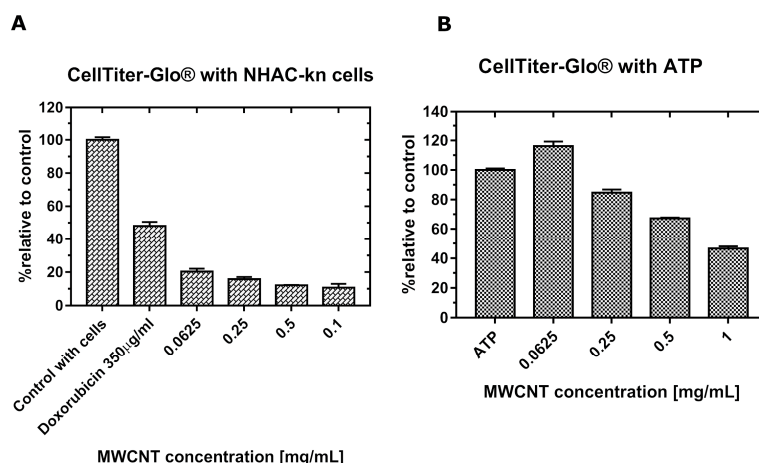
Figure 4. The plots represent relative cytotoxicity of MWCNT-Ox on NHAC-kn cells after 48 h (**A**) and signal of luminescence measured with the same concentrations of ATP and various concentrations of MWCNTs (**B**). Interference with the luminescent signal is visible. Doxorubicin as a positive control caused the death of over 50% of the cells.

3.3. ROS Assay

As in the test described above, the thermostable recombinant Ultra-Glo™ luciferase was used to convert the luciferin precursor to luciferin. As a positive control, 100 µM menadione—an organic chemical compound from the quinone group that induces the formation of reactive oxygen species was used, and this sample showed an over 4-fold increase in ROS production over control. The levels of hydrogen peroxide generation are shown in Figure 5.
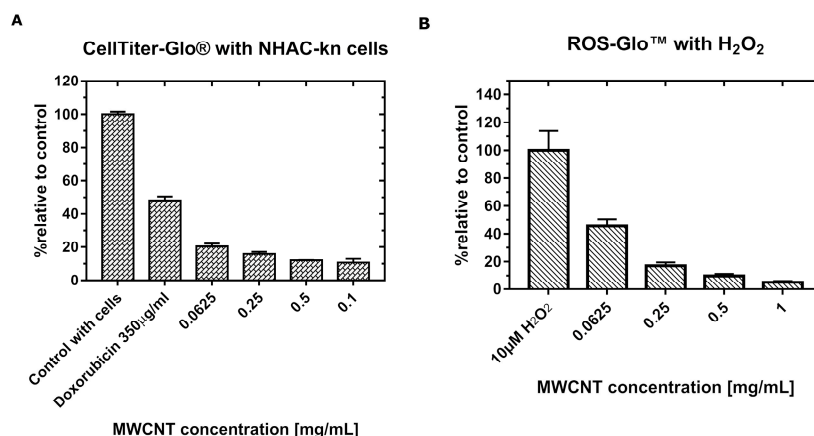
Figure 5. The plots represent the relative production of reactive oxygen species (ROS) in NHAC-kn cells after 48 h incubation with MWCNT-Ox (**A**) and signal of luminescence measured with the same concentrations of H_2O_2 and various concentrations of MWCNTs-Ox (**B**). A strong decrease in the luminescent signal is visible with increasing amounts of carbon nanotubes.

After 48 h of incubation of the cells with the MWCNT-Ox solutions, in the lowest examined concentration (0.0625 mg/mL), the signal was higher than in control. Then, with increasing concentrations, the signal is strongly diminished, which may suggest very low H_2O_2 production. However, when this result is compared to the viability test (Figure 4), this may be attributed to the much lower viable cell number.

Moreover, the experiment with MWNCTs and the same concentrations of H_2O_2 revealed strong interference with the signal. There are two possible mechanisms of these interactions: (1) MWCNTs scatter a luminescent signal or (2) ROS are scavenged by the MWCNTs, and both of these actions can

occur concomitantly. There is an indication that the latter mechanism occurs because the inhibition of the signal is stronger than measured with ATP.

3.4. Determination of Absorption and Luminescence Spectra

Recorded relative levels of absorbance show that relative absorbance increases significantly with increasing MWCNTs concentrations. As can be observed in Figure 6A, MWCNTs absorb a wide spectrum of light, which overlaps partly with the spectrum of light emitted by luciferase from CellTiterGlo assay (Figure 6B), with the maximum emission at λ = 532 nm.
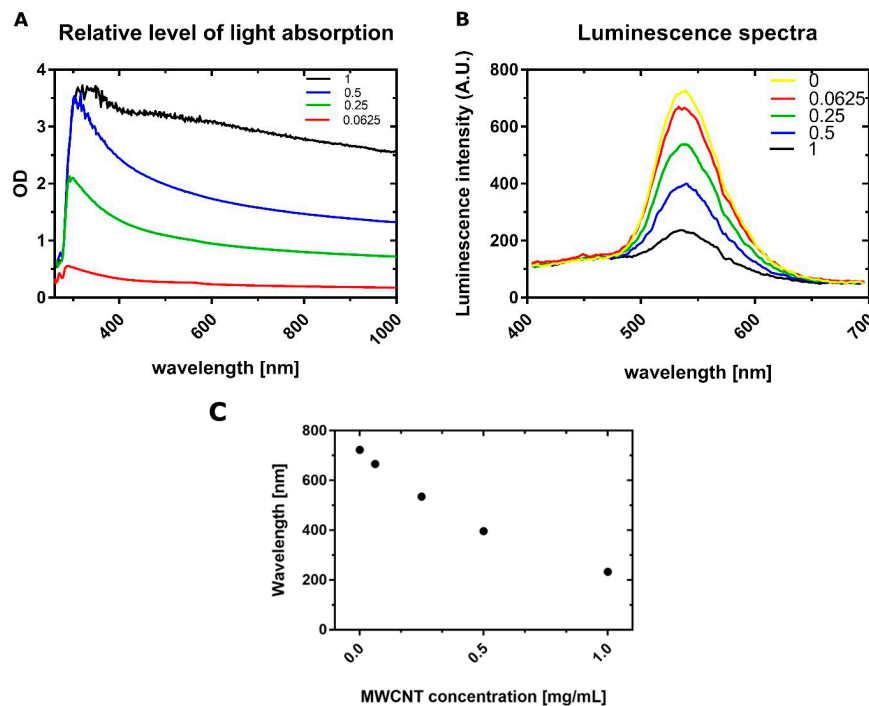
Figure 6. The Absorption spectrum of MWCNT-Ox used for experiments is shown on the (**A**) plot. The curves correspond to the respective concentrations of MWCNT-Ox. The maximum absorption is visible around 300 nm; however, it is observed throughout the whole range. The (**B**) plot shows luminescence spectra generated by the firefly luciferase from the CellTiter Glo assay, with a peak at λ = 532 nm. With an increasing amount of MWNCTs, the signal intensity is diminishing. When comparing both spectra, there is a visible overlap, which may indicate that some of the generated luminescent signals may be absorbed. The (**C**) plot represents a trend of decreasing maximum luminescence intensities with increasing concentrations of MWCNTs.

Luminescence spectra were obtained for all of the concentrations used (0, 0.0625, 0.25, 0.5, and 1 mg/mL), and it can be seen that with the increasing amount of MWCNTs, there is a stronger decrease in signal intensity, which confirms that MWCNTs interfere with the luminescent signal.

3.5. Quenching of Luminescent Signal

For both tests, it is shown that MWCNTs quench the luminescent signal (Figures 4B and 5B). The exact values of interference are shown in Tables 1 and 2.

Table 1. Table showing the amount of MWCNTs interference with the luminescent signal generated by the viability assay, with a fixed amount of ATP.

MWCNTs Concentration [mg/mL]	Percentage of Signal Relative to Control [%]	Amount of Interference [%]
0	100	-
0.0625	116.13	−16.13
0.25	84.63	+15.37
0.5	67.27	+32.73
1	46.51	+53.49

Table 2. Table showing the amount of MWCNTs interference with the luminescent signal generated by the ROS assay, with a fixed amount of H_2O_2.

MWCNTs Concentration [mg/mL]	Percentage of Signal Relative to Control [%]	Amount of Interference [%]
0	100	-
0.0625	45.73	+54.27
0.25	17.03	+82.96
0.5	9.78	+90.21
1	5.19	+94.8

As the concentration of MWCNTs increases, the luminescent signal decreases compared to the control, despite the presence of the same amount of substance (1 μM ATP and 10 μM H_2O_2). One exception is in the 0.0625 mg/mL sample, where the luminescent signal is even higher than in the control.

These numbers could potentially be taken into account to correct the obtained results. However, using percentages alone would yield unreliable values, because they are calculated from the measured luminescence intensities, which were obtained with a fixed amount of analyzed substance. The simple addition or subtraction of intensities does not apply either, because they should be measured with the same ATP amount, as was present in the well after cell lysis. The only possible way to obtain reliable results would be a complete separation of released ATP from MWCNTs, which is not possible, due to a few reasons. Firstly, the supernatant with MWCNTs could be discarded before performing the assay; however, after doing so, some amount of MWCNTs are embedded in the matrix, which is secreted by the chondrocytes. The detachment of cells and centrifugation does not separate them from the nanotubes, because they are present in the pellet. Centrifugation after lysis would also lead to errors because some amount of ATP would be present in the pellet, either adsorbed on the surface of the nanotubes or with cellular debris.

4. Discussion

In this paper, the cytotoxicity of functionalized, multiwalled carbon nanotubes on NHAC-kn human chondrocytes was investigated by analyzing cell viability and the level of generated reactive oxygen species, using luminescence-based tests. This method of detection was chosen because in the previous studies, it was shown that carbon nanotubes interfere with absorbance and fluorescence-based assays. Tests utilizing luminescence as a measurement method offers a number of advantages, such as higher sensitivity due to lower background, the endogenous production of a signal, without the need of an external excitation source, and a broad wavelength spectrum of emitted light. At first glance, assays performed in this paper are showing that prolonged incubation with functionalized MWCNT-Ox significantly decreases the number of viable chondrocytes. Similar results were obtained when examining the effect of SWCNTs on the proliferation of kidney epithelial cells HEK293 [24], MWCNTs on the proliferation of skin epithelial cells [40], and A549 lung adenoma cells [41,42]. All of these studies indicate the toxicity of these nanomaterials. However, the experiment performed with the same concentrations of MWCNT-Ox and a fixed amount of a compound that is detected by the test (ATP) showed different signal intensities in each of the examined concentrations (Figure 4B). This result proves the interaction of MWCNTs with the assay. Exposure of cells to a solution of functionalized

carbon nanotubes has shown to lead to the generation of ROS. Here, the ROS quantification assay was performed, and similar results as in the viability assay were observed (Figure 5A). With the lowest amount of MWCNTs, the assay reveals higher ROS generation than in control and a strong decrease with increasing concentrations. It was shown previously that carbon nanotubes may induce ROS production in cells; however, these values should be growing with higher carbon nanotube content. The decline shown here may be attributed to the much lower amount of viable cells. However, in an experiment, where only H_2O_2 was added to the MWCNT-Ox, an even stronger inhibition of signal was observed than in the analogous one with ATP. The possible explanation of this phenomenon is, additionally to luminescent signal absorption, the scavenging of generated ROS by the nanotubes. Additionally, absorption (Figure 6A) and luminescence spectra (Figure 6B) were obtained for all tested concentrations of MWCNT-Ox. MWCNTs showed a strong absorption of light, which partly overlaps with the luminescent spectrum. More importantly, the obtained luminescent spectra show a decrease in intensity with increasing MWCNT concentration. Therefore, the results of conducted experiments indicate that MWCNT-Ox interferes with the luminescent based-assays, yielding erroneous results.

To our knowledge, we are the first group to address the issue of the nanomaterials' interference with the luminescent assays. Similar experiments were carried out by Pem et al., where the interference of lanthanide-doped nanoparticles with common in vitro toxicity assays based on absorbance and fluorescence was examined, including ROS generation assays [43]. Together with previously published discrepancies in absorbance and fluorescence-based assays [36,37], this research casts doubt on many of the already published papers. For example, Ursini et al. performed cytotoxic, genotoxic, and inflammatory response to carboxyl-modified MWCNT on A549 and BEAS-2B cells [44]. To evaluate toxicity, WST-1 assay was used. A severe decrease in viability after incubation with increasing MWCNT-COOH concentrations was observed, with the number of 28.5% of viable cells at the highest evaluated concentration. This is the same pattern as the data presented in this paper. In order to evaluate the reliability of these results, similar control experiments as in this paper should be carried out. In this case, a known amount of hydrophilic formazan crystal formed from WST-1 should be incubated with respective MWCNT-COOH concentrations to verify whether carbon nanotubes do not interfere with the signal, yielding a false-positive result. Recently, a similar experiment with WST-1 assay was carried out by Scarcello et al. on manganese nanoparticles, with the conclusion that luminescence-based tests could be more appropriate for this type of analysis [45]. This further confirms that research on the interference of nanomaterials with luminescence-based assays is needed.

Another important aspect of carbon nanotubes toxicity is the impurities, which are often remnants of metal catalysts used in the synthesis. Carbon nanotubes for this paper were provided by the company, claiming at least 95% purity; therefore, we performed EDS analysis (Figure 2) to check the possible content of residual impurities.

Indeed, provided MWCNTs contained some metal impurities; however, after the functionalization process, it was not detected on the EDS analysis. Hence, we do not account for any interference with our measurements from it.

Further toxicological studies on in vitro and in vivo models should be developed to learn more about the effects of CNTs on health and body function. It would be desirable to learn more about the mechanism of ROS generation at the level of gene expression. Understanding these mechanisms will allow a better understanding of the interaction of cells with nanotubes, and it may perhaps develop ways to functionalize nanotubes to minimize these negative effects.

The interference of CNTs with the majority of assays is a serious issue. There is a growing number of research regarding 3D-cell scaffolds containing CNTs for application in regenerative medicine [46]. The viability of cells that are embedded in such structures is usually measured by these assays or their derivatives. In such composite materials, the CNTs are embedded in the scaffold. Therefore, they are non-removable before the assay, which may affect the final result, if CNTs are shown to interfere with the assay components. The lack of reliability of these tests casts even more emphasis on undertaking more in vivo studies, which should yield more trustworthy results.

On the other hand, an animal experiment is preceded by dosage determination based on in vitro assays; therefore, this may lead to improper experiment design. What is more, there are few in vivo animal studies in the literature that can better illustrate the total response of the body upon exposure to nanotubes. Currently, these studies focus on pulmonary, intraperitoneal, and subcutaneous administration. The level of toxicity induced by MWCNTs on the respiratory system of rats was assessed by the endotracheal aspiration of solutions at various concentrations. The toxic effect was dependent on the dose of carbon nanotubes and increased over time [47]. Orally administered SWCNTs and MWCNTs did not cause death or toxic effects in the tested rats. It is suggested that carbon nanotubes in the digestive system have formed agglomerates that have been removed from the body in the undigested form [48]. In contrast, the local application of SWCNTs to the skin of mice caused inflammation at the application site and the occurrence of oxidative stress [49]. It would be also reasonable to administer CNTs intravenously or to specific organs or body parts. In conclusion, despite years of research carried out, owing to the complexity of carbon nanotubes interactions with biological matter, combined with their physical and chemical properties, the methodology in determining the mechanisms of toxicity still needs to be improved and shifted toward in vivo experiments.

5. Conclusions

The conducted research shows that oxidized MWCNTs interfere with the luminescent signal generated by a commercially available assay, CellTiter Glo. This was confirmed by a series of experiments, where both absorbance and luminescent spectra were obtained. There is an overlap in these spectra, which may suggest that a part of the luminescent signal is quenched by MWCNTs. Importantly, a series of luminescent spectra with various amounts of MWCNTs showed that there is a decrease in signal intensity with increasing MWCNTs concentrations. Further studies elucidating the exact mechanism of this interference may help to overcome the limitations of the currently used assay.

References

1. Iijima, S. Helical microtubules of graphitic carbon. *Nature* **1991**, *354*, 56–58. [CrossRef]
2. Gulati, N.; Gupta, H. Two faces of carbon nanotube: Toxicities and pharmaceutical applications. *Crit. Rev. Ther. Drug Carr. Syst.* **2012**, *29*, 65–88. [CrossRef] [PubMed]
3. Ruoff, R.S.; Qian, D.; Liu, W.K. Mechanical properties of carbon nanotubes: Theoretical predictions and experimental measurements. *C. R. Phys.* **2003**, *4*, 993–1008. [CrossRef]
4. Peng, X.; Wong, S.S. Functional Covalent Chemistry of Carbon Nanotube Surfaces. *Adv. Mater.* **2009**, *21*, 625–642. [CrossRef]
5. Popov, V.N. Carbon nanotubes: Properties and application. *Mater. Sci. Eng. R Rep.* **2004**, *43*, 61–102. [CrossRef]
6. Ibrahim, K.S. Carbon nanotubes-properties and applications: A review. *Carbon Lett.* **2013**, *14*, 131–144. [CrossRef]
7. Kinloch, I.A.; Suhr, J.; Lou, J.; Young, R.J.; Ajayan, P.M. Composites with carbon nanotubes and graphene: An outlook. *Science* **2018**, *362*, 547–553. [CrossRef]
8. Lalwani, G.; Gopalan, A.; D'Agati, M.; Sankaran, J.S.; Judex, S.; Qin, Y.-X.; Sitharaman, B. Porous three-dimensional carbon nanotube scaffolds for tissue engineering. *J. Biomed. Mater. Res. Part A* **2015**, *103*, 3212–3225. [CrossRef]

9.   Gorain, B.; Choudhury, H.; Pandey, M.; Kesharwani, P.; Abeer, M.M.; Tekade, R.K.; Hussain, Z. Carbon nanotube scaffolds as emerging nanoplatform for myocardial tissue regeneration: A review of recent developments and therapeutic implications. *Biomed. Pharmacother.* **2018**, *104*, 496–508. [CrossRef]

10. Bianco, A.; Kostarelos, K.; Partidos, C.D.; Prato, M. Biomedical applications of functionalised carbon nanotubes. *Chem. Commun.* **2005**, 571. [CrossRef]

11. Semba, J.A.; Mieloch, A.A.; Rybka, J.D. Introduction to the state-of-the-art 3D bioprinting methods, design, and applications in orthopedics. *Bioprinting* **2020**, *18*, e00070. [CrossRef]

12. Wang, C.; Xia, K.; Wang, H.; Liang, X.; Yin, Z.; Zhang, Y. Advanced Carbon for Flexible and Wearable Electronics. *Adv. Mater.* **2018**, *31*, e1801072. [CrossRef] [PubMed]

13. Kumar, S.; Nehra, M.; Kedia, D.; Dilbaghi, N.; Tankeshwar, K.; Kim, K.-H. Carbon nanotubes: A potential material for energy conversion and storage. *Prog. Energy Combust. Sci.* **2018**, *64*, 219–253. [CrossRef]

14. Joddar, B.; Garcia, E.; Casas, A.; Stewart, C.M. Development of functionalized multi-walled carbon-nanotube-based alginate hydrogels for enabling biomimetic technologies. *Sci. Rep.* **2016**, *6*, 32456. [CrossRef]

15. Nardecchia, S.; Serrano, M.C.; Gutierrez, M.C.; Ferrer, M.L.; Del Monte, F. Modulating the cytocompatibility of tridimensional carbon nanotube-based scaffolds. *J. Mater. Chem. B* **2013**, *1*, 3064–3072. [CrossRef]

16. Chahine, N.O.; Collette, N.M.; Thomas, C.B.; Genetos, D.C.; Loots, G.G. Nanocomposite Scaffold for Chondrocyte Growth and Cartilage Tissue Engineering: Effects of Carbon Nanotube Surface Functionalization. *Tissue Eng. Part A* **2014**, *20*, 2305–2315. [CrossRef]

17. Mieloch, A.A.; Richter, M.; Trzeciak, T.; Giersig, M.; Rybka, J.D. Osteoarthritis Severely Decreases the Elasticity and Hardness of Knee Joint Cartilage: A Nanoindentation Study. *J. Clin. Med.* **2019**, *8*, 1865. [CrossRef]

18. Szymański, T.; Mieloch, A.A.; Richter, M.; Trzeciak, T.; Florek, E.; Rybka, J.D.; Giersig, M. Utilization of Carbon Nanotubes in Manufacturing of 3D Cartilage and Bone Scaffolds. *Materials* **2020**, *13*, 4039. [CrossRef]

19. Correa-Duarte, M.A.; Wagner, N.; Rojas-Chapana, J.; Morscheck, C.; Thie, M.; Giersig, M. Fabrication and Biocompatibility of Carbon Nanotube-Based 3D Networks as Scaffolds for Cell Seeding and Growth. *Nano Lett.* **2004**, *4*, 2233–2236. [CrossRef]

20. Trzeciak, T.; Rybka, J.D.; Akinoglu, E.M.; Richter, M.; Kaczmarczyk, J.; Giersig, M. In Vitro Evaluation of Carbon Nanotube-Based Scaffolds for Cartilage Tissue Engineering. *J. Nanosci. Nanotechnol.* **2016**, *16*, 9022–9025. [CrossRef]

21. Imaninezhad, M.; Schober, J.; Griggs, D.; Ruminski, P.; Kuljanishvili, I.; Zustiak, S.P. Cell Attachment and Spreading on Carbon Nanotubes Is Facilitated by Integrin Binding. *Front. Bioeng. Biotechnol.* **2018**, *6*, 1–12. [CrossRef] [PubMed]

22. Nomanbhay, S.; Raziah, A.Z.; Junizah, A.R. Carbon Nanotubes: A Review on Structure and Their Interaction with Proteins. *J. Chem.* **2013**, *2013*, 1–18. [CrossRef]

23. King, A.A.K.; Matta-Domjan, B.; Large, M.J.; Matta, C.; Ogilvie, S.P.; Bardi, N.; Byrne, H.J.; Zakhidov, A.; Jurewicz, I.; Velliou, E.; et al. Pristine carbon nanotube scaffolds for the growth of chondrocytes. *J. Mater. Chem. B* **2017**, *5*, 8178–8182. [CrossRef] [PubMed]

24. Cui, D.; Tian, F.; Ozkan, C.S.; Wang, M.; Gao, H. Effect of single wall carbon nanotubes on human HEK293 cells. *Toxicol. Lett.* **2005**, *155*, 73–85. [CrossRef]

25. Figarol, A.; Pourchez, J.; Boudard, D.; Forest, V.; Akono, C.; Tulliani, J.-M.; Lecompte, J.-P.; Cottier, M.; Bernache-Assollant, D.; Grosseau, P. In vitro toxicity of carbon nanotubes, nano-graphite and carbon black, similar impacts of acid functionalization. *Toxicol. In Vitro* **2015**, *30*, 476–485. [CrossRef]

26. Muller, J.; Huaux, F.; Moreau, N.; Misson, P.; Heilier, J.-F.; Delos, M.; Arras, M.; Fonseca, A.; Nagy, J.B.; Lison, D. Respiratory toxicity of multi-wall carbon nanotubes. *Toxicol. Appl. Pharmacol.* **2005**, *207*, 221–231. [CrossRef]

27. Snegin, E.; Gusev, A.; Barkhatov, A.; Vasyukova, I.; Artemchuk, O. Genotoxicity evaluation of multiwalled carbon nanotubes: In vivo studies in mice. *IOP Conf. Ser. Earth Environ. Sci.* **2020**, *433*. [CrossRef]

28. Takagi, A.; Hirose, A.; Nishimura, T.; Fukumori, N.; Ogata, A.; Ohashi, N.; Kitajima, S.; Kanno, J. Induction of mesothelioma in p53+/− mouse by intraperitoneal application of multi-wall carbon nanotube. *J. Toxicol. Sci.* **2008**, *33*, 105–116. [CrossRef]

29. Mutlu, G.M.; Budinger, G.R.S.; Green, A.A.; Urich, D.; Soberanes, S.; Chiarella, S.E.; Alheid, G.F.; McCrimmon, D.R.; Szleifer, I.; Hersam, M.C. Biocompatible Nanoscale Dispersion of Single-Walled Carbon Nanotubes Minimizes in vivo Pulmonary Toxicity. *Nano Lett.* **2010**, *10*, 1664–1670. [CrossRef]

30. Li, J.-G.; Li, W.-X.; Xu, J.-Y.; Cai, X.-Q.; Liu, R.-L.; Li, Y.; Zhao, Q.-F.; Li, Q. Comparative study of pathological lesions induced by multiwalled carbon nanotubes in lungs of mice by intratracheal instillation and inhalation. *Environ. Toxicol.* **2007**, *22*, 415–421. [CrossRef]

31. Sager, T.M.; Wolfarth, M.W.; Andrew, M.; Hubbs, A.; Friend, S.; Chen, T.-H.; Porter, D.W.; Wu, N.; Yang, F.; Hamilton, R.F.; et al. Effect of multi-walled carbon nanotube surface modification on bioactivity in the C57BL/6 mouse model. *Nanotoxicology* **2013**, *8*, 317–327. [CrossRef] [PubMed]

32. Aldieri, E.; Fenoglio, I.; Cesano, F.; Gazzano, E.; Gulino, G.; Scarano, D.; Attanasio, A.; Mazzucco, G.; Ghigo, D.; Fubini, B. The Role of Iron Impurities in the Toxic Effects Exerted by Short Multiwalled Carbon Nanotubes (MWCNT) in Murine Alveolar Macrophages. *J. Toxicol. Environ. Health Part A* **2013**, *76*, 1056–1071. [CrossRef] [PubMed]

33. Alarifi, S.; Ali, D. Mechanisms of Multi-walled Carbon Nanotubes–Induced Oxidative Stress and Genotoxicity in Mouse Fibroblast Cells. *Int. J. Toxicol.* **2015**, *34*, 258–265. [CrossRef] [PubMed]

34. Francis, A.P.; Thiyagarajan, D. Toxicity of carbon nanotubes: A review. *Toxicol. Ind. Health* **2018**, *34*, 200–210. [CrossRef]

35. Zhang, W.; Ding, Q.; Jinruan, J.; Fang, J. Biomolecular Interactions and Application of Carbon Nanotubes in Nanomedicine. *Austin Biomol. Open Access* **2016**, *1*, 1005.

36. Wörle-Knirsch, J.M.; Pulskamp, A.K.; Krug, H.F. Oops They Did It Again! Carbon Nanotubes Hoax Scientists in Viability Assays. *Nano Lett.* **2006**, *6*, 1261–1268. [CrossRef]

37. Casey, A.; Herzog, E.; Davoren, M.; Lyng, F.; Byrne, H.; Chambers, G. Spectroscopic analysis confirms the interactions between single walled carbon nanotubes and various dyes commonly used to assess cytotoxicity. *Carbon* **2007**, *45*, 1425–1432. [CrossRef]

38. Cree, I.A. Luminescence-Based Cell Viability Testing. *Biolumin. Methods Protoc.* **2003**, *102*, 169–178. [CrossRef]

39. Gergely, S.; Hegedűs, C.; Lakatos, P.; Kovács, K.; Gáspár, R.; Csont, T.; Virág, L. High Throughput Screening Identifies a Novel Compound Protecting Cardiomyocytes from Doxorubicin-Induced Damage. *Oxid. Med. Cell. Longev.* **2015**, *2015*, 1–12. [CrossRef]

40. Monteiro-Riviere, N.A.; Nemanich, R.J.; Inman, A.O.; Wang, Y.Y.; Riviere, J.E. Multi-walled carbon nanotube interactions with human epidermal keratinocytes. *Toxicol. Lett.* **2005**, *155*, 377–384. [CrossRef]

41. Ye, S.-F.; Wu, Y.-H.; Hou, Z.; Zhang, Q. ROS and NF-κB are involved in upregulation of IL-8 in A549 cells exposed to multi-walled carbon nanotubes. *Biochem. Biophys. Res. Commun.* **2009**, *379*, 643–648. [CrossRef] [PubMed]

42. Kyriakidou, K.; Brasinika, D.; Trompeta, A.; Bergamaschi, E.; Karoussis, I.; Charitidis, C. In vitro cytotoxicity assessment of pristine and carboxyl-functionalized MWCNTs. *Food Chem. Toxicol.* **2020**, *141*, 111374. [CrossRef]

43. Pem, B.; González-Mancebo, D.; Moros, M.; Ocana, M.; Becerro, A.I.; Pavičić, I.; Selmani, A.; Babič, M.; Jendelova, P.; Vrček, I.V.; et al. Biocompatibility assessment of up-and down-converting nanoparticles: Implications of interferences with in vitro assays. *Methods Appl. Fluoresc.* **2018**, *7*, 014001. [CrossRef] [PubMed]

44. Ursini, C.L.; Cavallo, D.; Fresegna, A.M.; Ciervo, A.; Maiello, R.; Buresti, G.; Casciardi, S.; Bellucci, S.; Iavicoli, S. Differences in Cytotoxic, Genotoxic, and Inflammatory Response of Bronchial and Alveolar Human Lung Epithelial Cells to Pristine and COOH-Functionalized Multiwalled Carbon Nanotubes. *BioMed Res. Int.* **2014**, *2014*, 1–14. [CrossRef] [PubMed]

45. Scarcello, E.; Lambremont, A.; Vanbever, R.; Jacques, P.J.; Lison, D. Mind your assays: Misleading cytotoxicity with the WST-1 assay in the presence of manganese. *PLoS ONE* **2020**, *15*, e0231634. [CrossRef] [PubMed]

46. Trzeciak, T.; Rybka, J.D.; Richter, M.; Kaczmarczyk, J.; Ramalingam, M.; Giersig, M. Cells and Nanomaterial-Based Tissue Engineering Techniques in the Treatment of Bone and Cartilage Injuries. *J. Nanosci. Nanotechnol.* **2016**, *16*, 8948–8952. [CrossRef]

47. Matsumoto, M.; Serizawa, H.; Sunaga, M.; Kato, H.; Takahashi, M.; Hirata-Koizumi, M.; Ono, A.; Kamata, E.; Hirose, A. No toxicological effects on acute and repeated oral gavage doses of single-wall or multi-wall carbon nanotube in rats. *J. Toxicol. Sci.* **2012**, *37*, 463–474. [CrossRef]

48. Liu, A.; Sun, K.; Yang, J.; Zhao, D. Toxicological effects of multi-wall carbon nanotubes in rats. *J. Nanopart. Res.* **2008**, *10*, 1303–1307. [CrossRef]

49. Murray, A.; Kisin, E.; Leonard, S.; Young, S.; Kommineni, C.; Kagan, V.; Castranova, V.; Shvedova, A.A. Oxidative stress and inflammatory response in dermal toxicity of single-walled carbon nanotubes. *Toxicology* **2009**, *257*, 161–171. [CrossRef]

Tomasz Szymański

Laboratory of Applied Biotechnology

Center for Advanced Technology

Adam Mickiewicz University in Poznań

e-mail: tomszy1@amu.edu.pl

Author contribution statement

I declare that I am the co-author of the article **"Carbon nanotubes interference with luminescence-based assays"** by Tomasz Szymański, Marcelina Kempa, Michael Giersig and Jakub Dalibor Rybka, published in *Materials* in 2020. The author's contribution is as follows:
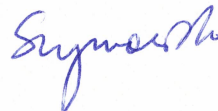
Tomasz Szymański designed the study and supervised the experiments. Tomasz Szymański made MWCNTs functionalization and measured cell viability in 2D cell cultures incubated with MWCNTs. Tomasz Szymański also made luminescence measurements of various MWCNTs solutions without cells, prepared samples for SEM, FT-IR, performed absorbance measurements, analyzed the data and created respective figures. Tomasz Szymański with Marcelina Kempa prepared the original draft.

Marcelina Kempa was responsible for MWCNTs purification, as well as preparation for TGA data analysis. She helped in cell culture and performed ROS measurement with MWCNTs. She also helped with the data analysis and preparation of figures for viability and ROS measurements.

Michael Giersig guided the research and revised the draft.

Jakub Dalibor Rybka guided and supervised the research and revised the draft. Jakub was responsible for the project management, funding management and corresponded with the journal and reviewers.

Date: 8.12.2023

Signature: *Szymański*

Rybka

prof. UAM dr hab. inż. Jakub D. Rybka

Dr hab. inż. Jakub Rybka, prof. UAM
Laboratory of Applied Biotechnology
Center for Advanced Technology
Adam Mickiewicz University in Poznań
e-mail: jrybka@amu.edu.pl

Author contribution statement

I declare that I am the co-author of the article **"Carbon nanotubes interference with luminescence-based assays"** by Tomasz Szymański, Marcelina Kempa, Michael Giersig and Jakub Dalibor Rybka, published in *Materials* in 2020. The author's contribution is as follows:

Tomasz Szymański designed the study and supervised the experiments. Tomasz Szymański made MWCNTs functionalization and measured cell viability in 2D cell cultures incubated with MWCNTs. Tomasz Szymański also made luminescence measurements of various MWCNTs solutions without cells, prepared samples for SEM, FT-IR, performed absorbance measurements, analyzed the data and created respective figures. Tomasz Szymański with Marcelina Kempa prepared the original draft.
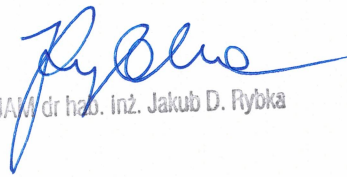
Marcelina Kempa was responsible for MWCNTs purification, as well as preparation for TGA data analysis. She helped in cell culture and performed ROS measurement with MWCNTs. She also helped with the data analysis and preparation of figures for viability and ROS measurements.

Michael Giersig guided the research and revised the draft.

Jakub Dalibor Rybka guided and supervised the research and revised the draft. Jakub was responsible for the project management, funding management and corresponded with the journal and reviewers.

Date: 0 8. 01. 2024

Signature:

prof. UAM dr hab. inż. Jakub D. Rybka

Michael Giersig

Department of Theory of Continuous Media and Nanostructures),
Institute of Fundamental Technological Research
Polish Academy of Sciences
Ul. Pawińskiego 5B; 02-106 Warsaw, Poland;
e-mail: mgiersig@ippt.pan.pl

Author contribution statement

I declare that I am the co-author of the article **"Carbon nanotubes interference with luminescence-based assays"** by Tomasz Szymański, Marcelina Kempa, Michael Giersig and Jakub Dalibor Rybka, published in *Materials* in 2020. The author's contribution is as follows:

Tomasz Szymański designed the study and supervised the experiments. Tomasz Szymański made MWCNTs functionalization and measured cell viability in 2D cell cultures incubated with MWCNTs. Tomasz Szymański also made luminescence measurements of various MWCNTs solutions without cells, prepared samples for SEM, FT-IR, performed absorbance measurements, analyzed the data and created respective figures. Tomasz Szymański with Marcelina Kempa prepared the original draft.

Marcelina Kempa was responsible for MWCNTs purification, as well as preparation for TGA data analysis. She helped in cell culture and performed ROS measurement with MWCNTs. She also helped with the data analysis and preparation of figures for viability and ROS measurements.

Michael Giersig guided the research and revised the draft.

Jakub Dalibor Rybka guided and supervised the research and revised the draft. Jakub was responsible for the project management, funding management and corresponded with the journal and reviewers.

Date: 2 2. 01. 2024

Signature: *prof. dr hab. Michał Giersig*

Marcelina Kempa

Laboratory of Applied Biotechnology
Center for Advanced Technology
Adam Mickiewicz University in Poznan
e-mail: mkempa@amu.edu.pl

Author contribution statement

I declare that I am the co-author of the article **"Carbon nanotubes interference with luminescence-based assays"** by Tomasz Szymański, Marcelina Kempa, Michael Giersig and Jakub Dalibor Rybka, published in *Materials* in 2020. The author's contribution is as follows:

Tomasz Szymański designed the study and supervised the experiments. Tomasz Szymański made MWCNTs functionalization and measured cell viability in 2D cell cultures incubated with MWCNTs. Tomasz Szymański also made luminescence measurements of various MWCNTs solutions without cells, prepared samples for SEM, FT-IR, performed absorbance measurements, analyzed the data and created respective figures. Tomasz Szymański with Marcelina Kempa prepared the original draft.

Marcelina Kempa was responsible for MWCNTs purification, as well as preparation for TGA data analysis. She helped in cell culture and performed ROS measurement with MWCNTs. She also helped with the data analysis and preparation of figures for viability and ROS measurements.

Michael Giersig guided the research and revised the draft.

Jakub Dalibor Rybka guided and supervised the research and revised the draft. Jakub was responsible for the project management, funding management and corresponded with the journal and reviewers.

Date: 07.12.2023

Signature: *Kempa Kornelia*

scientific reports

OPEN

Hyaluronic acid and multiwalled carbon nanotubes as bioink additives for cartilage tissue engineering

Tomasz Szymański[1,2], Julia Anna Semba[1,3], Adam Aron Mieloch[1], Piotr Cywoniuk[1], Marcelina Kempa[1,3] & Jakub Dalibor Rybka[1✉]

Articular cartilage and meniscus injuries are prevalent disorders with insufficient regeneration responses offered by available treatment methods. In this regard, 3D bioprinting has emerged as one of the most promising new technologies, offering novel treatment options. Additionally, the latest achievements from the fields of biomaterials and tissue engineering research identified constituents facilitating the creation of biocompatible scaffolds. In this study, we looked closer at hyaluronic acid and multi-walled carbon nanotubes as bioink additives. Firstly, we assessed the minimal concentrations that stimulate cell viability, and decrease reactive oxygen species and apoptosis levels in 2D cell cultures of normal human knee articular chondrocytes (NHAC) and human adipose-derived mesenchymal stem cells (hMSC-AT). In this regard, 0.25 mg/ml of hyaluronic acid and 0.0625 mg/ml of carbon nanotubes were selected as the most optimal concentrations. In addition, we investigated the protective influence of 2-phospho-L-ascorbic acid in samples with carbon nanotubes. Tests conducted on 3D bioprinted constructs revealed that only a combination of components positively impacted cell viability throughout the whole experiment. Gene expression analysis of *COL1A1*, *COL6A1*, *HIF1A*, *COMP*, *RUNX2*, and *POU5F1* showed significant changes in the expression of all analyzed genes with a progressive overall loss of transcriptional activity in most of them.

Joint degeneration resulting from articular cartilage and meniscus defects is one of the most prevalent disorders of the musculoskeletal system. Cartilage's low healing capacity and poor regeneration effects with available treatments motivate further research into new solutions[1]. A part of the effort is directed at new surgical techniques and more advanced biomaterials, facilitating the creation of biocompatible cartilage scaffolds[2]. Raising interest is observed in the field of biologically active materials, focused on the maintenance of cell viability and proper phenotype. Collagens in cartilage tissue form complex extracellular scaffolds to bear mechanical forces, maintain homeostasis and provide anchoring sites for chondrocytes, extracellular matrix (ECM) molecules, and growth factors[3]. For many years collagen was considered to be only a structural component of the cartilage matrix, but recently, its role in extracellular signaling, mainly via integrin receptors, was discovered[4]. Collagens regulate chondrocyte proliferation, metabolism, and differentiation; similarly to soluble signaling molecules. Additionally, they significantly suppress chondrocyte hypertrophy, which is the pathological process in osteoarthritic cartilage, leading to cell senescence and death. Interestingly, carbon nanotubes (CNTs) share similar dimensions to collagen fibrils, rendering them a potential collagen biomimetic[5,6]. Hyaluronic acid (HA) is another major ECM component, performing a dual role as a structural and signaling molecule. It has exceptional water retention properties, forming a gel-like environment within the tissue, and providing elasticity for the whole structure[7].

In this study, we investigated multi-walled carbon nanotubes (MWCNTs) and hyaluronic acid (HA) as bioink additives for the 3D bioprinting of cartilage constructs. 3D bioprinting is a tissue engineering technology, which allows for precise spatial deposition of cell-enriched biomaterials, and recreation of tissue-specific structures capable to restore, maintain or improve damaged tissue through 3D scaffolds[2].

Due to their unique biological and mechanical properties, carbon nanotubes are the subject of research in cartilage regenerative medicine. The MWCNTs are concentrically rolled graphene layers forming a cylindrical structure. Surfaces of synthetic materials functionalized with CNTs stimulate chondrocyte growth and facilitate

[1]Center for Advanced Technology, Adam Mickiewicz University, Poznan, Poland. [2]Faculty of Chemistry, Adam Mickiewicz University, Poznan, Poland. [3]Faculty of Biology, Adam Mickiewicz University, Poznan, Poland. ✉email: jrybka@amu.edu.pl

the maintenance of their native phenotype[8,9]. The incorporation of CNTs also improves the mechanical properties of constructs, rendering them useful in scaffold reinforcement[10]. Most studies emphasize concentration-dependent effects. The cytotoxicity of carbon nanotubes is frequently emphasized and observed through an increase in reactive oxygen species (ROS) production. To mitigate cellular damage elicited by high ROS levels, antioxidant compounds such as L-ascorbic can be utilized. Due to its additional role in collagen production, a more stable analog, 2-phospho- L-ascorbic acid, was used in our study[11–13].

In the case of cartilage tissue engineering, ECM components are of special interest not only due to their mechanical properties, ensuring the physiological functioning of cartilage as a shock absorber, but also due to their biological properties. Hyaluronic acid (HA) is a glycosaminoglycan prevalent in abundance in ECM of articular cartilage[14]. It provides antioxidative, anti-inflammatory, and chondroprotective effects, which are beneficial for cartilage repair. The concentration and molecular weight of HA determines its biological activity. This component was previously utilized as an additive to bioprint the articular cartilage constructs with auspicious stimulation of cell viability and phenotype[15]. HA has also been chemically modified to improve its mechanical, and biological properties, or enable UV cross-linking[16,17].

This study assesses the chondrogenic properties of multi-walled carbon nanotubes and hyaluronic acid as bioink additives. In the first step, the minimal stimulating concentration of these components was determined with the 2D culture of normal human knee articular chondrocytes (NHAC) and human adipose-derived mesenchymal stem cells (hMSC-AT). Then, cell-containing 3D constructs were created using extrusion-based 3D bioprinting and formulated bioink. The bioink composition was based on alginate, gelatin, and carboxymethylated cellulose nanocrystals (CCNC), supplemented with MWCNTs or HA. Subsequently, the viability and gene expression of chondrogenesis markers were evaluated.

Methods

MWCNTs functionalization.

MWCNTs were purchased and characterized as described in our previous work[18]. MWCNTs with diameters of 15–30 nm, lengths of 15–20 μm, and purity up to 95% produced by chemical vapor deposition (CVD) were functionalized by oxidation according to the following method. 30 mg of MWCNTs were sonicated at 70 °C in a mixture of concentrated sulfuric (H_2SO_4) and nitric (HNO_3) acids in a ratio of 3:1. Then, the mixture was neutralized with 300 ml of 3 M sodium hydroxide (NaOH). Purification of the oxidized carbon nanotubes was carried out in cycles of centrifugation and resuspension in miliQ water at $9000 \times g$ at 20 °C for: (a) 15 min, (b) 30 min, (c) 40 min, and then $12,000 \times g$ at 4 °C for 40 min. The resulting carbon nanotube solution was dried using a vacuum evaporator. The MWCNTs were suspended in a phosphate buffer (PBS). The mass of nanotubes in a given volume of the solution was determined by the thermogravimetric method to calculate the concentration of the functionalized MWCNTs (which was 2.02 mg/ml).

Cell culture.

Normal Human Articular Chondrocytes (NHAC, LONZA Catalog #: CC-2550) were cultured in CGM™ Chondrocyte Growth Medium (LONZA), while human adipose tissue-derived mesenchymal stem cells (hMSC-AT, PromoCell) were cultured in supplemented Mesenchymal Stem Cells Growth Medium 2 (PromoCell); both in a humidified 5% CO_2 atmosphere, at 37 °C in tissue culture flasks (Falcon®). The culture medium was changed every three days and cells were passaged with TrypLE (Gibco) at 80–85% confluency. Additionally, hMSC-AT were cultured in Mesenchymal Stem Cell Chondrogenic Differentiation Medium (PromoCell) as a reference for gene expression analysis.

Determination of the cell viability, reactive oxygen species, and apoptosis levels in 2D cell cultures stimulated with MWCNTs and 2-phospho-L-ascorbic acid.

For all tests, NHAC and hMSC-AT were seeded in a clear bottom 96-well plate (Corning) at a density of 1000 cells/well. After 24 h, medium with 0.015, 0.03, 0.0625, and 0.125 mg/ml MWCNTs was added to each well; the total volume was 100 μl medium/well. To investigate the antioxidant effect of vitamin C, the same replicates were performed with the addition of 50 μg/ml.

2-phospho-L-ascorbic acid in a cell culture medium. This salt was used instead of regular ascorbic acid, due to its increased stability in water solutions[19]. The viability was assessed with the CellTiter-Glo® Luminescent Cell Viability Assay (Promega) as described above.

The level of H_2O_2 and reactive oxygen species (ROS) were determined according to the manufacturer protocol of the ROS-Glo™ H_2O_2 Assay (Promega). Briefly, 24 h after seeding, 20 μl of H_2O_2 substrate solution was added to each well. The samples were incubated for 2 h at 37 °C with 5% CO_2. Subsequently, 100 μl of ROS-Glo™ Detection Solution was added to each well, and samples were incubated for 30 min at room temperature. The luminescent signal was read with a microplate reader (Infinite® 200 PRO, TECAN). ROS-Glo™ H_2O_2 Assay results were correlated with the CellTiter-Glo® Luminescent Cell Viability Assay. In an analogical way, Caspase-Glo® 3/7 Assay Systems (Promega) were conducted to investigate apoptosis via caspase activity. All samples were conducted in triplicate. The luminescence values were normalized to respective control samples (100%). The statistical significance was determined by a two-tailed Student's t-test (n = 3; additive vs control: $^*P < 0.05$; $^{**}P < 0.01$ and $^{***}P < 0.001$).

Determination of cell viability in 2D cultures supplemented with HA.

For all experiments, NHAC, and hMSC-AT cells were seeded in a clear bottom 96-well plate (Corning) at a density of 1000 cells/well. After 24 h, medium with 0.125, 0.25, 0.5, or 1 mg/ml HA (Contipro) was added to each well; the total volume was 100 μl medium/well. Cells were cultured in the supplemented medium at 37 °C with 5% CO_2. The experiment was performed according to the producer protocol of the CellTiter-Glo® Luminescent Cell Viability Assay (Promega). CGM™ medium and Mesenchymal Stem Cells Growth Medium 2 without HA were used as a control.

After 24 h, 48 h, and 72 h, 100 µl of CellTiter-Glo® Reagent was added to each well. The samples were incubated for 30 min at room temperature. The luminescent signal was read with a microplate reader (Infinite® 200 PRO, TECAN). All samples were conducted in triplicate. The luminescence values were normalized to respective control samples (100%). The statistical significance was determined by a two-tailed Student's t-test (n = 3; additive vs control: *P < 0.05; **P < 0.01 and ***P < 0.001).

The preparation of bioink. The bioink was prepared as follows. Weighted and UV-sterilized sodium alginate (Sigma-Aldrich) was dissolved in a sterile 4.6% (w/v) D-mannitol (Sigma-Aldrich) solution. Subsequently, weighted and UV-sterilized porcine skin gelatin (Sigma-Aldrich), and CCNC (Cellulose Lab) were separately added and mixed with the alginate solution with two syringes connected with the female/female Luer-lock adapter. The materials were shaken each time at 37 °C for at least 30 min with HulaMixer™ Sample Mixer, followed by overnight mixing. The final concentrations of bioink components were 4.0% gelatin, 0.75% alginate, and 1.4% CCNC. Before adding cells, HA or/and MWCNTs were added and bioink was additionally mixed with two syringes connected with the female/female Luer-lock adapter. The prepared bioink was mixed with 8×10^6 cells/ml of bioink in an analogical way. Only hMSC-AT were utilized for 3D bioprinting. Before bioprinting, the bioink with cells was placed in a cartridge and held at a 25 °C water bath to induce gelatin gelation.

The rheological tests. The rheological evaluation was performed on Anton Paar 302 rheometer, equipped with 25 mm, smooth, parallel plates (PP25) with bioink without cells and before crosslinking. The gap between plates was set to 1 mm and—unless stated otherwise—measurements were conducted at 23 °C. Performed rheological measurements were temperature sweep test and rotation. Temperature sweep experiments were performed at a rate of 2 °C/min from 20 to 40 °C. In the rotation study, the shear rate range was set to 0.01–1000.00 s^{-1}. A layer of silicone oil was spread over the verge surface of the sample to prevent water evaporation from bioink samples during rheological measurements. All rheological tests were performed in at least two repeats.

3D bioprinting. The BioX printer (Cellink) with temperature-control, pressure extrusion printhead was used, with printhead temperature set at 25 °C, and printbed temperature set at 10 °C.

After bioprinting, the constructs were crosslinked with sterile 200 mM CaCl$_2$ (Sigma-Aldrich) dissolved in 4.6% (w/v) D-mannitol (Sigma-Aldrich) for 10 min at room temperature.

The constructs were cultured in Mesenchymal Stem Cell Growth Medium 2 (Promocell), and the Mesenchymal Stem Cell Chondrogenic Differentiation Medium (Promocell) in the case of cells used as differentiation control. The constructs were cultured in standard conditions (37 °C, 5% CO$_2$) and the medium was changed every 3 days.

SEM–EDX. The constructs bioprinted without cells were subjected to Scanning Electron Microscopy (SEM) with Energy Dispersive X-Ray Analysis (EDX). The analyzed scaffolds were with or without the addition of the MWCNTs. The morphology of samples was characterized by scanning electron microscope Quanta FEG 250 (FEI) in low vacuum conditions at the pressure of 70 Pa with an electron beam energy of 10 keV. EDS spectra were collected with an electron beam energy of 30 keV using an EDS Octane SDD detector (EDAX). Prior to analysis, the scaffolds were frozen at −80 °C for 2 h and then lyophilized (Christ, Alpha 1–2 LDplus lyophilizer) for 12 h, at the pressure of 1 mBar. Subsequently, the pressure was decreased to 0.18 mBar and the process was carried out for another 4 h.

The live/dead assay of cells encapsulated in bioprinted construct. After 24 h, 14 days, and 21 days, bioprinted constructs were analyzed with the LIVE/DEAD assay performed according to the manufacturer`s protocol (LIVE/DEAD® Viability/Cytotoxicity Kit, Invitrogen). Stained cells were visualized on a confocal microscope (IX83, Olympus). Scans for viability counting were taken from the lateral part of three different constructs at each time point. From each of these scans, two middle slices were chosen for live and dead cell counting. Obtained images were analyzed with Fiji software using ITCN functionality. The viability was calculated as a % of live cells. The statistical significance was determined by two-tailed Student's t-test (n = 3; additive vs control: P^a < 0.05; P^b < 0.01 and P^c < 0.001; timepoint vs timepoint (within the particular additive group): *P < 0.05; **P < 0.01 and ***P < 0.001).

Analysis of gene expression of cell-laden constructs. Three constructs from each time point were dissolved in 100 mM sodium citrate containing 0.08 U/µl of Proteinase K and 1.0 U/µl of RNAse Inhibitor (A&A Biotechnology) with shaking at 37 °C for 5 min and followed by the RNA isolation with TriReagent (Sigma-Aldrich) and chloroform/phenol extraction. Isolated total RNA concentration was measured with the Qubit 4 fluorometer (Invitrogen) and reversely transcribed with the High-Capacity cDNA Reverse Transcription Kit (Thermo Scientific). Gene expression was analyzed from 7.5 ng of cDNA per sample with real-time PCR using Maxima SYBR Green/ROX qPCR Master Mix (Thermo Scientific) on QuantStudio 7 Flex (Applied Biosystems). The qPCR data were statistically analyzed with GraphPad Prism software. Relative expression was calculated with ddCt and referred to *RPS29* gene expression. The variations in gene expression were determined by two-tailed Student's t-test (n ≥ 2); P-values were considered significant as follows: additive vs control: P^a < 0.05; P^b < 0.01 and P^c < 0.001; timepoint vs timepoint (within the particular additive group): *P < 0.05; **P < 0.01 and ***P < 0.001. Sequences of primers used are listed in Supp. Tab. 1.

Results

Analysis of viability, ROS, and caspase 3/7 generation in 2D NHAC and hMSC-AT cell cultures.
In NHAC 2D culture, 1 mg/ml of HA addition had no significant effect on cell proliferation (Fig. 1a). The culture exposed to 0.25 mg/ml of HA showed negligible changes in viability after 24 h. However, increased proliferation was observed after 72 h of culture. Similar results were obtained for hMSC-AT (Fig. 2a). The highest increase in proliferation was observed at the HA concentration of 0.25 mg/ml. A decrease in cell viability of both NHAC and hMSC-AT cultures was observed for all MWCNTs concentrations. The highest decrease of about 50% in viability was observed for 0.125 mg/ml. Interestingly, in the culture with the lower range of MWCNTs concentrations (0.015 mg/mL and 0.03 mg/ml), cell viability was diminished in comparison to a higher concentration of 0.0625 mg/ml at all time points (Figs. 1b and 2b). Observed dependency was corroborated by analyses of ROS production and active caspases 3/7 (Figs. 1 c,d and 2c,d). The stable form of vitamin C (2-phospho-l-ascorbic acid) yields protective and antioxidative effects in the NHAC and hMSC-AT cell culture with CNTs. The strongest antioxidant effect of vitamin C is seen at the highest concentration of MWCNTs (0.125 mg/ml). Its supplementation causes a significant reduction in the production of reactive oxygen species and inhibits cell death compared to the medium without 2-phospho-l-ascorbic acid supplementation (Figs. 1 c,d and 2c,d).

Analysis of bioink and 3D bioprinting.
The addition of 0.25 mg/ml HA and 0.0625 mg/ml MWCNTs yielded the most beneficial effect in 2D tests, therefore these concentrations were selected for 3D bioprinting. The aim was to assess whether selected additives influence cell viability and induce chondrogenic differentiation in 3D culture. The hMSC-AT cell line at a concentration of 8×10^6 cells/ml was used in the study due to a higher proliferation rate than NHAC.

The MWCNTs or HA addition showed negligible influence on the rheological properties of bioinks. All of them exhibit a shear-thinning behavior and have similar cross-over temperatures (G' = G"), which signifies good printability (Fig. 3). Table 1 presents parameters set for 3D bioprinting.
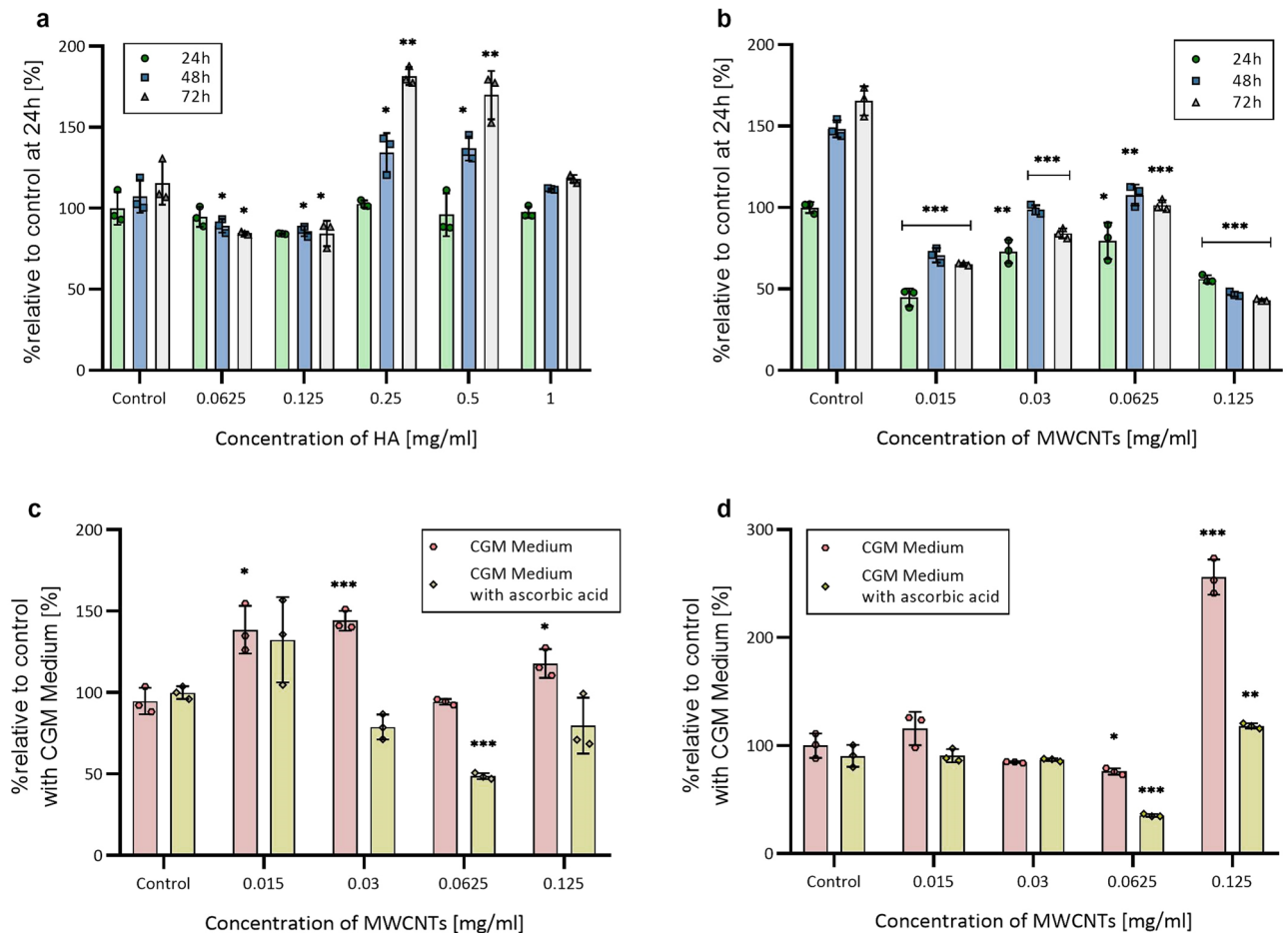

Figure 1. Relative cell viability, ROS levels and caspase 3/7 activity in 2D NHACs culture. (**a**) Relative viability of NHACs after exposure to different concentrations of HA. (**b**) Relative viability of NHACs after exposure to different concentrations of MWCNTs. (**c**) Relative ROS generation after 24 h exposure to MWCNTs. (**d**) Relative Caspase 3/7 activity after 24 h incubation with MWCNTs. The data are presented as the mean ± SD. The statistical significance was determined by two-tailed Student's t-test (n = 3; additive vs control: *P < 0.05; **P < 0.01 and ***P < 0.001).

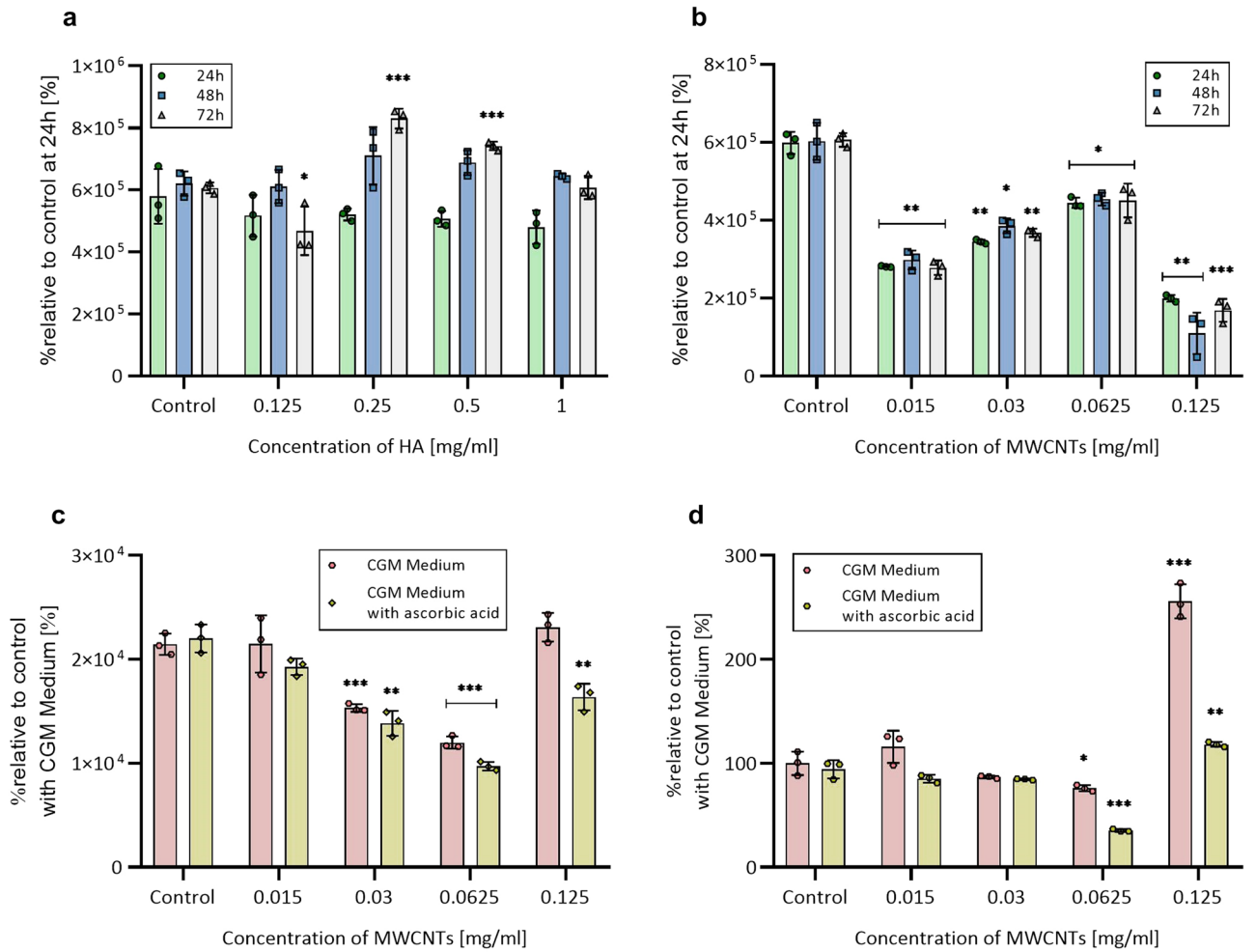**Figure 2.** Relative cell viability, ROS levels, and caspase 3/7 activity in 2D hMSC-AT culture. (**a**) Relativeiability of hMSC-AT after exposure to different concentrations of HA. (**b**) Relative viability of hMSC-AT after exposure to different concentrations of MWCNTs. (**c**) Relative ROS generation after 24 h exposure to MWCNTs. (**d**) Relative caspase 3/7 activity after 24 h incubation with MWCNTs. The data are presented as the mean ± SD. The statistical significance was determined by two-tailed Student's t-test (n = 3; additive vs control: *P < 0.05; **P < 0.01 and ***P < 0.001).
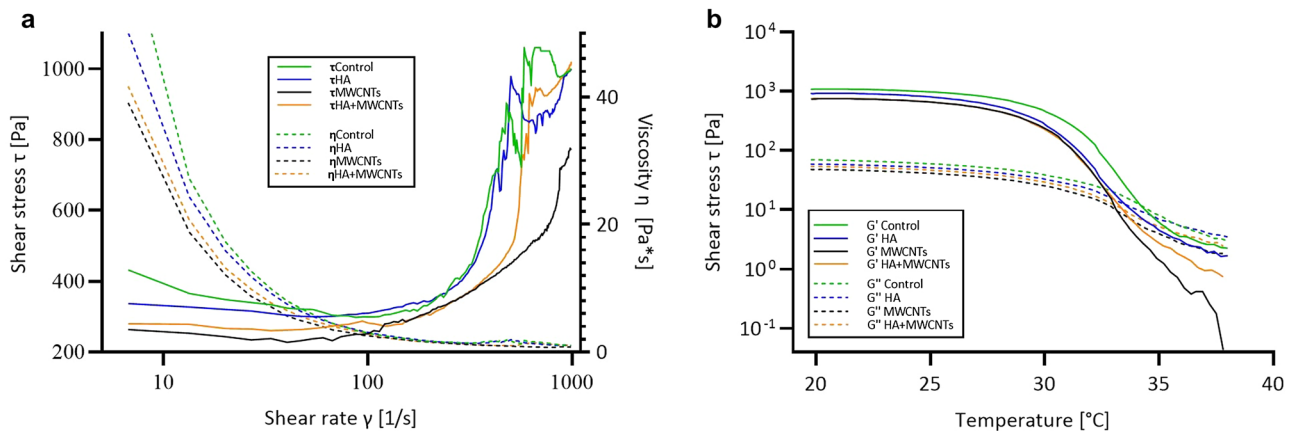

Figure 3. Rheological analysis of bioinks with MWCNTs or HA addition. Control is bioink without MWCNTs and HA. (**a**) Shear stress and viscosity as a function of shear rate. (**b**) The temperature-dependent functions of storage modulus G' and loss modulus G".

	No additives	Bioink with 0.25 mg/ml HA	Bioink with 0.0625 mg/ml MWCNTs	Bioink with 0.25 mg/ml HA and 0.0625 mg/ml MWCNTs
Needle	22 gauge (inner diameter = 410 μm)			
Pressure	60–68 kPa	65–70 kPa	55–60 kPa	65–70 kPa
Speed	14–15 mm/s	15–18 mm/s	14–15 mm/s	16–18 mm/s
Preflow	200 ms			
Postflow	0 ms			

Table 1. 3D bioprinting parameters.

SEM–EDX analysis showed insignificant changes in structure and elemental composition (Supp. Fig. 1). In the SEM images, regular pores can be observed, which match our bioprinting model. scaffolds also present highly fibrous structures.

Cell viability in bioprinted scaffolds. Live/dead assay was performed in order to determine the hMSC-AT viability in the 3D scaffolds (Fig. 4). In the control medium, a constant decrease in total viability was observed. Interestingly, the biggest decline in viability was observed in the differentiation medium, despite the cells having the highest transcriptional activity (see paragraph 3.4.). A similar decline was observed in HA-enriched constructs. In the case of MWCNTs-containing constructs, the decline was not observed, which implies a stimulating or protective effect on the cells. HA and MWCNTs combined were the only compositions, showing a synergistic effect, which has a positive impact on cell viability throughout the whole experiment.

HA and MWCNTs supplementation affect the expression of chondrogenic markers. To evaluate the chondrogenic potential of HA and functionalized MWCNTs, the gene expression analysis of genetic markers of chondrogenesis and stemness was performed (Fig. 5). Based on available data, the following genes were selected as chondrogenic markers: *COL1A1, COL6A1, COL10A1* and *COMP* (encoding collagen type I, VI, X, and Cartilage Oligomeric Matrix Protein, respectively—ECM components), *RUNX2, HIF1A,* and *SOX9*; (transcription factors)[3,20]. Additionally, to monitor the stemness of hMSCs we analyzed the expression of transcription factor Oct-4 (*POU5F1* gene)[21]. hMSC-AT-containing scaffolds of each bioink variant were maintained in culture for 1, 14, or 21 days. At each time point, expression of the hMSC-AT in bioink variants was normalized to hMSC-AT 3D bioprinted with bioink without additives (Fig. 5, green dashed lines). An additional group of control scaffolds was maintained in the chondrogenic medium for the same time intervals to define reference expression profiles in differentiated cells (DIFF) (Supp. Fig. 2). Gene expression profiles of cells from the same bioink variant between different time points were juxtaposed. A set of analyzed genes demonstrates expression fluctuations across subsequent time points (Fig. 5a–c,e,f) when compared to the control group (Fig. 5a–c,e,f, green dashed lines). The expression of two analyzed genes, *SOX9* and *COL10A1*, dropped below detectable lev-
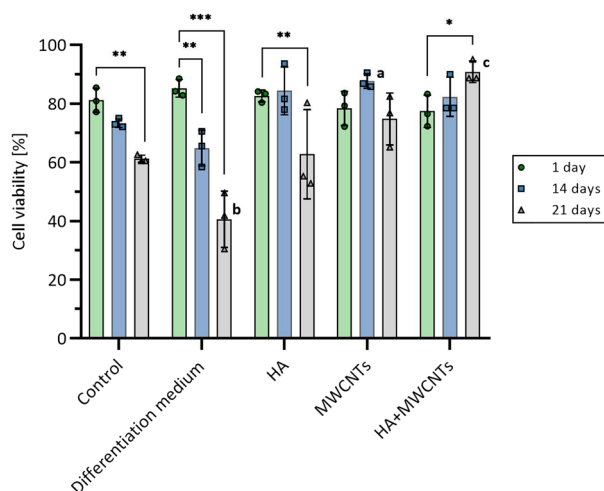

Figure 4. Viability of hMSC-AT cells in bioprinted scaffolds. Loss of viability over time can be observed in control media, supplemented with HA, and most profoundly, in commercial differentiation medium. Addition of the MWCNTs alone results in a protective or stimulating effect on cells, because the decrease in viability is not observed. Combined with HA, the viability has even increased over 21-day period. The data are presented as the mean ± SD. The statistical significance was determined by two-tailed Student's t-test (n = 3; additive vs control: [a]P < 0.05; [b]P < 0.01 and [c]P < 0.001; timepoint vs timepoint (within particular additive group): *P < 0.05; **P < 0.01 and ***P < 0.001).

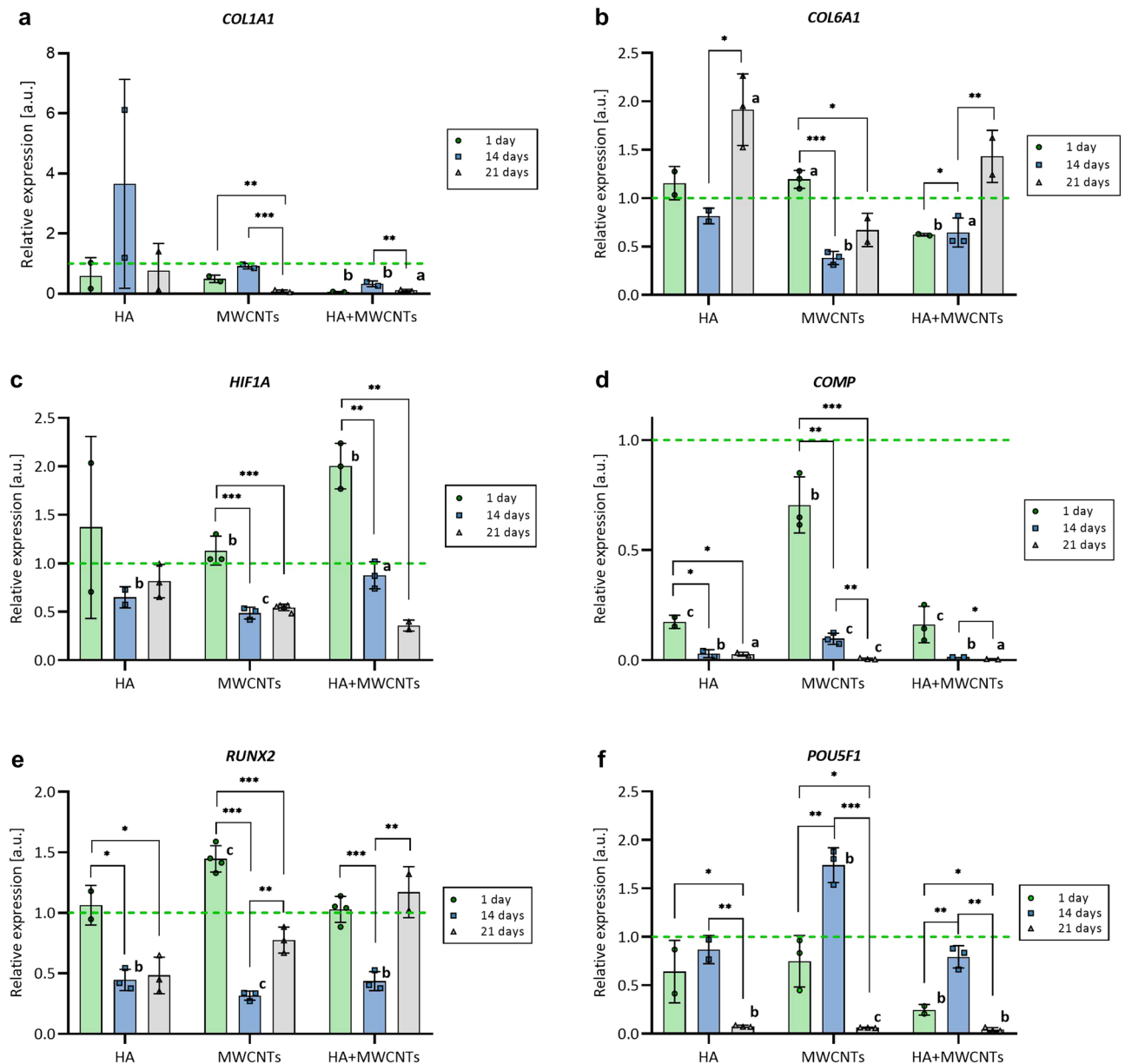**Figure 5.** Bioink additives affect the expression of chondrogenic markers. Real-time analysis of COL1A1 (**a**), COL6A1 (**b**), HIF1A (**c**), COMP (**d**), RUNX2 (**e**) and POU5F1 (**f**) gene expression in hMSCs 3D-printed with bioink containing 0.25 mg/ml of hyaluronic acid (HA), 0.0625 mg/ml of multi-walled carbon nanotubes (MWCNTs) or mix of HA and MWCNTs (HA + MWCNTs) (0.25 mg/ml and 0.0625 mg/ml, respectively) 1 day (1d), 14 days (14d) and 21 days (21d) post-printing. The expression of each variant is normalized to the average expression in hMSCs 3D-printed with bioink without additives at a particular time point (green dashed line). The statistical significance was determined by two-tailed Student's t-test (n ≥ 2; additive vs control (green dashed line): [a]P < 0.05; [b]P < 0.01 and [c]P < 0.001; timepoint vs timepoint (within particular additive group): *P < 0.05; **P < 0.01 and ***P < 0.001).

els on day 14 and 21, respectively, for all analyzed bioink variants including control scaffolds (data not shown), therefore, they were excluded from further analysis. Incubation for 21 days revealed an intense decrease of *COL1A1, HIF1A, COMP*, and *POU5F1* genes expression in MWCNTs and HA + MWCNTs bioink variants and *COMP* and *POU5F1* expression in HA variant (Fig. 5a,c,d,f). In parallel, expression analysis of the same genes in DIFF medium 21 days post-printing showed a rapid increase of *COL1A1* and *COMP* activity, and a significant decrease of *POU5F1* while expression of *HIF1A* remained unchanged (Supp. Fig. 2a,c,d,f). For HA and HA + MWCNTs variants, a significant increase in *COL6A1* expression was observed on day 21 (Fig. 5b) as well as for DIFF (Supp. Fig. 2b). The initial significant increase was also detected in *HIF1A* and *RUNX2* genes for MWC-NTs and HA + MWCNTs (*HIF1A*) and MWCNTs (*RUNX2*) followed by a deep decrease on day 14 (Fig. 5c,e). For MWCNTs on day 21 expression of *RUNX2* was restored to the control level as well as for HA + MWCNTs, yet, without expression boost on day 1 (Fig. 5e). Expression of *RUNX2* in DIFF progressively elevated (Supp.

Fig. 2e). Temporal transcriptional activation has also been observed for MWCNTs and HA + MWCNthe Ts in the *POU5F1* gene, where 14 days post-printing gene expression strongly increased to drop to a barely detectable level at day 21 (Fig. 5f) which reflects the expression profile of *POU5F1* in DIFF (Supp. Fig. 2f). Noteworthy, despite the same dynamics, *POU5F1* expression for HA + MWCNTs was much lower than for MWCNTs and did not reach the expression level observed in control scaffolds (Fig. 5f, 1 day, and 14 days).

Discussion

Bioink development is an inextricable part of 3D bioprinting for tissue engineering. Structural materials, like alginate or cellulose, are responsible for construct integrity and proper mechanical features; whereas biologically active substances are added to maintain cell functionality or stimulate various biological effects. This work investigated the influence of HA and functionalized MWCNTs firstly in 2D culture and then as additives to bioink designed for cartilage regeneration.

The toxicity of carbon nanotubes is a frequently raised concern regarding its utilization in tissue engineering[22]. The addition of the MWCNTs in all tested concentrations decreased cell viability and resulted in an increased ROS production in 2D cultures (Figs. 1b and 2b). These results confirm our previous reports[18]. Interestingly, R OS production diminished with increasing concentrations of MWCNTs, but when the concentration exceeded 0.0625 mg/ml, a robust generation of ROS occurred. This phenomenon could be elucidated by ROS scavenging facilitated by the CNTs, as described earlier. Our previous research reveals the interference of CNTs with luminescence-based assays, yielding nonrepresentative results, falsely indicating the high toxicity of this nanomaterial. However, at low concentrations used in this study, this interference may be omitted. Additionally, combining the assay with the measurement of caspase activity provides a double check on the reliability of the assay.

Additionally, to mitigate oxidative stress elicited by the MWCNTs, a more stable analog of vitamin C was tested. It has been demonstrated that ascorbic acid promotes chondrogenic cell differentiation, and helps to maintain a chondrogenic phenotype, especially in pathological conditions[23]. Our study corroborates the beneficial effects of ascorbic acid on oxidative stress and the viability of cells.

Alginate-HA bioink has been previously utilized to bioprint articular cartilage constructs[15]. In the study, the authors demonstrated that HA addition increased chondrogenic gene expression; however, in a contrast to our experimental design, a thermoplastic polymer was used as a structural material. The addition of HA was shown to affect the viscosity of bioink and, consequently, printability[24]. The rheological analysis of our bioinks showed inconsiderable variation. This discrepancy could be explained by the relatively low concentration of HA in the bioink (0.25 mg/ml).

The lowest level of the MWCNTs cytotoxicity in 2D culture was observed at a concentration of 0.0625 mg/ml which was subsequently used for bioink formulation. Cells cultured in 3D bioprinted constructs showed higher tolerance to increasing concentrations of carbon nanotubes, compared to 2D culture[25]. In 3D culture, carbon nanotubes are embedded in a hydrogel matrix, which limits their ability to be absorbed by the cells, while in 2D cultures carbon nanotubes diffuse into the medium facilitating cellular uptake by endocytosis[26]. In our previous study, 0.01% of CNTs embedded in polycaprolactone scaffold increased chondrocyte adhesion and proliferation[8].

Live/dead analysis showed that in the scaffold without additives (control and differentiation medium), as well as with HA, the viability of cells decreased over time. This is not the case in the scaffolds supplemented with MWCNTs. It may be attributed to the CNTs' resemblance to collagen fibrils, forming a 3D intricate mesh-like structure (Supp. Fig. 1), which may have a stimulating effect on the cells. Partial degradation of the HA-supplemented scaffolds could be caused by an increase in water content due to the strong hydrophilicity of HA, leading to the loss of integrity and subsequent degradation. Scaffolds with both MWCNTs and HA showed the highest viability of cells. They were also more stable than HA-supplemented scaffolds. This observation can further corroborate the CNTs' resemblance to collagens since collagen's main structural function is to provide tensile strength to the whole tissue.

In general, significant changes in expression of all analyzed genes with a progressive overall loss of transcriptional activity were observed (*COL1A1, HIF1A, COMP, POU5F1*—Fig. 5a,c,d,f, *COL10A1, SOX9*—data not shown). However, in DIFF samples the expression of *COL1A1* and *COMP* increased intensively while the *HIF1A* level remained stable (Supp. Fig. 2a,c,d). HIF1A protein is prone to oxygenation as a target of HIF hydroxylases and its level is elevated during hypoxia[27]. The initial increase of *HIF1A* expression observed on day 1 for all bioink variants may be due to culture format conversion from 2 to 3D which resulted in temporal hypoxia or hypoxia-like conditions, however, a stable level of *HIF1A* in DIFF does not support such hypothesis. On the other hand, the chondrogenic medium contains a variety of components that intensively stimulate the differentiation process (a detailed formulation of the medium was unavailable) some of which may exhibit antagonistic properties regarding *HIF1A* activation.

Since *HIF1A* positively regulates the expression of *SOX9*, it may explain the dramatic loss of its expression observed on days 14 and 21[28]. Collagen type I, VI, X, and COMP protein are constituents of cartilage ECM and their increased expression is observed at different stages of chondrogenic differentiation[3]. Although all bioink variants revealed an intense decrease in expression of *COL1A1* (except for HA, however, insignificant), *COL10A1,* and *COMP*, expression of *COL6A1* increased in HA and HA + MWCNTs. It also reflects a similar expression pattern in MWCNTs samples, yet, insignificant. It has been shown that the expression of *COL1A1* is prone to the presence of collagen type I-derived fragments[29,30]. As gelatin is one of the main components of the bioink formulation, it is plausible that short collagen fragments inhibit *COL1A1* transcription. A significant increase of *COL1A1* expression in DIFF might be, contrastingly, a result of the dominant stimulatory effect of the chondrogenic medium which ameliorates collagen fragment inhibitory properties. Little is known about the regulation of *COMP* expression. However, previous studies show that COMP binds to collagen type I which might point to mutual or synergistic regulation and explain the simultaneous decrease of *COMP* gene expression

in all bioink variants, in contrast to DIFF where expression of both genes is dramatically increased[31]. Collagen type X is abundant in hypertrophic chondrocytes, therefore, intense loss of its expression in bioprinted hMSCs might be a hallmark of early-stage chondrogenic differentiation[32]. Although collagen type VI comprises up to 1% of total collagen in articular cartilage it plays important role in ECM organization and governing chondrocyte fate and, therefore, serves as an indicator of chondrogenesis[33–35]. The moderate increase observed in HA and HA + MWCNTs corresponds to changes in *COL6A1* observed in DIFF. Although the magnitude of change in *POU5F1* expression in MWCNTs and HA + MWCNTs is notably lower, its profile is similar to this observed in DIFF. Interestingly, while the *POU5F1* gene tends to deactivate in differentiating cells, its expression at day 14 in DIFF (as well as in CNTs and HA + MWCNTs) strongly elevates to almost complete deactivation on day 21. That might point to significant transcriptional rearrangement in hMSCs during incubation in a chondrogenic medium but in the presence of MWCNTs or a mix of HA and MWCNTs as well. Taken together, the addition of HA or MWCNTs, alone or in tandem, to the bioink provokes alterations in the expression of genes related to chondrogenic differentiation. Although the expression patterns are not identical for all selected genes and the magnitude of observed changes is considerably lower when compared to the expression induced by the chondrogenic medium, effects elicited by additives, MWCNTs, and HA + MWCNTs, in the expression of *COL6A1*, *RUNX2*, and *POU5F1* might point to low-efficient or time-shifted differentiation.

Summary
The effects of hyaluronic acid and carbon nanotubes were investigated in 2D and 3D in vitro cell cultures. Results were concentration-dependent and differ in models (2D or 3D). HA stimulates cell viability in monolayer culture. In bioprinted constructs, MWCNTs have a beneficial influence on cell viability while HA inclusion in examined concentration has a negative impact on constructs integrity. The profile of the analyzed gene changed significantly and we observed the overall loss of transcriptional activity in most of them. These results suggest the need for more complex gene expression analysis combined with protein accumulation studies, also in extended time points. In general, promising results from 3D bioprinted scaffolds encourage undertaking in vivo tests to investigate the precise mechanism of CNTs' interaction with cells. This may elucidate further whether they act as collagen mimetics.

Data availability
All data generated or analyzed during this study are included in this published article [and its supplementary information files].

References
 1. Kwon, H. *et al.* Surgical and tissue engineering strategies for articular cartilage and meniscus repair. *Nat. Rev. Rheumatol.* **15**, 550–570 (2019).
 2. Semba, J. A., Mieloch, A. A. & Rybka, J. D. Introduction to the state-of-the-art 3D bioprinting methods, design, and applications in orthopedics. *Bioprinting* **18**, e00070 (2020).
 3. Gelse, K., Pöschl, E. & Aigner, T. Collagens—Structure, function, and biosynthesis. *Adv. Drug Deliv. Rev.* **55**, 1531–1546 (2003).
 4. Xin, W., Heilig, J., Paulsson, M. & Zaucke, F. Collagen II regulates chondrocyte integrin expression profile and differentiation. *Connect. Tissue Res.* **56**, 307–314 (2015).
 5. Holmes, D. F., Lu, Y., Starborg, T. & Kadler, K. E. Collagen fibril assembly and function. *Curr. Top. Dev. Biol.* **130**, 107–142 (2018).
 6. Koláčná, L. *et al.* Biochemical and biophysical aspects of collagen nanostructure in the extracellular matrix. *Physiol. Res.* **56**, 51–60 (2007).
 7. Garantziotis, S. & Savani, R. C. Hyaluronan biology: A complex balancing act of structure, function, location and context. *Matrix Biol.* **78–79**, 1–10 (2019).
 8. Mieloch, A. A., Semba, J. A. & Rybka, J. D. CNT-type dependent cellular adhesion on 3D-printed nanocomposite for tissue engineering. *Int. J. Bioprint.* **8**, 70–79 (2022).
 9. Chahine, N. O., Collette, N. M., Thomas, C. B., Genetos, D. C. & Loots, G. G. Nanocomposite scaffold for chondrocyte growth and cartilage tissue engineering: Effects of carbon nanotube surface functionalization. *Tissue Eng. Part A* **20**, 2305–2315 (2014).
10. Mirmusavi, M. H., Ahmadian, M. & Karbasi, S. Polycaprolactone-chitosan/multi-walled carbon nanotube: A highly strengthened electrospun nanocomposite Scaffold for cartilage tissue engineering. *Int. J. Biol. Macromol.* **209**, 1801–1814 (2022).
11. Pinnell, S. R. Regulation of collagen biosynthesis by ascorbic acid: A review. *Yale J. Biol. Med.* **58**, 553–559 (1985).
12. Murad, S. *et al.* Regulation of collagen synthesis by ascorbic acid. *Proc. Natl. Acad. Sci. USA* **78**, 2879–2882 (1981).
13. Ibold, Y. *et al.* Effect of different ascorbate supplementations on in vitro cartilage formation in porcine high-density pellet cultures. *Tissue Cell* **41**, 249–256 (2009).
14. Charan, T. R. *et al.* "Nanomaterials of curcumin-hyaluronic acid": Their various methods of formulations, clinical and therapeutic applications, present gap, and future directions. *Futur. J. Pharm. Sci.* **7**, 1–17 (2021).
15. Antich, C. *et al.* Bio-inspired hydrogel composed of hyaluronic acid and alginate as a potential bioink for 3D bioprinting of articular cartilage engineering constructs. *Acta Biomater.* **106**, 114–123 (2020).
16. Poldervaart, M. T. *et al.* 3D bioprinting of methacrylated hyaluronic acid (MeHA) hydrogel with intrinsic osteogenicity. *PLoS ONE* **12**, e0177628 (2017).
17. Hauptstein, J. *et al.* Hyaluronic acid-based bioink composition enabling 3D bioprinting and improving quality of deposited cartilaginous extracellular matrix. *Adv. Healthc. Mater.* **9**, 2000737 (2020).
18. Szymański, T., Kempa, M., Giersig, M. & Rybka, J. D. Carbon nanotubes interference with luminescence-based assays. *Materials (Basel)* **13**, 4270 (2020).
19. Hata, R.-I. & Senoo, H. L-Ascorbic acid 2-phosphate stimulates collagen accumulation, cell proliferation, and formation of a three-dimensional tissuelike substance by skin fibroblasts. *J. Cell. Physiol.* **138**, 8–16 (1989).
20. Di Cesare, P. E. *et al.* Expression of cartilage oligomeric matrix protein (COMP) by embryonic and adult osteoblasts. *J. Orthop. Res.* **18**, 713–720 (2000).
21. Niwa, H., Miyazaki, J. I. & Smith, A. G. Quantitative expression of Oct-3/4 defines differentiation, dedifferentiation or self-renewal of ES cells. *Nat. Genet.* **24**, 372–376 (2000).

22. Szymański, T. *et al.* Utilization of carbon nanotubes in manufacturing of 3D cartilage and bone scaffolds. *Materials* **13**, 4039 (2020).
23. Chang, Z., Huo, L., Li, P., Wu, Y. & Zhang, P. Ascorbic acid provides protection for human chondrocytes against oxidative stress. *Mol. Med. Rep.* **12**, 7086–7092 (2015).
24. Lee, S. J. *et al.* Three-dimensional printable hydrogel using a hyaluronic acid/sodium alginate bio-ink. *Polymers (Basel)* **13**, 1–8 (2021).
25. Chahine, N. O., Collette, N. M., Thomas, C. B., Genetos, D. C. & Loots, G. G. Nanocomposite scaffold for chondrocyte growth and cartilage tissue engineering: Effects of carbon nanotube surface functionalization. *Tissue Eng.-Part A* **20**, 2305–2315 (2014).
26. Maruyama, K. *et al.* Endocytosis of multiwalled carbon nanotubes in bronchial epithelial and mesothelial cells. *Biomed. Res. Int.* **2015** (2015).
27. Schofield, C. J. & Ratcliffe, P. J. Oxygen sensing by HIF hydroxylases. *Nat. Rev. Mol. Cell Biol.* **5**, 343–354 (2004).
28. Zhang, C. *et al.* Hypoxia-inducible factor-1 is a positive regulator of Sox9 activity in femoral head osteonecrosis. *Bone* **48**, 507–513 (2011).
29. Horlein, D., McPherson, J., Goh, S. H. & Bornstein, P. Regulation of protein synthesis: Translational controls by procollagen-derived fragments. *Proc. Natl. Acad. Sci. USA* **78**, 6163–6167 (1981).
30. Wiestner, M. *et al.* Inhibiting effect of procollagen peptides on collagen biosynthesis in fibroblast cultures. *J. Biol. Chem.* **254**, 7016–7023 (1979).
31. Rosenberg, K., Olsson, H., Mörgelin, M. & Heinegård, D. Cartilage oligomeric matrix protein shows high affinity zinc-dependent interaction with triple helical collagen. *J. Biol. Chem.* **273**, 20397–20403 (1998).
32. Smith, D. E. & Fisher, P. A. Identification, developmental regulation, and response to heat shock of two antigenically related forms of a major nuclear envelope protein in Drosophila embryos: Application of an improved method for affinity purification of antibodies using polypeptides. *J. Cell Biol.* **99**, 20–28 (1984).
33. Hou, W. *et al.* Cross-tissue characterization of heterogeneities of mesenchymal stem cells and their differentiation potentials. *Front. Cell Dev. Biol.* **9**, 3493 (2021).
34. Zelenski, N. A. *et al.* Type VI collagen regulates pericellular matrix properties, chondrocyte swelling, and mechanotransduction in mouse articular cartilage. *Arthritis Rheumatol.* **67**, 1286–1294 (2015).
35. Eyre, D. R., Weis, M. A. & Wu, J. J. Articular cartilage collagen: An irreplaceable framework?. *Eur. Cell. Mater.* **12**, 57–63 (2006).

Acknowledgements

Author contributions

J.D.R. guided and supervised the project. T.S. and A. A. M. designed and supervised the experiments. T.S., J.A.S., M.K. and P.C., conducted experiments, T.S. and J.D.R. contributed intellectually to the scientific design of the project. A.A.M. and J.D.R. mentored the technical part of the project; manuscript preparation T.S., J.A.S.; manuscript edition A.A.M, J.D.R.

Funding

Competing interests

The authors declare no competing interests.

Additional information

Supplementary Information The online version contains supplementary material available at https://doi.org/10.1038/s41598-023-27901-z.

Correspondence and requests for materials should be addressed to J.D.R.

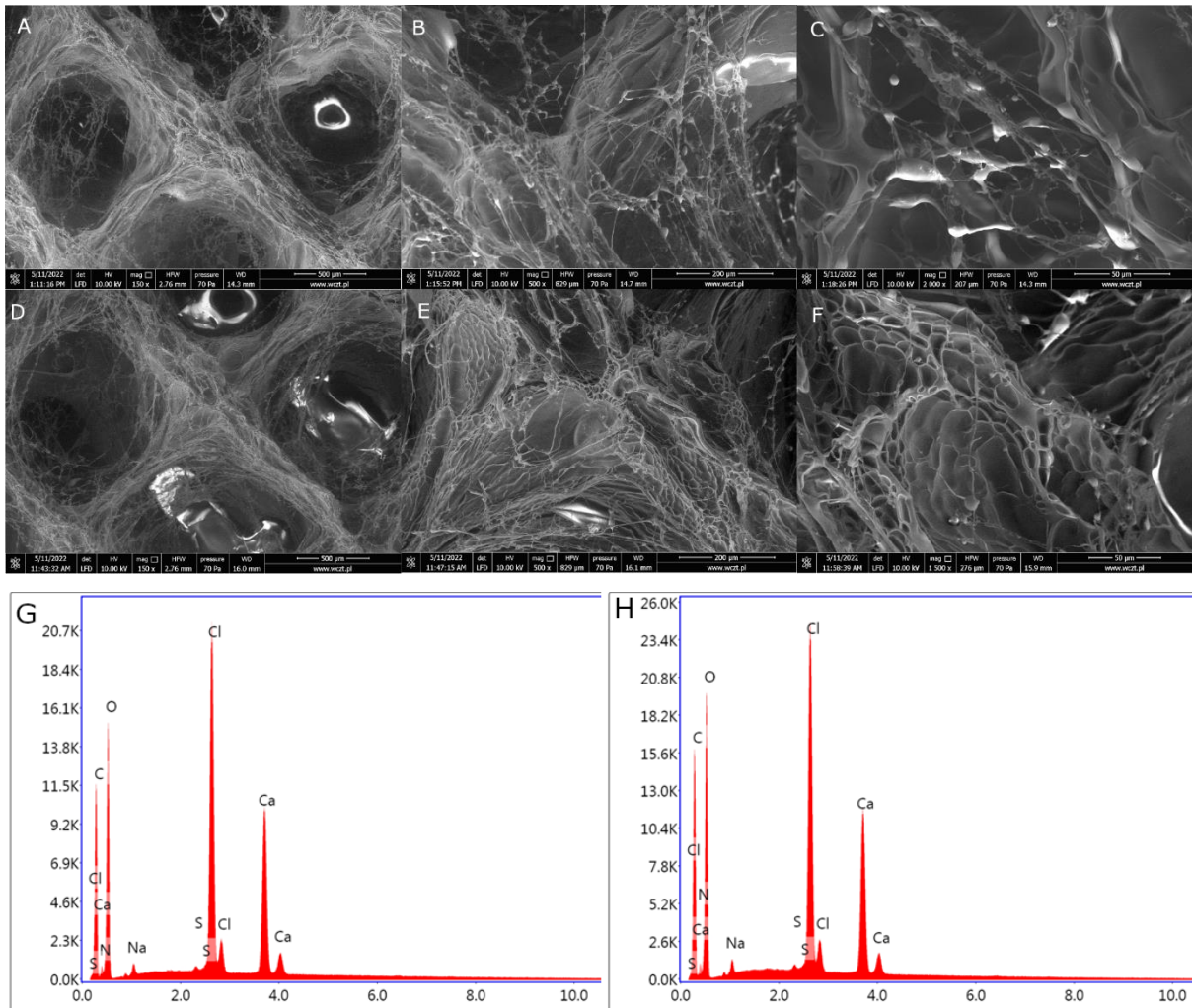**Reprints and permissions information** is available at www.nature.com/reprints.

Publisher's note Springer Nature remains neutral with regard to jurisdictional claims in published maps and institutional affiliations.
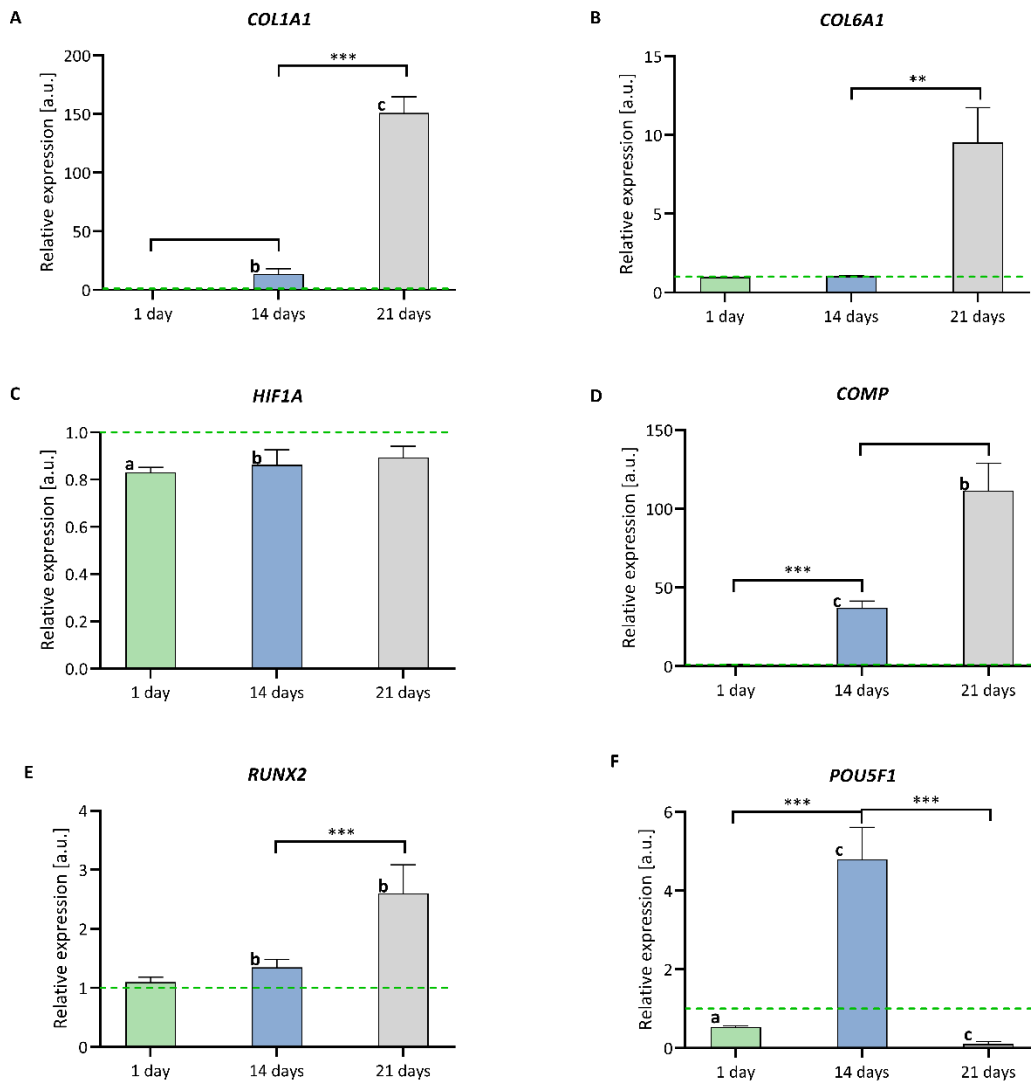
Supplementary data

Supplementary Figure 1. SEM and EDX analysis. SEM images of scaffolds without addition of the MWCNTs (A, B, C) and scaffolds supplemented with CNTs (D, E, F). EDX spectra of CNT supplemented (G) and non-supplmented scaffolds (H). There is no significant difference in atomic composition.

Supplementary Figure 2. **Differentiation medium affects expression of chondrogenic markers.** Real-time analysis of COL1A1 (A), COL6A1 (B), HIF1A (C), COMP (D), RUNX2 (E) and POU5F1 (F) gene expression in hMSCs 3D-printed with bioink without HA or MWCNTs supplementation 1 day (1d), 14 days (14d) and 21 days (21d) post-printing. Expression is normalized to average expression in hMSCs 3D-printed with bioink without additives and cultured in regular medium at particular time point (green dashed line). The statistical significance was determined by two-tailed Student's t-test (n≥2; chondrogenic vs control: P^a< 0.05; P^b < 0.01 and P^c < 0.001; timepoint vs time point P* < 0.05; P** < 0.01 and P*** < 0.001).

Supplementary Tabel 1. Primer sequences used in real-time analysis.

RPS29	forward 5'-AGATGGGTCACCAGCAGCTGTACTG-3'
	reverse 5'-AGACACGACAAGAGCGAGAA-3'
COL1A1	forward 5'-ACGTCCTGGTGAAGTTGGTC-3'
	reverse 5'-AGCCTCTCTCTCCTCTCTGACC-3'
COL6A1	forward 5'-CTCGTGGACAAAGTCAAGTCCT-3'
	reverse 5'-GTAGGTGCCCTTCCCAAAGTA-3'
COL10A1	forward 5'-TTACGCTGAACGATACCAAATG-3'
	reverse 5'-GACTTCCGTAGCCTGGTTTTC-3'
RUNX2	forward 5'-ACCAGATGGGACTGTGGTTACT-3'
	reverse 5'-TGTGAAGACGGTTATGGTCAAG-3'
HIF1A	forward 5'-CCAACAGTAACCAACCTCAGTG-3'
	reverse 5'-GCCTAAAAGTTCTTCTGGCTCA-3'
COMP	forward 5'-ACAATGACGGAGTCCCTGAC-3'
	reverse 5'-TCTGCATCAAAGTCGTCCTG-3'
SOX9	forward 5'-GACTCGCCACACTCCTCCT-3'
	reverse 5'-AGGTCTCGATGTTGGAGATGAC-3'
POU5F1	forward 5'-GGAGATATGCAAAGCAGAAACC-3'
	reverse 5'-CTCAAAATCCTCTCGTTGTGC-3'

Tomasz Szymański

Laboratory of Applied Biotechnology
Center for Advanced Technology
Adam Mickiewicz University in Poznan
e-mail: tomszy1@amu.edu.pl

Author contribution statement

I declare that I am the first author of the article "Hyaluronic acid and multiwalled carbon nanotubes as bioink additives for cartilage tissue engineering" by Tomasz Szymański, Julia Anna Semba, Adam Aron Mieloch, Piotr Cywoniuk, Marcelina Kempa and Jakub Dalibor Rybka, published in *Scientific reports* in 2023 and I am aware that this publication is a part of Julia Semba PhD dissertation. The author's contribution is as follows:

Tomasz Szymański designed the study and supervised the experiments. Tomasz Szymański made MWCNTs functionalization and determined the cell viability, reactive oxygen species, and apoptosis levels in 2D cell cultures stimulated with MWCNTs, 2-phospho-l-ascorbic acid, and hyaluronic acid. Tomasz Szymański with Julia Semba prepared the original draft and Supp. Figure 1.

Julia Semba co-designed the study. She was responsible for cell culture. Julia Semba prepared bioinks, made rheological analysis, and 3D bioprinted. Julia Semba prepared and analyzed SEM. Julia Semba with Piotr Cywoniuk prepared, made, and analyzed gene expression. Julia Semba with Tomasz Szymański prepared the original draft. She prepared Figures 1 to 3, as well as Figure 4 and Supp. Figure 1 with Tomasz Szymański and Figure 5 and Supp. Figure 2 with Piotr Cywoniuk.

Adam Mieloch designed the study, supervised the experiments, and revised the draft.

Piotr Cywoniuk helps with primer design and qPCR data analysis. Made Figure 5 and Supp. Figure 2 with Julia Semba.

Marcelina Kempa helped to determine the cell viability, reactive oxygen species, and apoptosis levels in 2D cell cultures stimulated with MWCNTs, 2-phospho-l-ascorbic acid, and hyaluronic acid.

Jakub Rybka guided and supervised the research and revised the draft. Jakub Rybka also acquired funding and corresponded with the journal and reviewers.

Date: 8.12.2023

Signature: *Szymoński*

prof. UAM dr hab. inż. Jakub D. Rybka

Dr Adam Mieloch

Laboratory of Applied Biotechnology
Center for Advanced Technology
Adam Mickiewicz University in Poznan
e-mail: amieloch@amu.edu.pl

Author contribution statement

I declare that I am the co-author of the article "Hyaluronic acid and multiwalled carbon nanotubes as bioink additives for cartilage tissue engineering" by Tomasz Szymański, Julia Anna Semba, Adam Aron Mieloch, Piotr Cywoniuk, Marcelina Kempa and Jakub Dalibor Rybka, published in *Scientific reports* in 2023 and I am aware that this publication is a part of Julia Semba PhD dissertation. The author's contribution is as follows:

Tomasz Szymański designed the study and supervised the experiments. Tomasz Szymański made MWCNTs functionalization and determined the cell viability, reactive oxygen species, and apoptosis levels in 2D cell cultures stimulated with MWCNTs, 2-phospho-l-ascorbic acid, and hyaluronic acid. Tomasz Szymański with Julia Semba prepared the original draft and Supp. Figure 1.

Julia Semba co-designed the study. She was responsible for cell culture. Julia Semba prepared bioinks, made rheological analysis, and 3D bioprinted. Julia Semba prepared and analyzed SEM. Julia Semba with Piotr Cywoniuk prepared, made, and analyzed gene expression. Julia Semba with Tomasz Szymański prepared the original draft. She prepared Figures 1 to 3, as well as Figure 4 and Supp. Figure 1 with Tomasz Szymański and Figure 5 and Supp. Figure 2 with Piotr Cywoniuk.

Adam Mieloch designed the study, supervised the experiments, and revised the draft.

Piotr Cywoniuk helps with primer design and qPCR data analysis. Made Figure 5 and Supp. Figure 2 with Julia Semba.

Marcelina Kempa helped to determine the cell viability, reactive oxygen species, and apoptosis levels in 2D cell cultures stimulated with MWCNTs, 2-phospho-l-ascorbic acid, and hyaluronic acid.

Jakub Rybka guided and supervised the research and revised the draft. Jakub Rybka also acquired funding and corresponded with the journal and reviewers.

Date: 04.12.2023

Signature:

dr Adam A. Mieloch

Dr Piotr Cywoniuk

Laboratory of Applied Biotechnology
Center for Advanced Technology
Adam Mickiewicz University in Poznan
e-mail: pcywoniuk@amu.edu.pl

Author contribution statement

I declare that I am the co-author of the article "Hyaluronic acid and multiwalled carbon nanotubes as bioink additives for cartilage tissue engineering" by Tomasz Szymański, Julia Anna Semba, Adam Aron Mieloch, Piotr Cywoniuk, Marcelina Kempa and Jakub Dalibor Rybka, published in *Scientific reports* in 2023 and I am aware that this publication is a part of Julia Semba PhD dissertation. The author's contribution is as follows:

Tomasz Szymański designed the study and supervised the experiments. Tomasz Szymański made MWCNTs functionalization and determined the cell viability, reactive oxygen species, and apoptosis levels in 2D cell cultures stimulated with MWCNTs, 2-phospho-l-ascorbic acid, and hyaluronic acid. Tomasz Szymański with Julia Semba prepared the original draft and Supp. Figure 1.

Julia Semba co-designed the study. She was responsible for cell culture. Julia Semba prepared bioinks, made rheological analysis, and 3D bioprinted. Julia Semba prepared and analyzed SEM. Julia Semba with Piotr Cywoniuk prepared, made, and analyzed gene expression. Julia Semba with Tomasz Szymański prepared the original draft. She prepared Figures 1 to 3, as well as Figure 4 and Supp. Figure 1 with Tomasz Szymański and Figure 5 and Supp. Figure 2 with Piotr Cywoniuk.

Adam Mieloch designed the study, supervised the experiments, and revised the draft.

Piotr Cywoniuk helps with primer design and qPCR data analysis. Made Figure 5 and Supp. Figure 2 with Julia Semba.

Marcelina Kempa helped to determine the cell viability, reactive oxygen species, and apoptosis levels in 2D cell cultures stimulated with MWCNTs, 2-phospho-l-ascorbic acid, and hyaluronic acid.

Jakub Rybka guided and supervised the research and revised the draft. Jakub Rybka also acquired funding and corresponded with the journal and reviewers.

Date: 8/12/2023

Signature: *Piotr Cywoniuk*

Dr hab. inż. Jakub Rybka, prof. UAM

Laboratory of Applied Biotechnology
Center for Advanced Technology
Adam Mickiewicz University in Poznan
e-mail: jrybka@amu.edu.pl

Author contribution statement

I declare that I am the corresponding author of the article "Hyaluronic acid and multiwalled carbon nanotubes as bioink additives for cartilage tissue engineering" by Tomasz Szymański, Julia Anna Semba, Adam Aron Mieloch, Piotr Cywoniuk, Marcelina Kempa and Jakub Dalibor Rybka, published in *Scientific reports* in 2023 and I am aware that this publication is a part of Julia Semba PhD dissertation. The author's contribution is as follows:

Tomasz Szymański designed the study and supervised the experiments. Tomasz Szymański made MWCNTs functionalization and determined the cell viability, reactive oxygen species, and apoptosis levels in 2D cell cultures stimulated with MWCNTs, 2-phospho-l-ascorbic acid, and hyaluronic acid. Tomasz Szymański with Julia Semba prepared the original draft and Supp. Figure 1.

Julia Semba co-designed the study. She was responsible for cell culture. Julia Semba prepared bioinks, made rheological analysis, and 3D bioprinted. Julia Semba prepared and analyzed SEM. Julia Semba with Piotr Cywoniuk prepared, made, and analyzed gene expression. Julia Semba with Tomasz Szymański prepared the original draft. She prepared Figures 1 to 3, as well as Figure 4 and Supp. Figure 1 with Tomasz Szymański and Figure 5 and Supp. Figure 2 with Piotr Cywoniuk.

Adam Mieloch designed the study, supervised the experiments, and revised the draft.

Piotr Cywoniuk helps with primer design and qPCR data analysis. Made Figure 5 and Supp. Figure 2 with Julia Semba.

Marcelina Kempa helped to determine the cell viability, reactive oxygen species, and apoptosis levels in 2D cell cultures stimulated with MWCNTs, 2-phospho-l-ascorbic acid, and hyaluronic acid.

Jakub Rybka guided and supervised the research and revised the draft. Jakub Rybka also acquired funding and corresponded with the journal and reviewers.

Date: 0 8. 01. 2024

Signature:

prof. UAM dr hab. inż. Jakub D. Rybka

Julia Semba

Laboratory of Applied Biotechnology
Center for Advanced Technology
Adam Mickiewicz University in Poznan
e-mail: jsemba@amu.edu.pl

Author contribution statement

I declare that I am the co-author of the article **"Hyaluronic acid and multiwalled carbon nanotubes as bioink additives for cartilage tissue engineering"** by Tomasz Szymański, Julia Anna Semba, Adam Aron Mieloch, Piotr Cywoniuk, Marcelina Kempa and Jakub Dalibor Rybka, published in *Scientific reports* in 2023. The author's contribution is as follows:

Tomasz Szymański designed the study and supervised the experiments. Tomasz Szymański made MWCNTs functionalization and determined the cell viability, reactive oxygen species, and apoptosis levels in 2D cell cultures stimulated with MWCNTs, 2-phospho-1-ascorbic acid, and hyaluronic acid. Tomasz Szymański with Julia Semba prepared the original draft and Supp. Figure 1.

Julia Semba co-designed the study. She was responsible for cell culture. Julia Semba prepared bioinks, made rheological analysis, and 3D bioprinted. Julia Semba prepared and analyzed SEM. Julia Semba with Piotr Cywoniuk prepared, made, and analyzed gene expression. Julia Semba with Tomasz Szymański prepared the original draft. She prepared Figures 1 to 3, as well as Figure 4 and Supp. Figure 1 with Tomasz Szymański and Figure 5 and Supp. Figure 2 with Piotr Cywoniuk.

Adam Mieloch designed the study, supervised the experiments, and revised the draft.

Piotr Cywoniuk helps with primer design and qPCR data analysis. Made Figure 5 and Supp. Figure 2 with Julia Semba.

Marcelina Kempa helped to determine the cell viability, reactive oxygen species, and apoptosis levels in 2D cell cultures stimulated with MWCNTs, 2-phospho-1-ascorbic acid, and hyaluronic acid.

Jakub Rybka guided and supervised the research and revised the draft. Jakub Rybka also acquired funding and corresponded with the journal and reviewers.

Date: 28. 12. 2023
Signature: *Semba Julia*